

Maternal influenza and its consequences for offspring's immunity

Dissertation zur Erlangung des Doktorgrades
der Naturwissenschaften (Dr. rer. nat.)

des Fachbereiches Chemie
der Fakultät Mathematik, Informatik und Naturwissenschaften
der Universität Hamburg

Vorgelegt von
Henning Magnus Peter Jacobsen
aus Schleswig

Hamburg, 2020

Die vorliegende Arbeit mit dem Titel „Maternal Influenza and its Consequences for Offspring’s Immunity“ wurde im Zeitraum vom 01. November 2016 – 03. August 2020 am Heinrich-Pette-Institut, Leibniz Institut für Experimentelle Virologie (Abteilung 61: Virale Zoonose – One Health) in Hamburg angefertigt.

Reviewer: Prof. Dr. Gülsah Gabriel

Second Reviewer: Prof. Dr. Wolfram Brune

Date of Thesis Defense: October 23, 2020

Approval for Publication: October 27, 2020

Publications related to this study (as of July 2020)

Henning Jacobsen, Kerstin Walendy-Gnirß, Nilgün Tekin-Bubenheim, Isabel Ben-Batalla, Nikolaus Berenbrok, Lucas Scholl, Vinicius Pinho dos Reis, Annette Gries, Hanna Jania, Nancy Mounogou Kouassi, Arne Düsedau, Gundula Pilnitz-Stolze, Aicha Jeridi, Ali Önder Yildirim, Helmut Fuchs, Valerie Gailus-Durner, Claudia Stöger, Martin Hrabe de Angelis, Fiona Culley, Peter Openshaw, Jochen Behrends, Sonja Loges, Bianca Schneider, Gülsah Gabriel. Murine Offspring Born to Influenza A Virus Infected Mothers Present Increased Vulnerability Towards Infections in Later Life. *Nature Microbiology* (2020, submitted)

Other publications (As of July 2020)

Maria Schroeder, Berfin Tuku, Dominik Jarczak, Axel Nierhaus, Tian Bai, **Henning Jacobsen**, Martin Zickler, Zacharias Mueller, Stephanie Stanelle-Bertram, Andreas Meinhardt, Jens Aberle, Stefan Kluge, Gülsah Gabriel. Low Testosterone, High Estradiol and Cytokine Storm in Critically Ill Male COVID-19 Patients. (2020, in preparation).

Henning Jacobsen, Madhusudan Rajendran, Angela Choi, Haakon Sjursen, Karl A. Brokstad, Rebecca J. Cox, Peter Palese, Florian Krammer, Raffael Nachbagauer. Influenza Virus Hemagglutinin Stalk-Specific Antibodies in Human Serum are a Surrogate Marker for In Vivo Protection in a Serum Transfer Mouse Challenge Model. *mBio* 8:e01463-17 (2017)

Geraldine Engels, Alexandra Maximiliane Hierweger, Julia Hoffmann, Rene Thieme, Swantje Thiele, Stephanie Bertram, Carola Dreier, Patricia Resa-Infante, **Henning Jacobsen**, Kristin Thiele, Malik Alawi, Daniela Indenbirken, Adam Grundhoff, Svenja Siebels, Nicole Fischer, Violeta Stojanovska, Damia Muzzio, Federico Jensen, Khalil Karimi, Hans-Willi Mittrücker, Petra Clara Arck, and Gülsah Gabriel. Pregnancy-Related Immune Adaptation Promotes the Emergence of Highly Virulent H1N1 Influenza Virus Strains in Allogeneically Pregnant Mice. *Cell Host & Microbe* 21, 321–333 (2017).

Table of contents

1. Zusammenfassung.....	1
2. Abstract	2
3. Introduction.....	3
3.1. Influenza	3
3.2. The influenza virus.....	3
3.2.1. Taxonomy	3
3.2.2. Virion structure	4
3.3. Virus ecology	5
3.4. Virus drift and shift.....	6
3.5. Influenza pandemics.....	7
3.6. Preventive and curative strategies.....	8
3.6.1. Vaccines.....	8
3.6.2. Antiviral treatment.....	9
3.7. Risk groups for influenza	10
3.7.1. The elderly (≥ 65 years of age)	10
3.7.2. Individuals with chronic medical conditions	11
3.7.3. Infants and young children (< 5 years of age)	11
3.7.4. Pregnant women	12
3.8. Immunology during pregnancy	13
3.9. Maternal immune activation and offspring's health.....	14
3.10. Animal models to study maternal immune activation.....	16
3.10.1. Artificial models of maternal immune activation.....	18
3.10.2. Maternal immune activation models using IAV	18
4. Aim.....	20
5. Results	21
5.1. Influenza A virus mediated maternal immune activation	21
5.2. Maternal immune activation and pregnancy outcomes	27
5.3. Effects on offspring's immunity.....	31
5.3.1. Offspring infection with influenza B virus	35
5.3.2. Offspring infection with <i>Staphylococcus aureus</i>	38
5.3.3. Adoptive transfer of alveolar macrophages.....	42
5.4. Discussion	45
6. Outlook.....	49
7. Materials and Methods	51

7.1.	Materials.....	51
7.1.1.	Chemicals.....	51
7.1.2.	Buffers and solutions.....	52
7.1.3.	Kits	53
7.1.4.	Antibodies.....	54
7.1.5.	Enzymes.....	56
7.1.6.	DNA oligonucleotides	56
7.1.7.	Narcotics and supplements	56
7.1.8.	Bacterial strains	57
7.1.9.	Media for bacterial culture.....	57
7.1.10.	Eukaryotic cell lines	57
7.1.11.	Media and supplements for eukaryotic cell culture	57
7.1.12.	Virus strains	58
7.1.13.	Consumables	59
7.1.14.	Safety gear	60
7.1.15.	Laboratory equipment.....	60
7.1.16.	Software	62
7.2.	Methods	63
7.2.1.	Ethics statement.....	63
7.2.2.	Cells and virus.....	63
7.2.3.	Hemagglutination assay	63
7.2.4.	Determination of viral titers.....	64
7.2.5.	Methicillin resistant <i>Staphylococcus aureus</i> (MRSA)	64
7.2.6.	Determination of bacterial titers.....	65
7.2.7.	Animal experiments	65
7.2.8.	Lung function.....	67
7.2.9.	Immunohistology and histopathology	68
7.2.10.	Immune cell analysis and sorting	68
7.2.11.	Cytokine and hormone measurement	70
7.2.12.	Nutrient gene RT-qPCR of placental tissue	71
7.2.13.	Sex determination by PCR	72
7.2.14.	Data analysis.....	72
7.2.15.	Collaborations	73
7.2.15.1.	Lung function.....	73
7.2.15.2.	Nutrition gene RT-qPCR of placental tissue	73
7.2.15.3.	Analysis of cell populations by flow cytometry	74

7.2.15.4. Measurement of testosterone from plasma	74
7.2.15.5. Immunohistology and histopathology	74
8. Literature	75
I. Supplements – Hazardous materials	84
II. Supplements – Figures	87
III. Supplements – List of tables and figures.....	95
IV. License agreements, reprint of figures.....	97
Danksagung	98
Eidesstattliche Erklärung.....	100

Abbreviations

ALD	Autism-like disorder
AM	Alveolar macrophage
BM2	BM2 protein
BSA	Bovine serum albumin
BSL	Bio safety level
CD	Cluster of differentiation
CDC	Center for Disease Control (US)
cDNA	Complementary DNA
CFU	Colony forming units
CMP	Common myeloid progenitor
CNS	Central nervous system
CVV	Candidate vaccine virus
d p.i.	Days post infection
dDCs	Decidual dendritic cells
DEPC	Diethylpyrocarbonate
DMSO	Dimethylsulfoxide
DNA	Deoxyribonucleic acid
dNKs	Decidual natural killer cells
dNTP	Deoxyribonucleoside triphosphate
D-PBS	Dulbecco's phosphate-buffered saline
E	Embryonic / gestational day
EDTA	Ethylenediaminetetraacetic acid
ELISA	Enzyme-linked immuno-sorbent assay
EMA	European Medicines Agency
EU	European Union
FACS	Fluorescence-activated cell sorting
FBS	Fetal bovine serum
GMP	Granulocytic macrophage progenitor
Grb10	Growth factor bound protein 10
HA	Hemagglutinin

HCl	Hydrochloric acid
HE	Hematoxylin-Eosin (staining)
HPAIV	Highly pathogenic influenza A virus
HSC	Hematopoietic stem cell
IAV	Influenza A virus
IBV	Influenza B virus
ICV	Influenza C virus
Igf2	Insulin-like growth factor 2
IIV	Inactivated influenza vaccine
KCl	Potassium chloride
LAIV	Live-attenuated influenza vaccine
LH/CG	Luteinizing hormone/chorionic gonadotropin
LPAIV	Low pathogenic influenza A virus
LPS	Lipopolysaccharide
M1	Matrix protein 1
M2	Matrix protein 2
MDCK	Mardin-Darby Canine Kidney (cell line)
MEM	Minimum essential medium
MEP	Megakaryocyte-erythroid progenitor
MIA	Maternal immune activation
MOI	Multiplicity of infection
MRSA	Methicillin-resistant <i>Staphylococcus aureus</i>
MS	Mannitol salt phenol red (agar plates)
NA	Neuraminidase
NaCl	Sodium chloride
NAI	Neuraminidase inhibitors
NaOH	Sodium hydroxide
NB	Glycoprotein NB
NEP	Nuclear export protein (also NS2)
NS2	Non-structural protein 2 (also NEP)
OD	Optical density
P/S	Penicillin & Streptomycin

Abbreviations

PA	Polymerase acidic protein
PB1	Polymerase basic protein 1
PB2	Polymerase basic protein 2
PBS	Phosphate-buffered saline
PCR	Polymerase chain reaction
PFU	Plaque forming units
Poly(I:C)	Polyinosinic:polycytidylic acid
RBC	Red blood cell
RIV	Recombinant influenza vaccine
RNA	Ribonucleic acid
RNP	Ribonucleoprotein complex
RT	Room temperature
RT-qPCR	Real-time quantitative PCR
SGA	Small for gestational age
Slc	Solute carrier (protein family)
SPF	Specified pathogen free
TLR	Toll-like receptor
TPCK	Tosyl phenylalanyl chloromethyl ketone
TSB	Tryptic soy broth
UKE	University Medical Centre Hamburg-Eppendorf

1. Zusammenfassung

Influenza stellt eine bedeutende Bedrohung für die menschliche Gesundheit dar. Saisonale Epidemien sind jedes Jahr verantwortlich für bis zu fünf Millionen schwere Erkrankungen. Aktuelle Studien modellieren, dass jedes Jahr bis zu 650.000 Menschen an Influenza sterben, davon bis zu 72.000 in Europa. Obgleich eine Influenza A Virus-Infektion bei gesunden Menschen häufig nur mit milden bis mäßigen Symptomen einhergeht, können vor allem schwangere Frauen schwere Komplikationen entwickeln. Dies ist von besonderer Bedeutung, da eine mütterliche Influenza auch einen schädigenden Effekt auf die kindliche Entwicklung haben kann – mit unkalkulierbaren Folgen für das Kind.

Mittels eines neu etablierten „*two hit*“ Mausmodells wird in dieser Studie der Einfluss einer mütterlichen Influenza A Virus Infektion (*first hit*) auf die Immunität der Nachkommen gegen eine respiratorische Infektion (*second hit*) im späteren Leben untersucht. Ein wichtiger Aspekt dieser Arbeit ist der direkte Vergleich zwischen Influenza A Virus (IAV)-bedingte maternaler Immunaktivierung (MIA) und artifizieller MIA durch das Immunstimulanz Poly(I:C).

In dieser Studie konnte gezeigt werden, dass MIA in Mäusen generell zu Nachkommen mit einem stark verminderten Geburtsgewicht führt. In diesen Nachkommen wurden darüber hinaus Frequenzabberationen der hämatopoetischen Stammzellen beobachtet, die mit einer veränderten Immunzellfrequenz in Milz und Lunge einhergehen. Infektionsexperimente der Nachkommen zeigen, dass nur die Nachkommen, die von IAV infizierten Müttern geboren wurden, eine erhöhte Anfälligkeit gegenüber respiratorischen Infektionen aufweisen. Weitere Experimente bestätigen, dass funktionell beeinträchtigte alveolare Makrophagen eine wichtige Rolle bei dieser erhöhten Anfälligkeit spielen könnten.

Diese Ergebnisse zeigen, dass eine mütterliche Influenza einen nachhaltigen Einfluss auf die Nachkommen haben und so deren Anfälligkeit gegenüber Infektionen im späteren Leben erhöhen kann. Diese Erkenntnisse stärken die Empfehlung mütterlicher Influenza-Impfungen und ebnen gleichzeitig den Weg detaillierter Studien in Bezug auf die Immunontogenese der Nachkommen im Kontext mütterlicher Infektionen.

2. Abstract

Influenza is a major health concern worldwide. Seasonal epidemics cause up to five million severe cases with substantial mortality every year. Recent studies model that worldwide up to 650,000 people die of influenza-associated disease and that up to 72,000 of these deaths occur in Europe. Although most individuals with influenza will experience mild to moderate disease, pregnant women are at increased risk to develop severe complications. Importantly, maternal influenza might also be harmful to the unborn child with unforeseeable consequences for offspring's health; yet insights into the underlying mechanisms of maternal infection and potential long-term health deficits remain unclear.

Using a novel „two-hit” murine model, the impact of maternal influenza A virus infection (first hit) on offspring's vulnerability to respiratory infection (second hit) in later life was assessed. An important aspect of this work is the direct comparison of influenza A virus-induced maternal immune activation (MIA) and artificially induced MIA by poly(I:C).

In this study it was shown that early gestational influenza- as well as poly(I:C)-induced MIA leads to very low birth weight fetuses. Offspring born to MIA mice exhibit dysregulated hematopoietic stem cell frequencies with subsequently affected immune cell frequencies in spleen and lung. Importantly, challenge studies with this offspring revealed that only mice born to IAV-infected mothers were more vulnerable towards respiratory infection. Subsequent experiments confirmed that functionally impaired alveolar macrophages might be a key contributor towards increased vulnerability in affected offspring.

These findings show that maternal influenza may have long-term postnatal effects on offspring, increasing the vulnerability to infections in later life. These results do not only strengthen the evidence base favoring widespread adoption of influenza vaccination in pregnancy but also allow more precise future research in regards of maternal influenza-related immune ontogeny of the offspring.

3. Introduction

3.1. Influenza

Influenza is a major health concern worldwide. Seasonal epidemics cause up to five million severe cases with substantial mortality every year. Recent studies model that worldwide up to 650.000 people die of influenza-associated disease and that up to 72.000 of these deaths occur in Europe.¹ Influenza is one of the most important respiratory illnesses exhibiting a strong seasonal pattern with peak activity during the winter². Human influenza is caused by the influenza viruses of type A (IAV), B (IBV) and to a small account influenza C (ICV)^{3,4}.

3.2. The influenza virus

3.2.1. Taxonomy

Influenza viruses belong to the *Orthomyxoviridae* family of single-stranded RNA viruses⁵. Influenza A viruses are classified into subtypes, based on their major surface proteins hemagglutinin (HA) and neuraminidase (NA) whereas influenza B viruses are classified into the two major lineages B/Yamagata and B/Victoria^{4,5}.

So far, 18 HA and 11 NA subtypes have been described. Whereas all HA and NA subtypes, except for H17N10 and H18N11, can affect aquatic waterfowl, H1N1 and H3N2 are the major subtypes affecting the human population.^{6,7} H17N10 and H18N11 influenza viruses were just recently found in bats and represent new subtypes that are evolutionarily distinct from all other circulating strains⁸.

The influenza virus nomenclature is standardized and consists of the species of isolation (non-human only), location of isolation, isolate number, year and HA and NA subtype (IAV only)⁹. One example would be A/Hamburg/NY1580/09 H1N1.

3.2.2. Virion structure

By electron microscopy, influenza A and B viruses show spherical or filamentous shapes with a diameter of 100 nm or a length of up to 300 nm, respectively (Figure 1)¹⁰. The virion lipid envelope carries the two major surface glycoproteins HA and NA in a 1:4 ratio as well as a smaller number of matrix ion channels (M2) pervading the lipid membrane^{11,12}. The viral core is enclosed by a matrix of M1 proteins and inside the core, the nuclear export protein (NEP or NS2) and the ribonucleoprotein complexes (RNP) can be found. The RNPs consist of the viral RNA segments and the heterotrimeric RNA-dependent RNA polymerase that is composed of the polymerase subunits PB1, PB2 and PA.⁹ The influenza B virion structure is similar while carrying the surface proteins NB and BM2 instead of M2. Influenza C viruses only carry one surface proteins that corresponds to HA and NA, functionally.¹¹

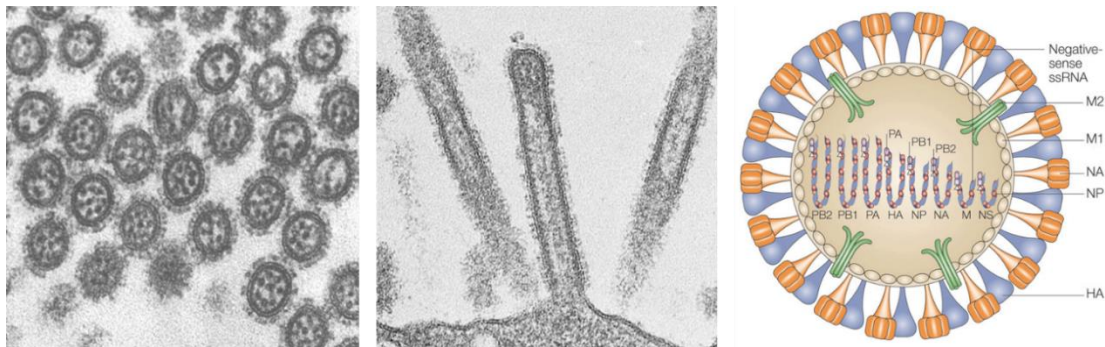


Figure 1: Influenza A virion morphology and structure. The influenza A virion has a spherical (left, adapted from ¹³) or filamentous (middle, adapted from ¹³) phenotype with a diameter of 100 nm or a length of up to 300 nm. The lipid envelope with the two major surface glycoproteins HA and NA contains a smaller number of matrix ion channels (M2) spanning the lipid membrane. Inside the viral core of M1 proteins the nuclear export protein (NEP or NS2) and the ribonucleoprotein complexes (RNP) can be found. The RNPs consist of the viral RNA segments and the heterotrimeric RNA-dependent RNA polymerase that is composed of the polymerase subunits PB1, PB2 and PA (right, adapted from ¹⁴).

3.3. Virus ecology

Aquatic wild birds are considered the main reservoir for influenza A viruses and except for bat-origin influenza viruses (H17N10, H18N11), all IAV subtypes have been initially isolated from avian hosts^{7,15–17}.

Generally IAV do only cause no or minimal signs of disease in wild birds and such viruses are called low pathogenic influenza A viruses (LPIAV) but in the last decades also highly pathogenic influenza A viruses (HPIAV) have been observed^{18,19}.

Occasionally, IAV can cross the species barrier and transmit from wild birds into a broad variety of other vertebrate hosts including domestic animals like poultry or swine from where it can quickly spread into the human population (Figure 2)^{20,21}. After transmission into a new host, adaptive mutations of the virus may increase replicative fitness. Furthermore interspecies transmission and coinfection of different IAV might even lead to the emergence of new IAV subtypes (see 3.4)^{15,22,23}.

For successful interspecies transmission, many molecular determinants were described²⁴. With the cellular plasma membrane being the first barrier that needs to be overcome by the virus, glycoconjugates containing S-acetylneuraminic (sialic acid) residues were identified as the primary receptor for the viral HA²⁵. While avian-adapted IAV use α 2,3-linked sialic acids, mammalian-adapted IAV use α 2,6-linked sialic acids²⁶. Importantly, both sialic acid isoforms are present in the human respiratory tract; although α 2,6-linked sialic acids are more prevalent in the upper respiratory tract, while α 2,3-linked sialic acids are mainly expressed in the lower respiratory tract²⁷. This might explain the fact, that humans can be infected with bird-adapted influenza A viruses, although efficiency of transmission is strongly reduced²⁸.

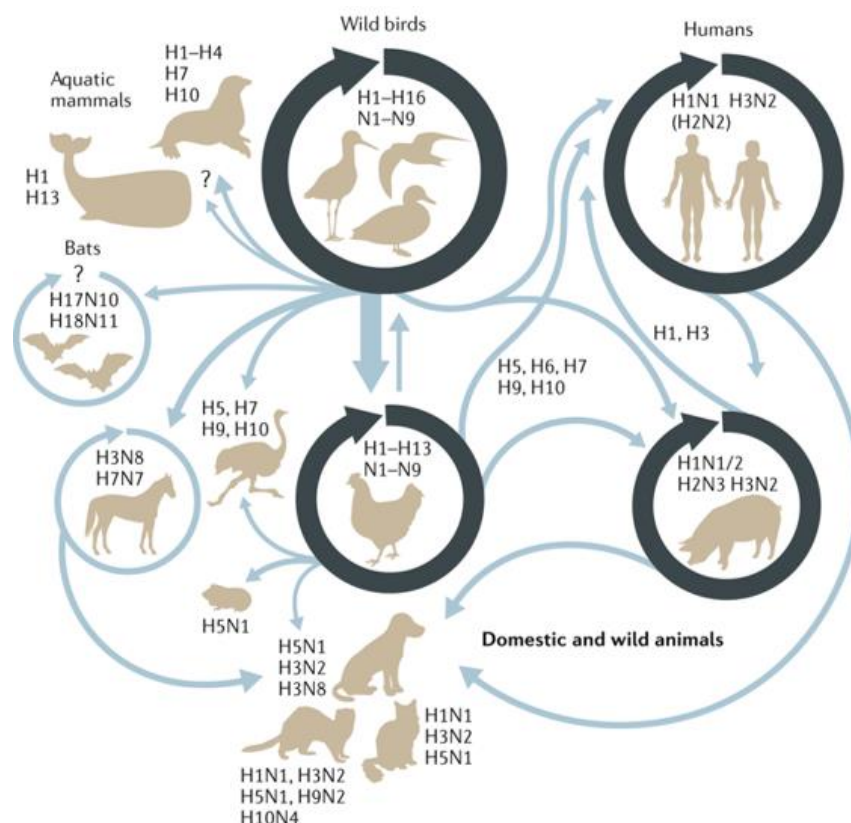


Figure 2: Interspecies transmission and hosts of IAV. Aquatic wild birds are considered the main host for IAV. Except for bat-origin influenza viruses (H17N10, H18N11), all IAV subtypes have been initially isolated from avian hosts. Many IAV subtypes can cross into a broad variety of vertebrate hosts but mainly H1N1 and H3N2 subtypes are responsible for human infection. Adapted from ²⁹.

3.4. Virus drift and shift

Lack of proofreading function of the viral RNA-dependent RNA polymerase is causative for the genetic instability of the virus and the emergence of drift mutants. Although most of these mutants are not replication competent, this mechanism constantly gives rise to new viruses with unique and immunogenically unknown antigens, especially HA and NA. This effect is called antigenic drift and is the main reason for the need of annually reformulated vaccines.^{30,31}

In addition, coinfection of a mammalian cell with different influenza A virus subtypes might lead to the reassortment of RNA segments between these viruses and subsequent formation of new influenza A virus subtypes²³. Reassortment is possible because of the segmented nature of the viral genome and occurs when at least two distinct strains co-infect one cell³². Swine are of special importance to this process, because they are susceptible to infection with

viruses adapted to humans and birds and thus allow for reassortment of these viruses³². Their broad susceptibility to bird- and human-adapted influenza A viruses results at least in part from the presence of both α 2,6- and α 2,3-linked sialic acid receptors on the epithelia of their upper respiratory tract³³. The fact that influenza viruses that normally circulate in three distinct species can meet within pigs led to their labeling as a “mixing vessel”, ideal for the genesis of novel reassortants with high pandemic potential^{34,35}.

Importantly, viruses that arise from this process called antigenic shift, might display antigenic features against which the human population might be mostly naïve. Thus, antigenic shift is the main driver of pandemic outbreaks and the sustained introduction of new influenza A viruses into the human population.²²

3.5. Influenza pandemics

Although it is likely that pandemics already occurred before, only after the begin of modern virology, influenza pandemics were recorded and thoroughly investigated. Four worldwide pandemics raised since the early 20th century: in 1918, 1957, 1968 and - most recently - in 2009 (Figure 3)^{14,23,36}. The largest pandemic so far happened in 1918 and the H1N1 virus infected one third of the world’s population causing approximately 50 million deaths^{37,38}. In 1957 an H2N2 virus caused the so called ‘Asian flu’ which affected up to 50% of the world’s population and caused more than 1 million deaths¹⁴. The third pandemic started in 1968 with an H3N2 virus and comparable morbidity and mortality to Asian flu. The last pandemic happened in 2009 as a result of genetic reassortment of three different viruses in pigs³⁹. The 2009 pandemic H1N1 (pH1N1) IAV quickly became the most predominant influenza virus strain worldwide and caused about 500.000 deaths within the first 12 months of circulation⁴⁰. Viruses introduced into the human population continue to adapt due to drift mutations and remain circulating in the human population as shown in Figure 3^{23,41}.

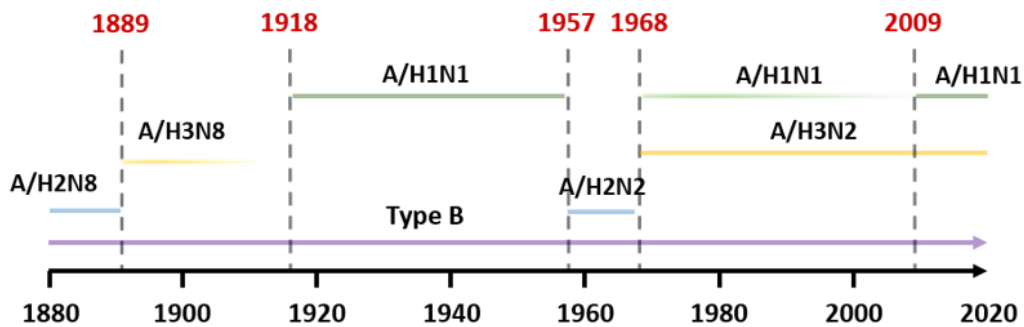


Figure 3: Influenza A virus pandemics. Four worldwide pandemics occurred since the early 20th century: in 1918, 1957, 1968 and in 2009. Viruses introduced into the human population continue to adapt due to drift mutations and remain circulating in the human population.

3.6. Preventive and curative strategies

3.6.1. Vaccines

Arguably, for prevention and control of influenza the best method is vaccination, as it is safe, reduces illness and is well suitable for groups at risk for complications^{42–45}. Currently, three categories of vaccines are approved by national administrations: the most common detergent-split inactivated influenza vaccines (IIV), recombinant influenza vaccines (RIV) and live attenuated influenza vaccines (LAIV). IIVs are composed of three (trivalent) or four (tetraivalent) candidate vaccine viruses (CVV) including one H1N1, one H3N2 and one or two influenza B viruses from the Victoria and/or Yamagata lineage. These vaccines are either produced in eggs or in eukaryotic cell lines, inactivated, purified and detergent split. The antigen is mainly composed of the viral HA protein.^{46,47} RIV are solely composed of HA proteins from the annual CVVs and these proteins are exclusively produced in insect cells⁴⁸. Like IIV, LAIV are also composed of three or four CVVs. Importantly these viruses have been engineered to show limited replication in the upper respiratory tract by only growing at or below 33 °C^{49,50}. Because they contain attenuated live viruses, LAIV elicit the most robust immune response but are usually not recommend for use in high risk groups^{51,52}. Although vaccination is considered safe and efficient, recommendations and vaccine compliance differ internationally. Coverage rates within the European Union (EU) for important risk groups vary between 2 to 73% for the elderly population, 16 to 57 % for individuals with chronic medical conditions and 1 to 59% for pregnant women (2016-17).⁵³

Importantly, genetic drift of circulating influenza viruses requires annual updates of the vaccines to keep up with viral evolution. This effect is reinforced by the fact that most available vaccines are directed against the HA antigen that is subject to high rates of drift mutations. Thus, recent research is about to address more universal and long-lasting influenza vaccine candidates by targeting more conserved epitopes like the HA stalk or internal proteins^{47,54,55}. Because vaccine composition needs to be estimated in advance of the upcoming season, annual strain mismatches lead to an overall vaccine efficacy that rarely exceeds 50%⁵⁶⁻⁵⁸.

3.6.2. Antiviral treatment

Treatment of severe influenza presents multiple challenges and for successful treatment it is highly important that antiviral medication is initiated as soon as possible after illness onset⁵⁹. Currently available European Medicines Agency (EMA) approved antiviral medications include neuraminidase inhibitors (NAI) and M2 inhibitors (

Table 1). Notably, M2 inhibitors are not active against influenza B strains and there is widespread resistance among current H1N1 and H3N2 influenza A strains⁶⁰. Also NAI resistant viruses emerge quickly and controlling e.g. Tamiflu resistance has become a major public health issue⁶¹.

In the last years, several antivirals targeting the viral polymerase complex have been identified and are in clinical testing. Currently, three antivirals (favipiravir, pimodivir and baloxavir) targeting different polymerase subunits (PB1, PB2 and PA, respectively) have been found to be inhibitory for Influenza A viruses, including those resistant to NAIs. Favipiravir and baloxavir were also found to inhibit influenza B viruses. Importantly, monotherapy of pimodivir and baloxavir are associated with high frequencies of emergence of escape variants, that can be reduced by combination therapy and synergistic interactions with NAIs. Thus, current clinical studies focus on combination therapies using e.g. oseltamivir and polymerase inhibitors.⁶²

Currently approved antiviral treatment is recommended and considered safe for individuals from all risk groups except very young children⁶³.

Table 1: EMA approved antiviral medications. Currently available EMA approved antiviral medications including neuraminidase inhibitors and M2 inhibitors, 2018.⁶⁰

Neuraminidase inhibitors	
Tamiflu (oseltamivir)	EMA authorized in all EU member states
Alpivab (peramivir)	EMA authorized in all EU member states
Relenza (zanamivir)	Authorized at national level in all EU member states
M2 inhibitors	
Amantadine	Authorized at national level in all EU member states
Rimantadine	Authorized at national level in all EU member states

3.7. Risk groups for influenza

Most individuals with influenza will experience mild to moderate disease that is cleared within one or two weeks⁶⁴. However, there are groups that have an increased risk of transmission and/or developing severe disease. Risk groups are commonly assessed by national and international authorities based on clinical correlation and their evaluation slightly differs between countries. Nevertheless, the following risk groups are described by all major health authorities.^{65–69}

3.7.1. The elderly (≥ 65 years of age)

It is well known that people with 65 years and older are at increased risk of developing serious complications from influenza, compared to young and healthy adults^{70–72}. This is, in part, due to increasing immune senescence of the host and decreasing efficacy of vaccines^{72–74}. Age-related changes in immune function cover a broad variety of mechanisms and are a continuous subject of research. Well known changes are delayed lymphocyte proliferation, decreased cytotoxic T-cell activity, increased memory T cell response and altered cytokine expression patterns⁷⁵. But also a lower antioxidant status and higher levels of reactive oxygen

species were proposed to correlate to increased vulnerability towards Influenza A virus infection⁷⁶. Recent studies highlight the importance of hormonal changes in the elderly and they provide strong evidence that sex hormones as well as metabolic hormones play a crucial role in increased vulnerability towards infections^{77,78}. Especially elevated progesterone levels in males and elevated testosterone levels in females were correlated to increased mortality⁷⁷. It is estimated that about 70 – 80% of influenza-related deaths occur in this risk group⁷².

3.7.2. Individuals with chronic medical conditions

Underlying medical conditions such as immunosuppression, metabolic disease, cardiac disease or disease that affects the lung are important risk factors for severe influenza-related complications^{79–81}. During the 2009 pandemic an average of 40% and up to 78% of hospitalized patients had underlying medical conditions^{79,80}. The most reported conditions were pregnancy, asthma, obesity, chronic obstructive pulmonary disease (COPD), neurologic, and cardiac disease⁸². Reported co-morbidity was associated to complications like viral or bacterial pneumonia, and acute respiratory distress syndrome (ARDS)^{81,83}. Additionally, the risk of admission to an intensive care unit (ICU) were found to be increased in patients with at least one underlying medical condition⁸⁴. Findings from the 2009 pandemic provide evidence that the impact of co-morbidities might be also influenced by age, as for example neurologic conditions were found to be more common in ICU-admitted children, while asthma and obesity were prominent in both children and adult patients^{84,85}. The Center for Disease Control and Prevention (CDC) lists all conditions that are known to increase the risk of getting serious complications⁶⁸.

3.7.3. Infants and young children (< 5 years of age)

Many studies have shown that infants and young children present higher influenza incidence and attack rates compared to adults^{82,86–90}. A recent meta-analysis estimated that 90 million children aged <5 years are affected by influenza every year⁹¹. Importantly, infants below the age of 5 years are significantly more likely to develop clinical influenza⁹². Within this group,

infants below the age of six months are at highest risk of severe complications⁹³. During and after the 2009 pandemic infants and young children had the highest rate of hospitalization and death⁹³⁻⁹⁵. Current studies estimate that annually up to 100.000 infants die because of influenza and noteworthy, 99% of all influenza-related deaths in children seem to occur in developing countries⁹¹. Although especially infants below the age of six months are at increased risk of complication, options for antiviral treatment and prevention are limited. Most antivirals as well as vaccination are not approved for use in these children^{90,96}. Thus maternal vaccination is the most effective measurement to protect infants during their first months of life⁹³.

3.7.4. Pregnant women

Influenza is more likely to cause severe illness in pregnant women compared to the general population⁹⁷. Diverse and striking changes of the maternal physiology and the immune system make pregnant women more vulnerable towards influenza-related complications⁹⁸⁻¹⁰⁰. Importantly maternal flu might also be harmful to the unborn child¹⁰¹⁻¹⁰³. Pregnant women show an increased risk for severe morbidity, mortality, need for cesarean section and stillbirth^{98,101,102,104}. Since the focus of this study is on the interplay of influenza virus infection and pregnancy, this topic will be described in more detail on the following pages.

3.8. Immunology during pregnancy

Allogeneic pregnancy creates a unique immunological situation. The placenta, which is in direct contact to the maternal immune system, expresses antigens derived from the father. To tolerate these foreign antigens, the maternal immune system needs to mount many processes of immunological adaptation. In healthy pregnancies these adaptations suppress rejection of the fetus¹⁰⁵. These processes include the restriction of T cell migration to the feto-maternal interface due to epigenetic silencing mechanisms¹⁰⁶. Decidual dendritic cells (dDCs) are arrested in a tolerogenic state, reflected by a reduced expression of costimulatory surface markers^{107,108}. Also the generation of CD4⁺ and CD8⁺ regulatory T cells (Treg) as well as a special subset of decidual natural killer cells (dNKs) plays an important role in sustaining tolerance towards the fetus^{105,109,110}. Further B cell modification and adaptation was described to promote fetal tolerance¹¹¹. These changes collectively orchestrate an anti-inflammatory and tolerogenic environment that allows placental development and suppresses fetal rejection. Importantly, these mechanisms also go in line with a reduced secretion of type I interferons and inflammatory cytokines as well as a reduced ability for antigen presentation during pregnancy. This state of adapted immunity subsequently leads to an increased vulnerability towards infections that can ultimately create a contradictory need of maintaining fetal tolerance versus mounting an anti-inflammatory immune response.¹⁰⁰ Many challenges can interfere with this feto-maternal immune cross-talk and have a severe impact on maternal health, pregnancy outcome and offspring's development¹⁰⁵. Figure 4 depicts the contradictory demands for the immune system to adapt to pregnancy and to mount an immune response towards maternal infection with the influenza virus.

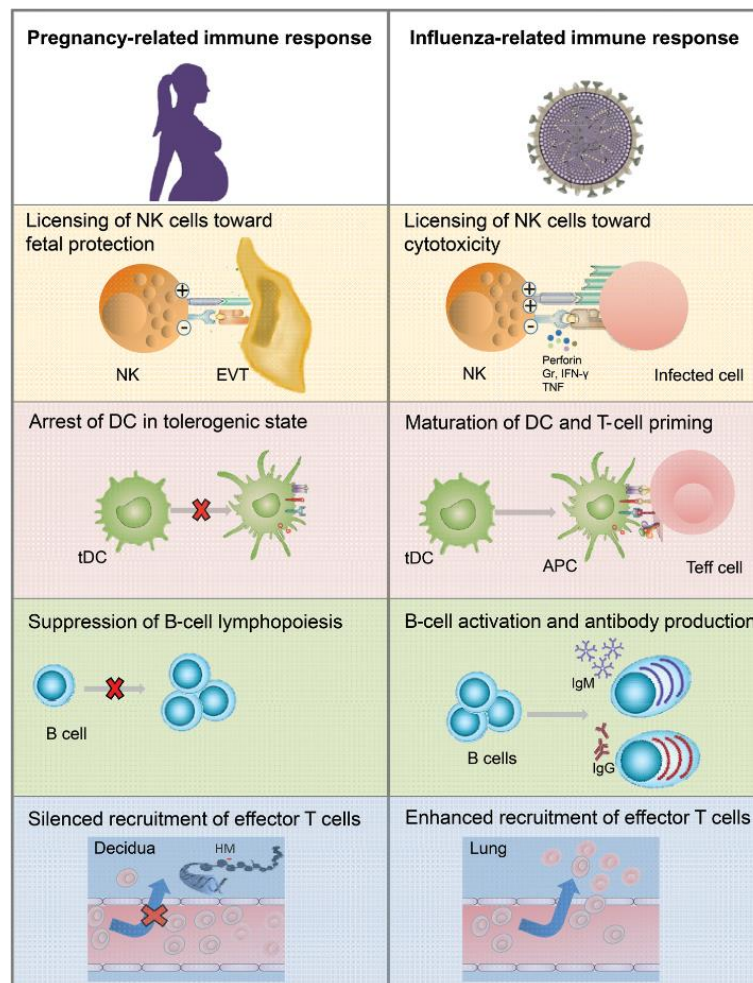


Figure 4: Contradictory demands for the immune system to adapt to pregnancy and to mount an immune response towards maternal infection with the influenza virus¹¹². Left: Pregnancy-related mechanisms of immune adaptation are needed to allow immune tolerance towards the allogenic fetus. Licensing of NK cells towards dNK cells by extravillous trophoblast cells. Arrest of decidual DCs in tolerogenic state by suppression of stimulatory surface markers. Reduction of B cell proliferation by estrogen-mediated suppression of B cell lymphopoiesis¹¹³. Epigenetically silenced recruitment of effector T cells in the decidua¹⁰⁶. Right: Activation of the innate immune system by influenza virus infection. Antigen-mediated activation of NK cells towards a cytotoxic state. Activation of the adaptive immune system by antigen presenting cells. Antigen carrying DCs interact with T cells and induce DC maturation and T effector cell priming. Recruitment of effector T cells to infected tissue by chemokine receptor ligands.¹¹²

3.9. Maternal immune activation and offspring's health

Importantly, maternal influenza might also be harmful to the unborn child with unforeseeable consequences for offspring's health. It is well known that maternal immune activation (MIA) defined by elevated pro-inflammatory cytokine responses (e.g. IL-6, IL-17A) that might be induced by external stressors of various etiology, is a major contributor to

neurodevelopmental disorders in the offspring^{114–116}. Many factors involved in fetal brain development operate during prenatal stages of life, a window of critical vulnerability during central nervous system (CNS) development¹¹⁷. Epidemiological studies implicate an increased risk for schizophrenia or autism-like disorders (ALD) in offspring born to prenatally infected mothers^{118,119}. Although many studies were performed on the role of MIA on neurodevelopmental disorders in the offspring, the underlying mechanisms remain yet mostly elusive. Increased levels of the pro-inflammatory cytokines IL-6 and TNF- α were determined as risk factors for altered fetal brain development¹⁰³. Also, maternal stress hormones or glucocorticoids entering the fetal circulation were described to affect hippocampal ontogeny^{120,121}. Nevertheless, the lack of proper animal models and conclusive clinical data did not yet allow for consequent studies of the complex interactions within this multidimensional process.

Besides, there is increasing knowledge that this phenomenon is likely not restricted to neurodevelopmental disease. Maternal infection and vaccination were reported to also affect the offspring's immune system in various ways¹²². The association of in utero environmental stress and disease outcome in later life is thought to be related to so-called fetal programming.

Recent studies strengthen the hypothesis, that maternal infection may “prime” the developing immune system by mechanisms that go beyond the sole transfer of maternal antigens¹²³. In utero exposure to maternal inflammatory markers, such as cytokines and chemokines has been reported to affect fetal immune cell activation. MIA seems to increase the concentration of proinflammatory cytokines such as IL 2, IL-6 and TNF α and to delay the development of innate immunity in the offspring^{124,125}. There is also evidence that the maturation of the adaptive immune system might be influenced by the preferential development of Th17 cells in MIA offspring¹²⁶.

Not only in utero priming, but also epigenetic modifications may contribute to fetal programming. Many stressors were described to affect fetal programming by epigenetic means¹²⁷. Best studied are nutritional factors, that were clearly linked to metabolic disease and cancer in the offspring¹²⁸. But also, high corticosterone exposure, steroid hormones or fetal hypoxia seem to disturb fetal epigenetic development resulting in later life disease¹²⁷. Importantly, also MIA was linked to adverse epigenetic programming, but a detailed

understanding of maternal infections and fetal epigenetics remains elusive and proper models are missing ¹²⁹.

In general, MIA-related effects on the offspring's immune system are commonly described by a disturbed cytokine balance or dysregulated frequencies of immune cells and conclusive mechanistical insights or functional studies on the offspring's immune system remain missing.

Additionally, most work on the impact of MIA on offspring's immunity has been done using animal - especially rodent - models. Several important limitations of these studies might explain a high degree of contradictory findings as well as limited translational value to clinical findings. Thus, current animal models used in MIA research will be described in the following sections.

3.10. Animal models to study maternal immune activation

Animal models of MIA are widely used as experimental tools to study immune-mediated or neurodevelopmental disorders in the offspring¹³⁰. Originally developed to support epidemiological implications of MIA mediated neuropsychiatric illnesses in the offspring, these models had a significant impact on research focused on the developmental and neuroimmunological origin of these diseases^{131,132}. Most animal models utilize artificial immune activators like polyriboinosinic-polyribocytidilic acid (poly(I:C)) or lipopolysaccharide (LPS) to induce MIA. The increasing importance of these studies is clearly reflected by the consequent increase of studies using for example poly(I:C) in the context of MIA research (Figure 5)¹³³.

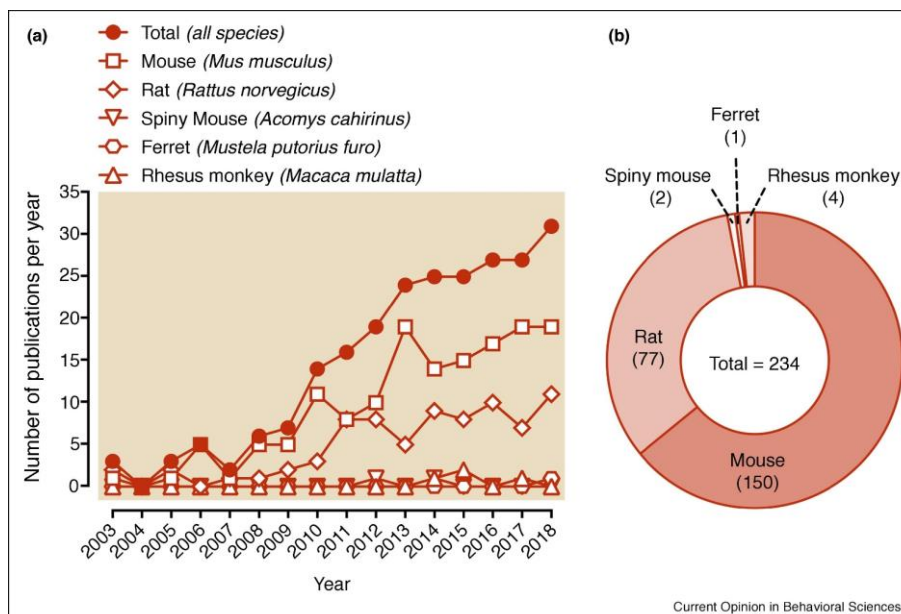


Figure 5: Number of studies using a poly(I:C) based model of MIA from 2003 to 2018. (a) Number of published articles per year and species. (b) total number of publications per species.¹³³

The use of different and inconsistent MIA models goes in line with many possible reasons for variability, subsequently limiting translational value and reproducibility. Important factors might be the chosen species, the type of immunogen that is used as well as dosing and route of administration. The vast majority of MIA studies are performed in rodents like mice and rats¹³³.

Recent epidemiological findings additionally revealed the importance of gestational timing and MIA indication. Yet, most MIA studies were performed in mid or late gestation models and little is available about MIA during early fetal development^{117,133}. Although sex and age of the offspring was reported to be another important factor responsible for variable outcome, especially sex-specific effects were neglected for a long time in animal models^{134,135}. Many more sources of variability were proposed and consistent approaches to address mechanistic questions remain missing¹³³.

Finally, it needs to be highlighted that almost all work on MIA in animal models, irrespective of the immunogen, was carried out in syngeneically mated mice, which limits the translational relevance for human pathologies as it was shown that syngeneically mated mice do not mount the same immunological adaptation during pregnancy as allogeneic pregnant mice do¹⁰⁰.

3.10.1. Artificial models of maternal immune activation

The most common models to study MIA are based on treatment of the pregnant animal with immunogenic substances like the bacterial endotoxin LPS or with poly(I:C). LPS is a cell wall component of gram-negative bacteria binding to Toll-Like Receptor (TLR) 2 and 4 while poly(I:C) is a synthetically produced double stranded RNA analog (dsRNA) binding to TLR 3^{136,137}. Both reagents are potent activators of the mammalian immune system and LPS- as well as poly(I:C)-based approaches have been linked to MIA-related adverse outcomes in several studies¹³⁸. MIA models using artificial immunogens possess specific advantages and disadvantages and the suitability of these approaches strongly depends on the research question that is addressed. Importantly, the induction of MIA by poly(I:C) application leads to sickness-like-behavior in the animal with profound symptoms and immune activation that is however restricted to a period of 24 – 48 hours¹³⁹. This allows for a precise timing of the immunogenetic impact and indeed studies utilizing poly(I:C) induced MIA were decisive for the elucidation of distinct windows of vulnerability during pregnancy^{116,140}. Additionally, the use of artificial immunogens allows for a well-controlled immune stimulation and subsequent studies on dose-dependency^{141,142}. On the other side, a major drawback of these immunogens is the limited set of immune responses elicited^{136–139} whereas viral infections, such as influenza, do not only lead to a more broad immune activation but also activate the innate as well as the adaptive immune system.

3.10.2. Maternal immune activation models using IAV

Although less commonly used in animal models, influenza based MIA studies are of increasing importance, especially addressing its role in neuropsychiatric disease in the offspring^{138,143–145}. Animal models using influenza virus-induced MIA are relatively rare but have been of significant importance to understand the immune adaptation during pregnancy as well as immune activation to influenza virus infection^{146–148}. However, as described above a viral infection can cause mild to severe illness in pregnant mice in a dose-dependent manner and the state of immune activation covers a period of up to two weeks. So, influenza virus

infections do not reflect a precisely timed immunogenetic impact. Indeed, it presents a long-lasting state of MIA that underlies a high degree of variability.

Noteworthy, most studies performed in mice introduce the influenza virus during mid or late gestation^{100,146,147} limiting translational value, because data from human studies show that primarily early gestational stress is responsible for long-term health deficiencies in the offspring¹⁴⁹.

With very few exceptions, MIA studies utilizing influenza viruses are restricted to the use of influenza A viruses of the subtype H1N1. This needs to be considered, since also other influenza A virus subtypes as well as influenza B viruses are of clinical relevance for pregnant women. Indeed, one study found that also influenza B virus infection during pregnancy go in line with severe outcomes in a murine model, but conclusive and clearly comparative studies using different influenza viruses remain missing¹⁵⁰.

4. Aim

The aim of this study is to establish a “two hit” model to study the impact of maternal influenza A virus infection on offspring’s immunity to later life infections. A comparative approach using poly(I:C)-induced, artificial MIA and IAV-induced MIA upon early gestation is used to decipher pathogen-related effects on offspring’s immunity.

While most current animal models of maternal immune activation or maternal influenza utilize syngeneic breeding and late-gestational MIA, this study aims to provide a MIA model that is clinically more relevant. Allogeneic breeding is used as it is necessary to reflect pregnancy-related immunological adaptations that are crucial to study maternal immune activation and its legacy for the offspring. Additionally, this work sets a focus on early gestational MIA as it has been shown that early gestation might be a window of highest vulnerability, but conclusive animal models remain missing.

Most studies on the impact of MIA on offspring’s health solely focus on neurodevelopmental disorders and although clinical findings implicate severe effects on offspring’s immunity, only little evidence is provided by mechanistical studies. Thus, in this study a “two hit” model is used to investigate the impact of maternal influenza A virus infection (first hit) on offspring’s vulnerability to later life infection (second hit) with Influenza B virus or *Staphylococcus aureus*.

5. Results

5.1. Influenza A virus mediated maternal immune activation

With beginning of this study, there was no allogeneic mouse model for early gestational influenza A virus infection available. Although epidemiological findings highlight that early gestation is the most vulnerable window for MIA associated effects on fetal development, in most studies MIA is induced at or after gestational day 10, considered mid to late gestation^{100,149}. To overcome limitations of late gestational challenge models, first aim of this study was to establish a mouse model for influenza related maternal immune activation (MIA) during early, allogenic pregnancy. Additionally, we aimed to directly compare artificial MIA, induced by poly(I:C) to IAV-derived MIA. Whereas poly(I:C) is known to cause a strong, but only short lasting immune activation, we have previously shown, that infection with IAV during pregnancy leads to significant and long-lasting morbidity in pregnant mice^{100,139}. A direct comparison of both models will allow to link the outcome to more specific mechanisms and the overall character of allogeneic pregnancy and MIA. Furthermore, early gestational MIA will be subsequently utilized as a “first hit” to study potential immunological effects in the offspring.

Infection of BALB/c-mated allogeneic pregnant C57Bl/6 females at early gestation (gestational day 5.5, E5.5) with a dose of 10^3 plaque forming units (PFU) of the pH1N1 2009 influenza A virus (IAV) resulted in mild disease displayed by delayed weight gain during pregnancy compared to PBS-treated dams. In parallel, poly(I:C)-treated (4 mg/kg) dams showed weight loss that was restricted to day 1 post infection (d p.i.) compared to PBS-treated dams (Figure 6a). Higher dosage of poly(I:C) as mostly used in other studies (20 mg/kg) at E5.5 resulted in abortion of most pregnancies (Supplementary figure 1). Both, IAV-infection, and poly(I:C)-treatment were non-lethal (Figure 6b).

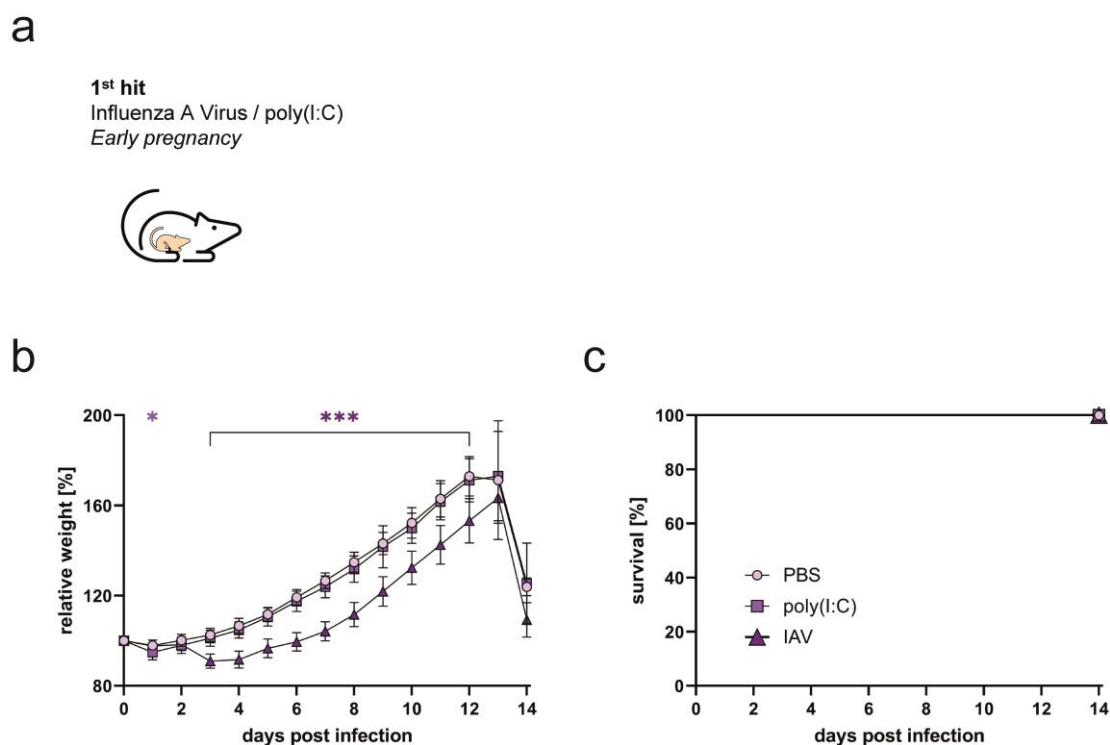


Figure 6. 1st hit: IAV-infection but not poly(I:C)-treatment during early gestation leads to mild and non-lethal disease. (a) The first hit was performed during early pregnancy by application of either poly(I:C) or infection with IAV. (b and c) Pregnant C57Bl/6 mice were treated with 4 mg/kg poly(I:C) (n = 24) or infected with 10^3 PFU of IAV (n = 24) on day 5.5 of gestation. PBS-treated dams were used as controls (n = 20). Weight development (b) and survival (c) were determined within 14 d p.i. The statistical significance for weight (b) was calculated by multiple unpaired t-test (two-tailed) with correction for multiple comparisons using the Bonferroni-Dunn method. Survival data (b) were analyzed using a log rank test for trend. Levels of statistical significance were defined as * $p < 0.05$, *** $p < .001$.

To confirm infection of the mice, viral replication was quantified by titration of lung homogenates and detection of the viral NP antigen by histology of lungs isolated on day 1, 3 and 6 post infection. Virus was detectable exclusively in lungs from IAV-infected dams (Figure 7a). Additionally, the relative lung weight of mice was increased in mice infected with IAV on day 6 post infection compared to lungs from PBS- or poly(IC)-treated mice, indicating strong infiltration to the tissue (Figure 7b). IAV nucleoprotein staining confirmed viral replication in lungs from infected dams whereas lungs from PBS and poly(I:C)-infected mice were negative for viral antigens (Figure 7c).

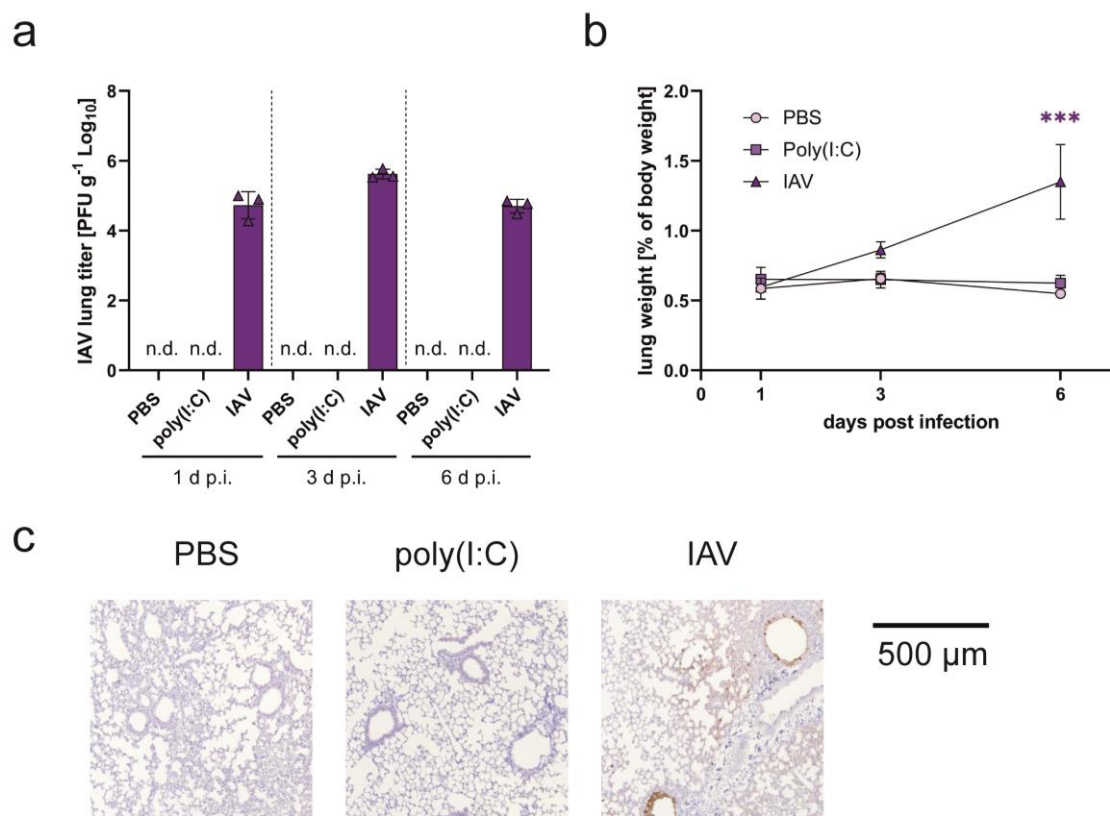


Figure 7. 1st hit: IAV-infection during early gestation leads to viral replication and inflammation of the lung. (a-b) Viral lung titers (a) and lung weight (b) at indicated days post early gestational treatment with PBS (n = 3), poly(I:C) (n = 6) or infection with IAV (n = 3). (c) Representative immunohistology of IAV NP antigen in maternal lungs at 3 days post infection, Scale bar = 500 μ m. Values (a,b) are shown as mean and error bars as SD. Significance was calculated using unpaired t-test (two-tailed) with Welch's correction (***) $p < .001$, n.d. = not detectable).

Next, major pro-inflammatory cytokines were assessed in maternal plasma and lung at 1, 3 and 6 days post infection. High elevations of the pro-inflammatory cytokines IL-6, TNF- α and MCP-1, that are linked to MIA^{115,138} were found in both maternal lung and plasma. Levels for IL-6, TNF- α and MCP-1 were significantly increased in lungs 6 days after infection with IAV compared to lungs from animals treated with PBS or poly(I:C) (Figure 8a-c). Plasma cytokine levels were generally lower. Animals treated with poly(I:C) presented higher levels of IL-6, TNF- α and MCP-1 on day 1 post treatment, whereas IAV-infected mice had increased plasma levels of IL-6 and TNF- α on day 6 post infection (Figure 8d-f). Data for IL-1 β , IL-2, IL-10 and IL-17A are shown in Supplementary figure 2.

Notably, only IAV infection caused an increase of inflammatory cytokines in the lung while application of poly(I:C) only affected plasma cytokine levels.

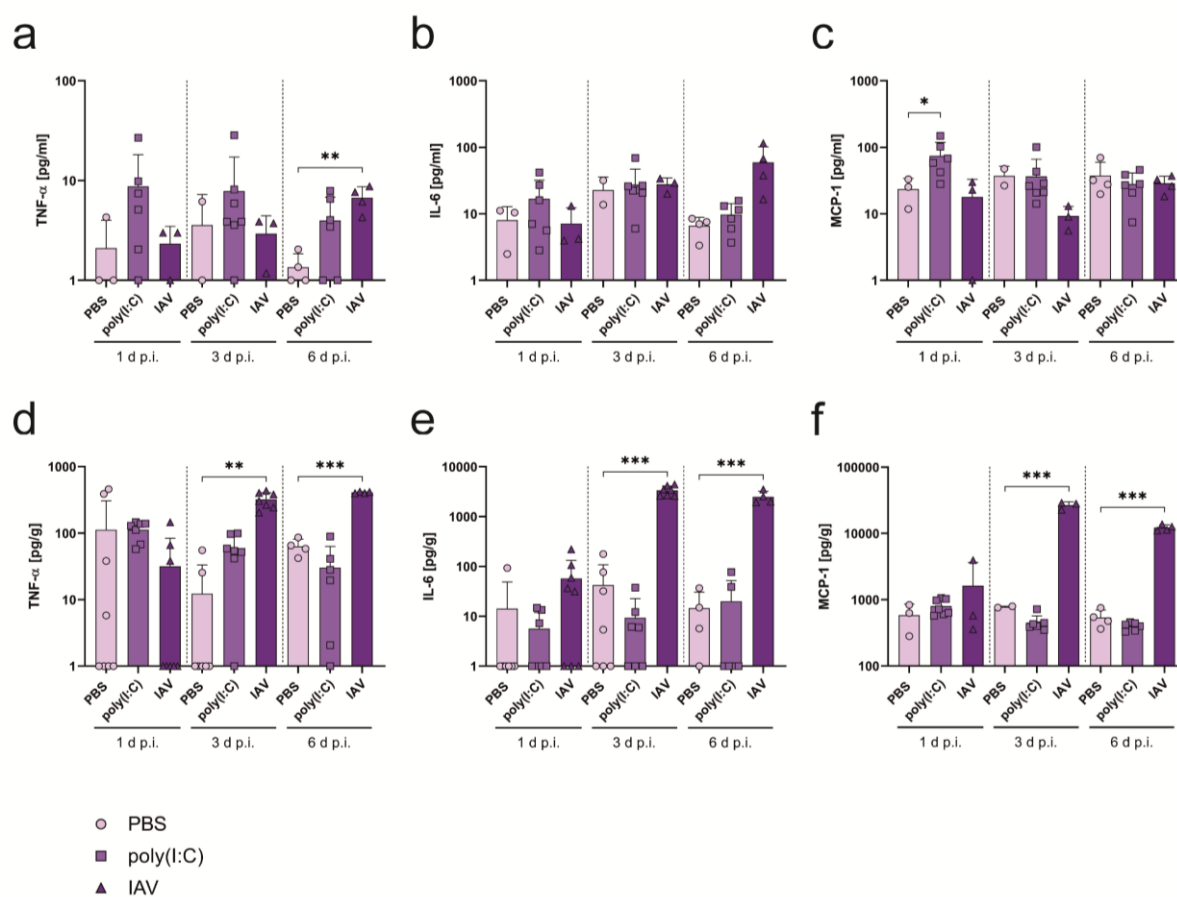


Figure 8. 1st hit: IAV-infection and poly(I:C)-treatment lead to MIA displayed by increased levels of pro-inflammatory cytokines. (a-c) Cytokines (TNF- α [a], IL-6 [b], and MCP-1 [c]) determined by Luminex assay in lungs of pregnant mice treated with PBS (n = 3), poly(I:C) (n = 6-7) or infected with IAV (n = 3-4) at E5.5, measured at 1, 3 and 6 d p.i. (d-f) Cytokines (TNF- α [d], IL-6 [e], and MCP-1 [f]) determined by Luminex assay in plasma of pregnant mice treated with PBS (n = 8, one outlier), poly(I:C) (n = 6-7) or infected with IAV (n = 4-8) at E5.5, measured at 1, 3 and 6 d p.i. Values are normalized to organ weight. All data are presented as mean and SD. Cytokine levels that were below detection limit were set to the kit's lower detection limit of 1 pg/g. The statistical significance was calculated by unpaired t-test (two-tailed) with Welch's correction (*p<0.05, **p<0.01, ***p<.001). Mathematical outliers were determined using Grubb's test.

Another important hallmark of MIA is the indirect dysregulation of maternal hormones, especially pregnancy hormones like progesterone and corticosterone^{151–153}. This dysregulation can influence disease outcome and affect offspring development, therefore also maternal hormones were measured during the course of infection (Figure 9). Both, corticosterone, and progesterone levels were slightly increased upon maternal immune activation with IAV. Only subtle effects were observed in dams treated with poly(I:C). No changes were observed in maternal testosterone levels (Supplementary figure 3).

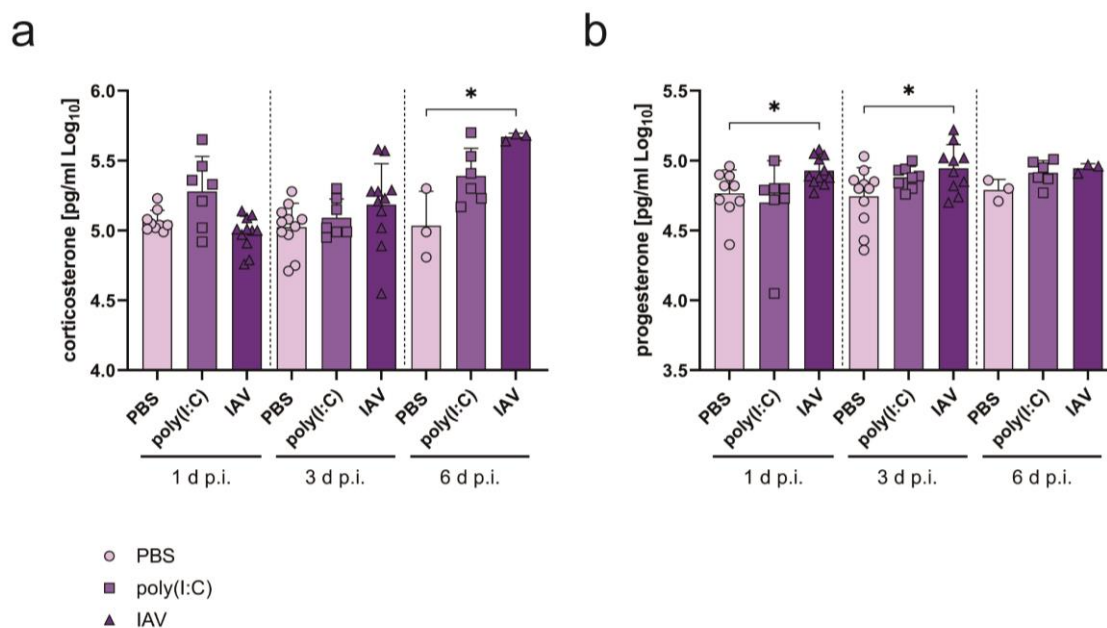


Figure 9. 1st hit: IAV-infection during early gestation causes increased levels of corticosterone and progesterone. Corticosterone (a) and progesterone (b) determined by ELISA in plasma of pregnant mice treated with PBS (n = 3-11), poly(I:C) (n = 6-8) or infected with IAV (n = 3-11) at E5.5, measured at 1, 3 and 6 d p.i. All data are presented as mean and SD. The statistical significance was calculated by unpaired t test (two-tailed) with Welch's correction (*p<0.05).

Corticosterone is known to affect placental growth and mRNA expression as well as nutrient allocation to the fetus^{154,155}. Thus, placental weight and mRNA expression of nutrient supply genes were analyzed on gestational day E17.5. Importantly, insufficient or dysregulated transfer of nutrients from mother to fetus was shown to correlate to MIA associated risk factors like low birth weight^{156,157}. Placental weight was increased in both, mice treated with poly(I:C) and mice infected with IAV compared to PBS controls (Figure 10 a). Increased placental weight might be a sign of placental lesions or compensatory effects and correlates to adverse peri-natal outcomes in humans¹⁵⁸. Subsequent mRNA analysis revealed no changes in growth factor bound protein 10 (Grb10). On the other hand, significant dysregulations were observed in insulin-like growth factor 2 (Igf2, poly(I:C) only) and in two amino acid transporter genes the solute carrier family member 1 and 2 (Slc38a1, Slc38a2) (Figure 10 b).

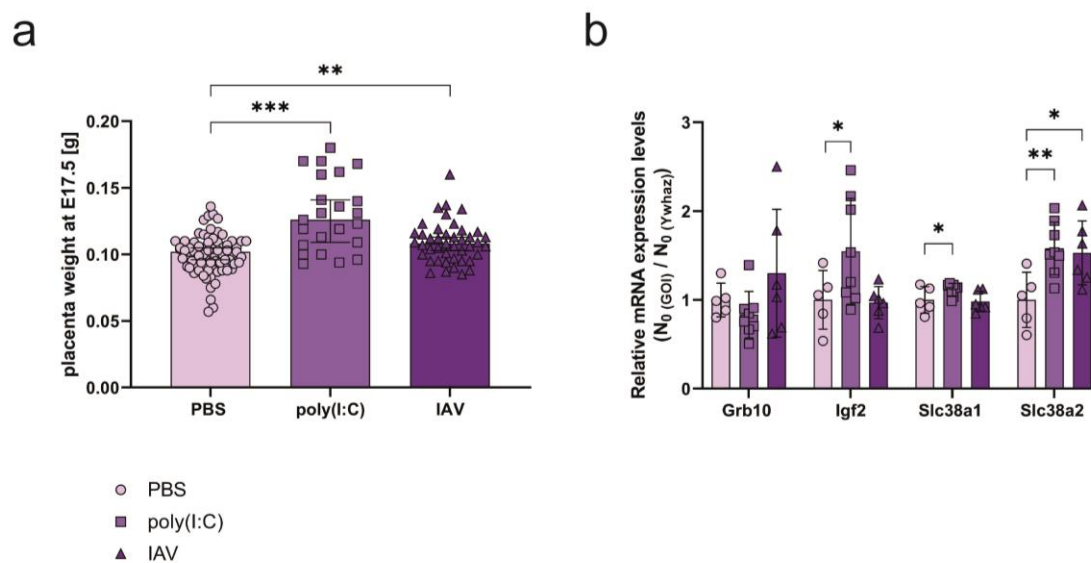


Figure 10. 1st hit: Poly(I:C)-treatment and IAV-infection during early gestation affect placental weight and nutrient gene expression. (a) Placenta weight from dams treated with PBS (n = 72), treated with poly(I:C) (n = 23) or infected with IAV (n = 43) at E17.5. (b) Relative mRNA expression of nutrient supply genes of growth inhibitory gene *Grb10* (growth factor receptor bound protein 10), growth stimulatory gene *Igf2* (insulin-like growth factor II), *Slc38a1* (solute carrier family 38, member 1) and *Slc38a2* (solute carrier family 38, member 2) of placentas from fetuses from PBS (n = 5), poly(I:C) (n = 8) or IAV (n = 6) infected dams. The relative expression of PBS was set to 1 for each gene after normalization to the housekeeping gene *Ywhaz*. All data are presented as mean and SD. The statistical significance was calculated by unpaired t-test (two-tailed) with Welch's correction (* $p < 0.05$, ** $p < 0.01$, *** $p < 0.001$).

In summary, these data show that both MIA models, using either poly(I:C) or IAV during early gestation present major hallmarks of MIA that were linked to stress-related adverse pregnancy outcomes. Nevertheless, both models display distinct features of MIA which needs to be highlighted. Only maternal IAV infection caused a constantly reduced weight gain, whereas the weight of poly(I:C)-treated mice was only affected shortly after treatment. This goes in line with pro-inflammatory cytokine levels, which were found to be increased only immediately after treatment in poly(I:C)-treated dams, whereas the overall cytokine response in IAV-infected mice was stronger and prolonged. Also, poly(I:C) seems to lead to an early increase of corticosterone, while IAV infection increased corticosterone levels in delayed but more pronounced manner. Importantly the effects on the placenta seem to be similar between dams after poly(I:C)-treatment or IAV-infection.

5.2. Maternal immune activation and pregnancy outcomes

As described before, increased maternal cytokine and hormone levels as well as an increased placental weight are hallmarks for adverse pregnancy outcomes. To assess MIA related effects of both poly(I:C)-treatment and IAV-infection during early gestation, the primary pregnancy outcome and fetal health were assessed. Gestational length was unaffected by maternal poly(I:C)-treatment or IAV-infection (Figure 11b). Pregnant dams were euthanized at gestational day E17.5, considered two days before birth to avoid loss of impaired or even dead fetuses immediately after birth. Fetal explants allowed for evaluation of the gestational outcome as well as weight and size of the fetuses. Litter size was determined for both pre-delivery outcomes (E17.5) and post-natal outcomes (2-week-old offspring) in order to evaluate fetal and neonatal viability (Figure 11c). Additionally, viability was assessed for sex-dependency by comparing the litters sex distribution pre- and post-partum from PBS-, poly(I:C)-treated and IAV-infected mothers (Figure 11d). Neither poly(I:C)-treatment nor infection with IAV had any effects on the litter-size or sex of the offspring, both in utero and post-natally. These findings implicate that poly(I:C)- as well as IAV- induced MIA does not lead to in-utero lethality in this model.

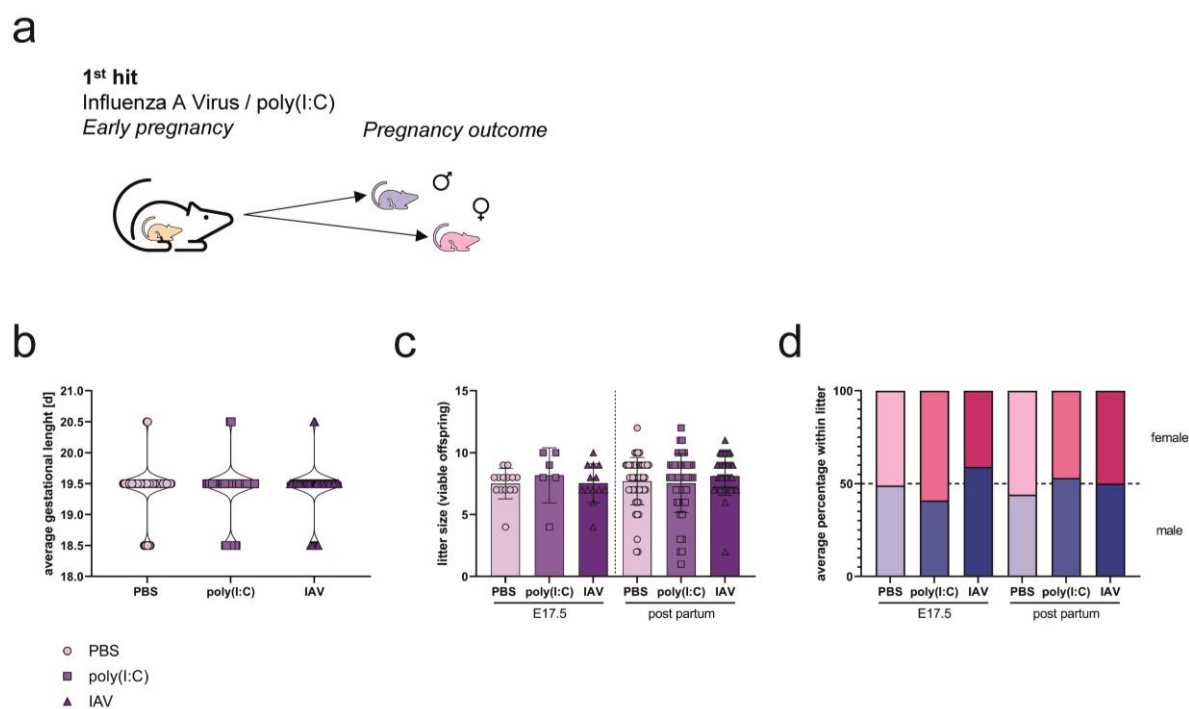


Figure 11. 1st hit: IAV- and poly(I:C)-induced MIA does not affect primary pregnancy outcome. (a) Pregnancy outcome was assessed at embryonic day 17.5 or post-partum with 2-week-old offspring. (b) Gestational length of dams that were treated with PBS (n = 66), treated with 4 mg/kg poly(I:C) (n = 65) or infected with 10^3 PFU IAV (n = 61). (c) Litter size of PBS-treated dams at E17.5 (n = 14) and 2 w p.p. (n = 53), poly(I:C)-treated dams at E17.5 (n = 6) and 2 w p.p. (n = 48) and IAV-infected dams at E17.5 (n = 13) and 2 w p.p. (n = 43). Only viable fetuses were counted. Data are presented as mean and SD. (d) Percentage of male and female fetuses per litter for PBS-treated dams at E17.5 (n = 10) and 2 w p.p. (n = 53), poly(I:C)-treated dams at E17.5 (n = 6) and 2 w p.p. (n = 48) and IAV-infected dams at E17.5 (n = 13) and 2 w p.p. (n = 43). Only viable fetuses were counted. Fetal sex was determined by PCR, sex of 2-week-old offspring was determined by physiological examination. The statistical significance was calculated by unpaired t-test (two-tailed) with Welch's correction (no effects achieved statistical significance).

Although fetal viability was not affected, low birth weight and intra-uterine growth restriction are among the most important risk factors for long-term health deficiencies in the offspring¹⁵⁹. To assess how these are affected by IAV-infection or artificial immune activation, fetal weight and size were measured at gestational day E17.5 (Figure 12). Indeed, fetuses from poly(I:C)-treated and IAV-infected mothers show significantly decreased weight and crown-to-rump length compared to fetuses from PBS-treated mice (Figure 12a,b), suggesting that both MIA models in this study have a striking and comparable effect on fetal growth, despite the fact that MIA markers were found to be more pronounced in IAV-infected dams.

These data show that both maternal IAV infection and poly(I:C) treatment lead to a significant fetal phenotype called small for gestational age (SGA), characterized by low birth weight and body size^{160,161}.

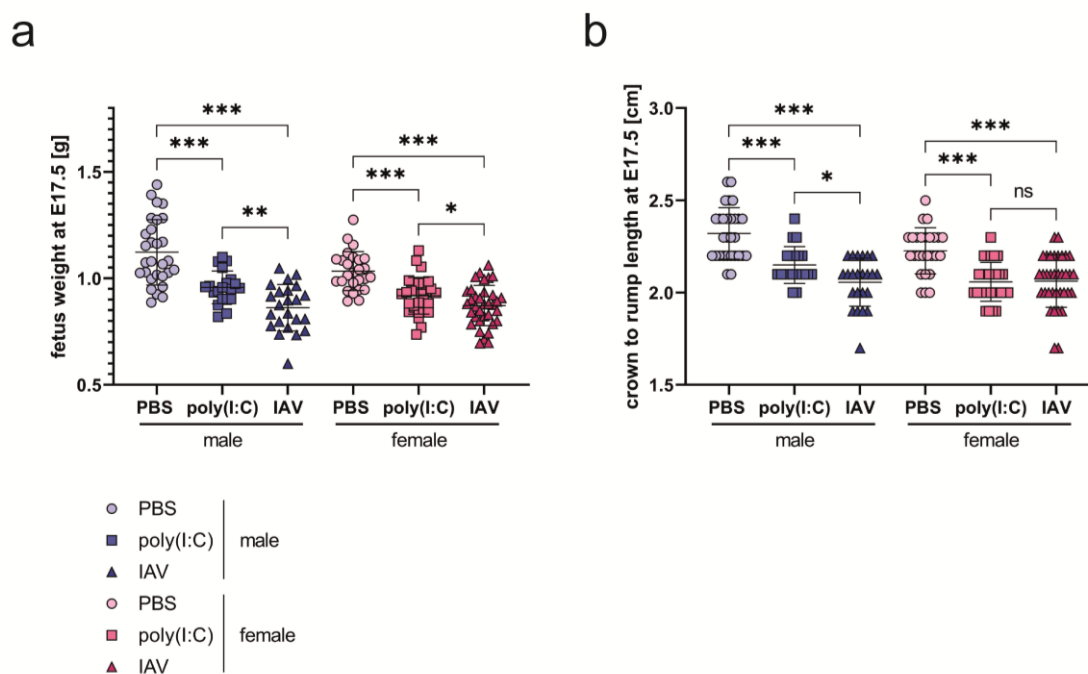


Figure 12: 1st hit: IAV- and poly(I:C)-induced MIA leads to low-birth-weight offspring. Fetus weight (a) and crown to rump length (b) as determined on E17.5 for PBS-treated dams (n = 29 males, 26 females), poly(I:C)-treated dams (n = 20 males, 29 females) and IAV-infected dams (n = 23 males, 35 females). Only viable fetuses were included. All data are presented as mean and SD. The statistical significance was calculated by unpaired t-test (two-tailed) with Welch's correction (*p<0.05, **p<0.01, ***p<0.001).

Long-term observations showed that offspring born to poly(I:C)-treated mothers were able to catch up in regards of body weight with offspring born to PBS-treated mothers within the first two weeks of life. On the other side, offspring born to IAV-infected mothers continued to show low body weight until early adulthood (Figure 13a,b). This indicates that maternal IAV-infection but not poly(I:C)-treatment influences offspring's health even beyond childhood. To exclude maternal health and subsequent impairments in brood care, offspring born to PBS-treated mothers were exchanged with offspring born to IAV-infected mothers and vice versa, immediately after birth (Figure 13c). Observation of the weight gain during the first two weeks of life revealed that IAV-infected mothers can provide equal brood care independent of their

early gestational MIA insult, reflected by comparable relative weight gain of all litters after exchange.

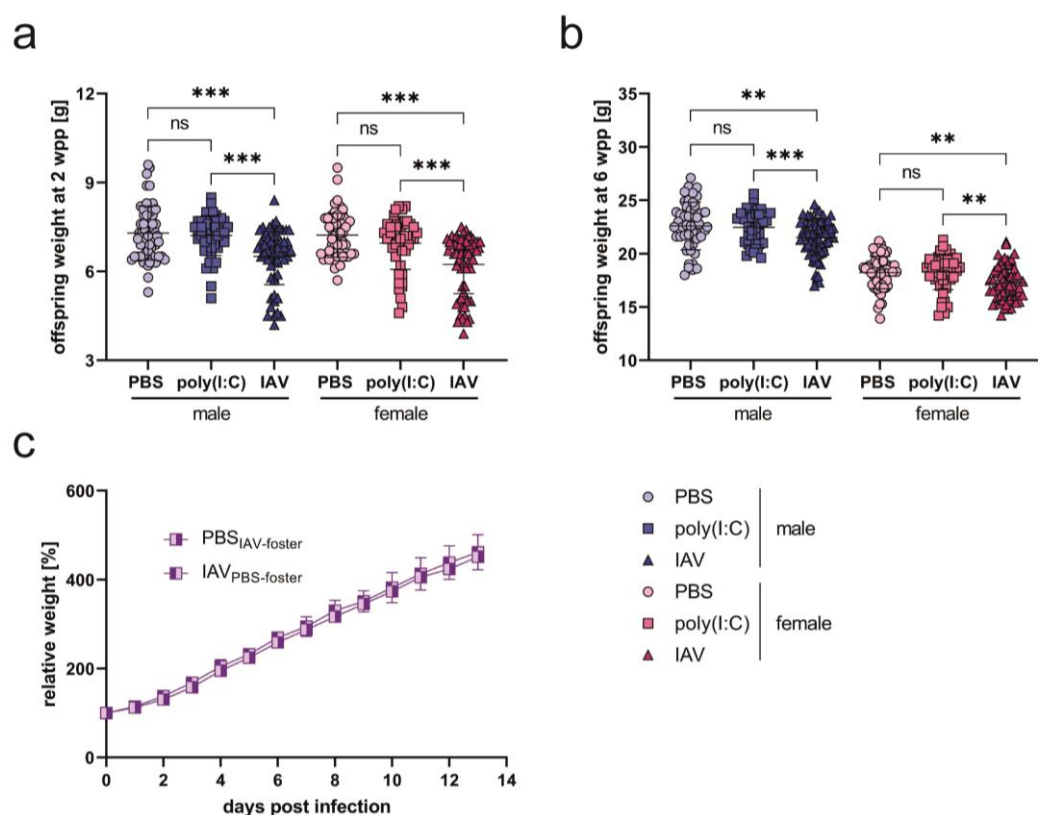


Figure 13. Offspring's health: Offspring born to IAV-infected dams present prolonged low body weight that is not affected by brood care. (a) Offspring weight at 2 weeks of age born to mothers treated with PBS (n = 54 males, n = 56 females), poly(I:C) (n = 47 males, n = 49 females) and IAV (n = 59 males, (n= 67 females). (b) Offspring weight at 6 weeks of age born to mothers treated with PBS (n = 48 males, n = 57 females), poly(I:C) (n = 36 males, n = 46 females) and IAV (n = 69 males, (n= 57 females). (c) Offspring born to PBS treated mothers was exchanged with offspring born to IAV-infected mothers immediately after birth and weight gain was observed for each animal individually during the first two weeks of life. Each group consisted of two litters with eight pups each. All data are presented as mean and SD. The statistical significance for (a) and (b) was calculated by unpaired t test (two-tailed) with Welch's correction (*p<0.05, **p<0.01, ***p<.001). Data on weight were analyzed using multiple unpaired t-test (two-tailed) with correction for multiple testing (Bonferroni-Dunn) (no effects achieved statistical significance).

In summary, this model provides a link between virus-induced MIA and fetal growth restriction. Interestingly, maternal IAV-infection but not poly(I:C)-treatment seems to affect long-term health of the offspring. This might be a strong implication for underlying impairments in the offspring which are not immediately visible upon gestational outcome. This inapparent effect is well studied for neurological disorders in the offspring and there is by now clear evidence, that MIA is linked to such disorders in the offspring^{103,114,149}.

Importantly, subsequent analysis of the offspring's physiology revealed that SGA did not affect lung physiology and pathology in adult offspring (Supplementary figure 4). A detailed understanding about other possible health-impairments like alterations of the offspring's immune system remain elusive and were focus of this study.

5.3. Effects on offspring's immunity

Previous animal studies proposed a link between MIA and immune cell dysregulation in the offspring^{162,163}. To establish a link between MIA and potential immunological aberrations in the offspring, bone marrow, spleens, and lungs of two- and six-week old offspring were analyzed for major immune cell frequencies using flow cytometry.

First, the bone marrow of two-week-old mice was assessed for the frequency of hematopoietic stem cells (HSC) and progenitor cells (Figure 14 a). These progenitors give rise to all hematopoietic cells and ensure life-long supply of mature immune cells. Dysregulation of these cells can disturb a balanced production of mature lineages with detrimental consequences for overall immunity^{164–166}.

In two-week-old offspring, both populations were found upregulated in offspring born to IAV-infected dams, compared to offspring born to PBS- or poly(I:C)-treated mice (Figure 14b,c). Interestingly, no differences were observed in offspring born to poly(I:C)-treated mothers, suggesting that immune stimulation in the mother alone does not lead to dysregulation of hematopoietic stem and progenitor cells in the offspring. Additionally, common myeloid progenitors (CMP) as well as granulocyte-macrophage progenitors (GMP) were found increased in offspring born to IAV-infected dams (Figure 14d,e). CMPs are directly derived from hematopoietic progenitors and differentiate into GMPs and megakaryocyte-erythroid progenitor cells (MEP) generating basically all types of myeloid cells. GMPs produce granulocytic lineages and macrophages. No dysregulation was observed in MEPs which differentiate into megakaryocyte erythrocyte lineage cells (Figure 14f).¹⁶⁷ Interestingly, very similar results were found in 6-week-old offspring, providing evidence, that these effects are of long-lasting nature (Supplementary figure 5a-e).

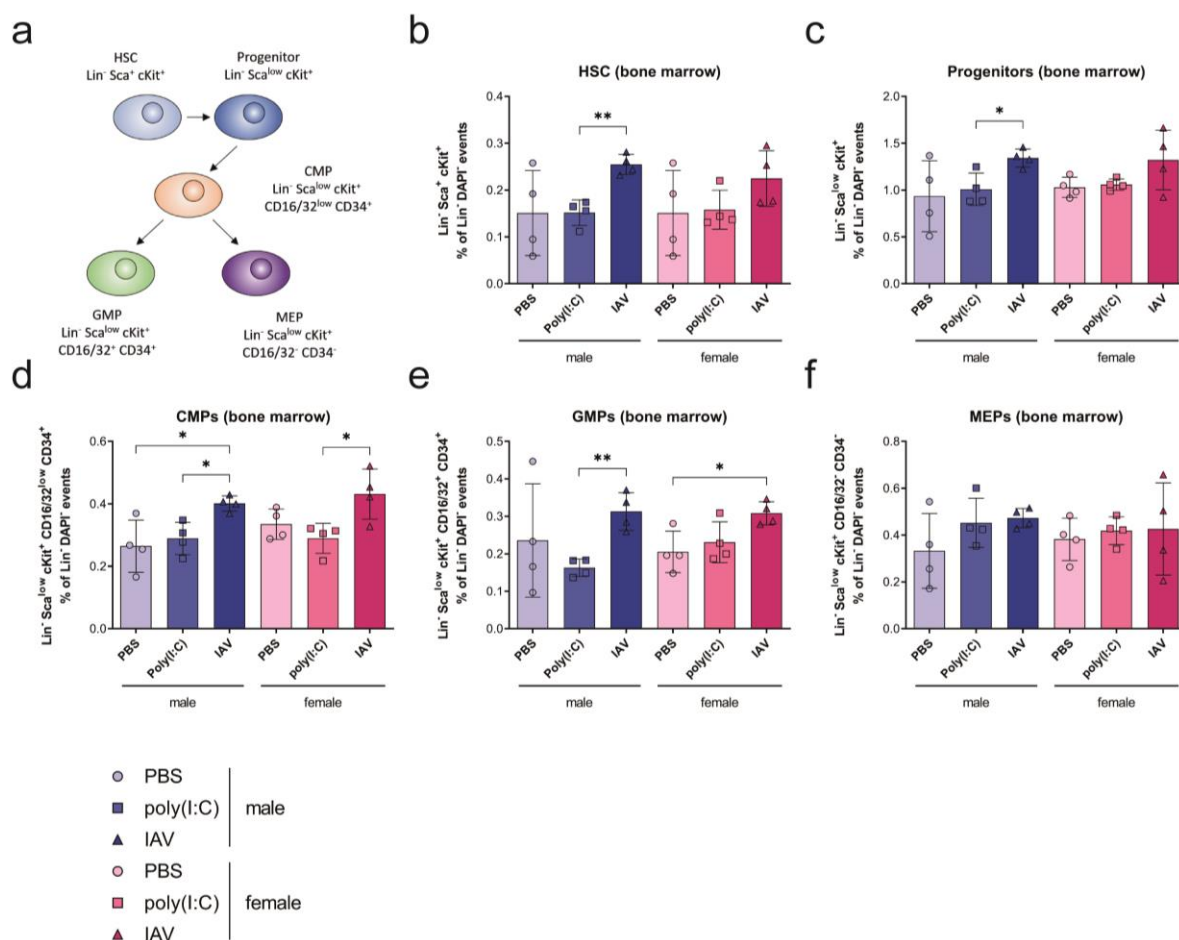


Figure 14. Offspring's health: Early gestational influenza affects 2-week-old offspring's hematopoiesis. (a) Markers used to define respective stem and progenitor cell populations by flow cytometry in this study. (b-f) Frequency of Lin⁻ Sca⁺ cKit⁺ cells (b), Lin⁻ Sca^{low} cKit⁺ cells (c), Lin⁻ Sca^{low} cKit⁺ CD16/32^{low} CD34⁺ cells (d), Lin⁻ Sca^{low} cKit⁺ CD16/32⁺ CD34⁺ cells (e) and Lin⁻ Sca^{low} cKit⁺ CD16/32⁻ CD34⁺ cells (f) as % of Lin⁻ DAPI⁺ events in the bone marrow of 2-week-old offspring (n = 4) born to early gestational PBS-treated, poly(I:C)-treated or IAV-infected dams, as assessed by flow cytometry. If fewer measurement points than the indicated n are visible in the graphs, the ones not shown were excluded as technical outliers. All data are presented as mean and SD. The statistical significance was calculated by unpaired t-test (two-tailed) with Welch's correction (*p < 0.05, **p < 0.01).

As such a significant dysregulation in immune cell progenitor and stem cells is most likely to affect down-stream hematopoiesis and consequently also immune cell frequencies in peripheral organs, major immune cell subtypes of the innate and adaptive immune system were analyzed in spleen and lung by flow cytometry. To provide a first overview about potential consequences, we analyzed a subset of major immune cell subtypes in the offspring's spleens and lungs.

Indeed, B cell frequencies were reduced in lungs but not spleens from juvenile offspring born to IAV-infected dams (Figure 15a,d). Additionally, while NK cell frequencies were enhanced in

spleens, they were drastically decreased in lungs from offspring born to IAV-infected mice (Figure 15b,e). Interestingly, regulatory T cell (Treg) frequencies on the other side seem to be increased in those offspring's lungs (Figure 15c,f). In contrast to the findings for hematopoietic stem cells, this clear phenotype was not or only to lesser extent present in adult offspring (Supplementary figure 5f-k).

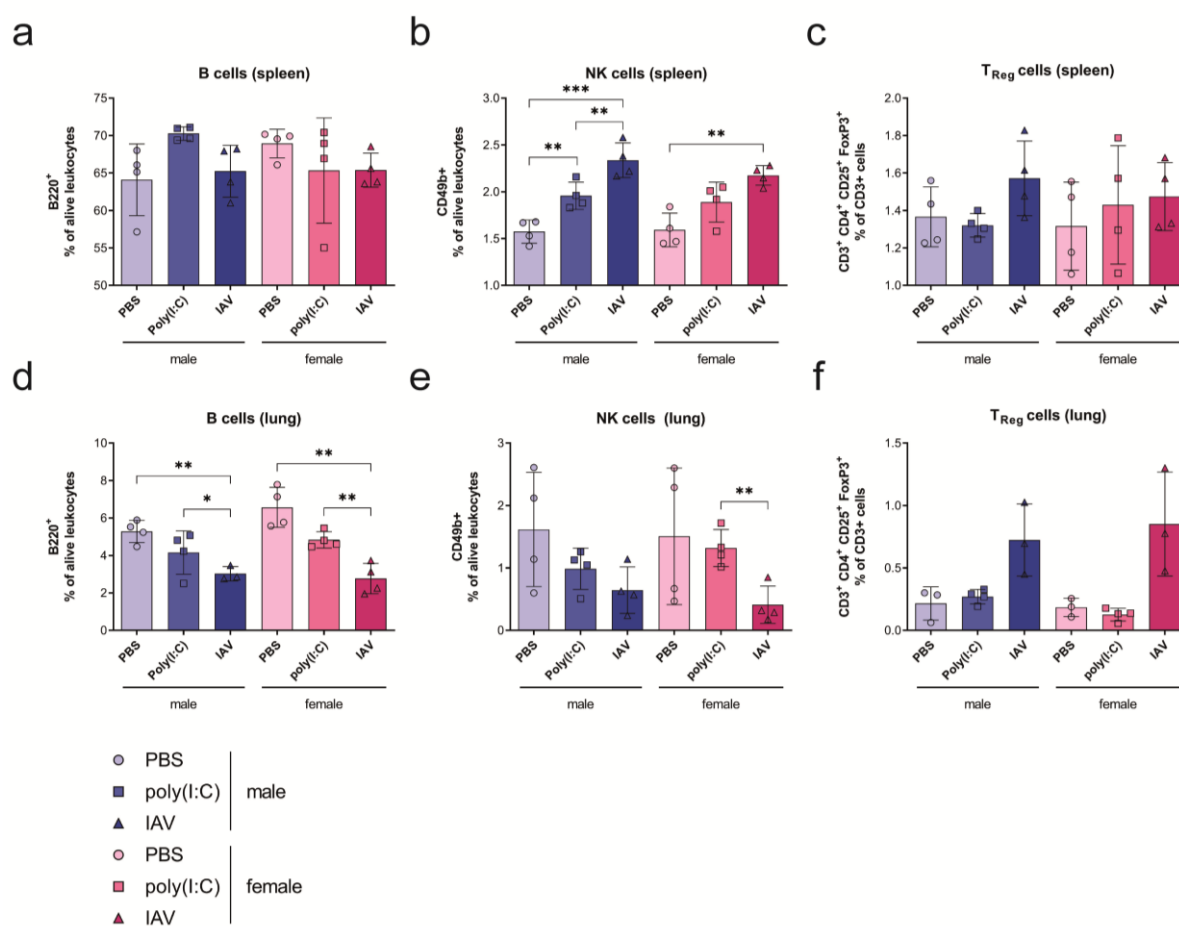


Figure 15. Offspring's health: Early gestational influenza affects 2-week-old offspring's peripheral immune cell frequencies. Frequency of B220⁺ cells (a and d), CD49b⁺ cells (b and e), CD3⁺ CD4⁺ CD25⁺ FoxP3⁺ cells (c and f) as % of alive leukocytes in spleens (a-c) or lungs (d-f) of 2-week-old offspring (n = 4) born to early gestational PBS-treated, poly(I:C)-treated or IAV-infected dams, as assessed by flow cytometry. If fewer measurement points than the indicated n are visible in the graphs, the ones not shown were excluded as technical outliers. All data are presented as mean and SD. The statistical significance was calculated by unpaired t-test (two-tailed) with Welch's correction (*p<0.05, **p<0.01, ***p<0.001).

In the context of respiratory immunity, also alveolar macrophages (AM) play a pivotal role during early stages of infection, especially during early life¹⁶⁸. They are in close contact to the epithelial cells of the alveoli and are crucial for tissue homeostasis and repair, clearance of

surfactant and cell debris, pathogen recognition and clearance and also for initiation and resolution of lung inflammation^{169,170}. Under physiological conditions, they produce low levels of inflammatory cytokines and suppress inflammation and adaptive immunity¹⁶⁹. Therefore, also alveolar macrophages were analyzed in two- and six-week-old offspring by flow cytometry. The results show a slight upregulation of alveolar macrophages as well a tendency for increased activation marker (CD11c) expression in both juvenile and adult offspring born to IAV-infected dams (Figure 16, Supplementary figure 5I).

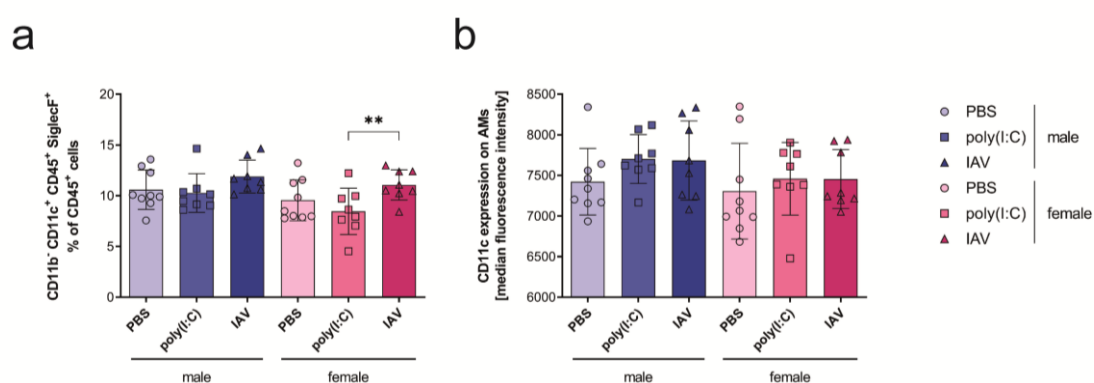


Figure 16. Offspring's health: Early gestational influenza might affect alveolar macrophages in 2-week-old offspring's lung. (a) Frequency and CD11c expression as median fluorescence intensity (b) of CD11b⁺ CD11c⁺ CD45⁺ SiglecF⁺ cells as % of CD45⁺ cells in lung of 2-week-old offspring (n = 8-9) born to early gestational PBS-treated, poly(I:C)-treated or IAV-infected dams, as assessed by flow cytometry. If fewer measurement points than the indicated n are visible in the graphs, the ones not shown were excluded as technical outliers. All data are presented as mean and SD. The statistical significance was calculated by unpaired t test (two-tailed) with Welch's correction (**p<0.01).

Overall, these findings demonstrate that influenza-related maternal immune activation during early gestation has long-lasting effects on hematopoiesis in juvenile offspring. This effect translates into aberrant immune cell frequencies in juvenile, but not adult offspring. Importantly, no sex-specific differences were observed within offspring born to poly(I:C)-treated or IAV-infected offspring.

To understand whether these effects might ultimately affect functional immunity in the offspring, a "two hit" model was utilized to challenge the immune system of juvenile and adult offspring born to MIA mothers.

5.3.1. Offspring infection with influenza B virus

Challenge experiments with 2- and 6-week old offspring born to poly(I:C)-treated or IAV-infected dams as well as born to control dams were performed to evaluate functional immunity in this offspring. To first validate the “two hit” model, homologous and semi-homologous second hits were performed on two-week-old offspring. Thus, offspring born to PBS-treated or IAV- (H1N1) infected dams were infected with either the same H1N1 virus (homologous) or a H3N2 reassortant (6+2 in WSN backbone, semi-homologous) at 2 weeks of age. Juvenile offspring presented full protection against homologous challenge and partial protection against semi-homologous protection, as expected due to perinatal transfer of protective antibodies (Supplementary figure 6) confirming the validity of the preclinical two-hit animal model.

As maternal influenza A virus infection elicits protective immunity against a subsequent challenge with IAV in the offspring, a challenge model using influenza B virus (IBV) was chosen as a heterologous viral pathogen to study functional immunity in the offspring. Importantly, anti-IAV antibodies do not cause significant protection against IBV¹⁷¹. Two-week-old mice born to MIA affected (poly(I:C)-treated or IAV-infected) or control-treated mothers were infected intra-nasally with a sublethal dose of IBV. Infected mice were monitored for 14 days and signs of disease as well as weight development was recorded. Additionally, plasma and lungs were isolated from offspring at 1, 3 and 6 days post infection to study cytokine expression.

Upon infection with 10^5 PFU of IBV (B/Lee/40) in two-week-old offspring, male but not female offspring born to IAV-infected mothers present increased lethality compared to offspring born to poly(I:C)- or PBS-treated dams (Figure 17a,b). In contrast, no differences were observed in morbidity upon second hit in adult offspring born to poly(I:C)-treated or IAV-infected dams compared to offspring born to control dams (Figure 17 c,d).

These data show that juvenile, but not adult offspring born to MIA dams are more vulnerable towards an unrelated viral infection during early life and that this effect seems to be sex specific with stronger vulnerability in male offspring. Nevertheless, since the same infection dosage was used for juvenile and adult offspring, it might be that the challenge dose in adult offspring was too low to achieve distinguishable effects in these mice. Thus, potential impairments in adult offspring cannot be fully excluded.

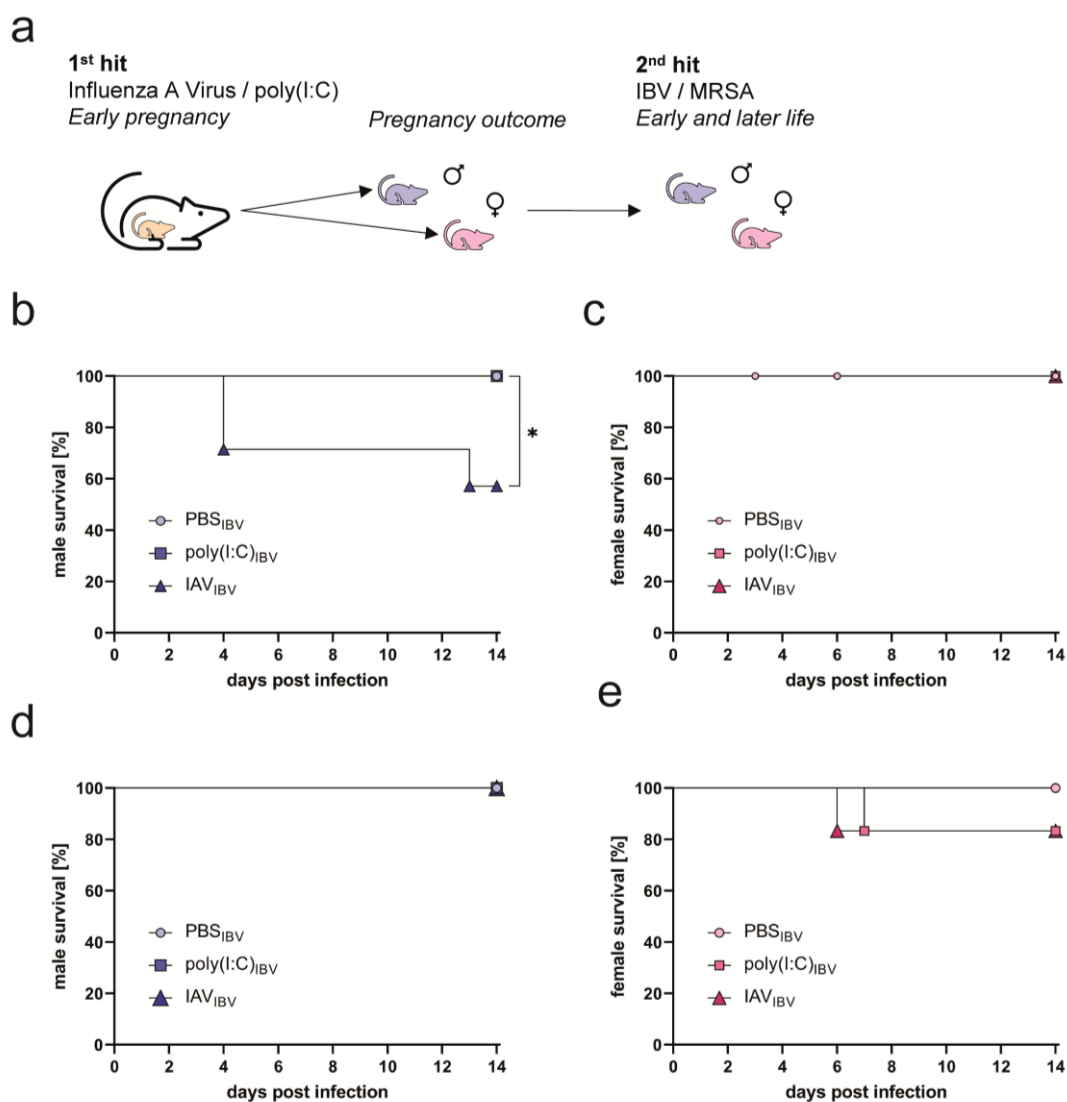


Figure 17. 2nd hit: Male offspring born to IAV-infected dams show increased vulnerability towards early life IBV infection. (a) Second hit experiments were performed in two- and six-week-old offspring using IBV for a respiratory challenge. (b) 2-week-old male offspring born to PBS- (n = 5), poly(I:C)-treated (n = 5) or IAV-infected (n = 7) dams were infected with 10^5 PFU of IBV. Survival was determined within 14 d p.i. (c) 2-week-old female offspring born to PBS- (n = 7 [day 3], 6 [day 6], 4 [day 14]), poly(I:C)-treated (n = 8) or IAV-infected (n = 9) dams were infected with 10^5 PFU of IBV. Survival was determined within 14 d p.i. or until organ explants. Due to less available female offspring for PBS groups, also animals from organ explant experiments were included until the day of explant, as indicated above. (d) 6-week-old male offspring born to PBS- (n = 5), poly(I:C)-treated (n = 8) or IAV-infected (n = 8) dams infected with 10^5 PFU of IBV. Survival was determined within 14 d p.i. (e) 6-week-old female offspring born to PBS- (n = 4), poly(I:C)-treated (n = 6) or IAV-infected (n = 6) dams infected with 10^5 PFU of IBV. Survival was determined within 14 d p.i. The statistical significance was calculated by Log Rank test for trend (* $p < 0.05$).

To further characterize increased morbidity in these mice, cytokine levels were measured in lung homogenates explanted at 1, 3 or 6 days post infection.

As expected, increased vulnerability of juvenile offspring born to IAV-infected dams seem to correlate with increased inflammatory cytokine response early after infection (Figure 18a-c). In line with this observation, no increase in cytokine levels was observed in adult offspring but IL-2 was found to be decreased in offspring born to IAV-infected dams. Evaluation of sex-specific effects was not possible due to small group sizes. No changes were observed for IL-1 β , IL-10 or IL-17A in both juvenile and adult offspring (Supplementary figure 7).

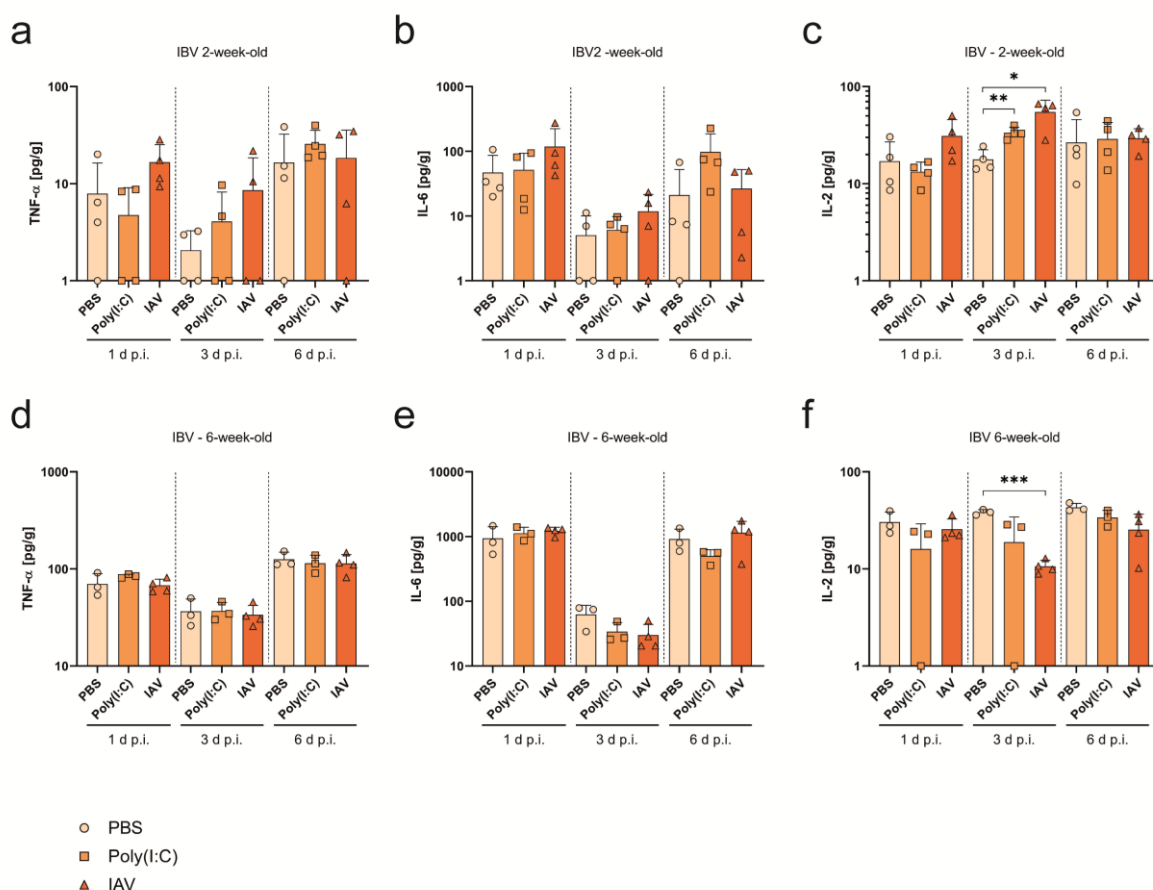


Figure 18. 2nd hit: Offspring born to IAV-infected dams show increased vulnerability towards early life IBV infection. (a-c) Cytokines (TNF- α [a], IL-6 [b], and IL-2 [c]) determined by Luminex assay in lungs of 2-week-old offspring (both sexes) born to PBS- or poly(I:C)-treated or IAV-infected offspring (n = 4) after infection with 10⁵ PFU of IBV measured at 1, 3 or 6 d p.i. (d-f) Cytokines (TNF- α [d], IL-6 [e], and IL-2 [f]) determined by Luminex assay in lungs of 6-week-old offspring (both sexes) born to PBS- or poly(I:C)-treated or IAV-infected offspring (n = 3-4) after infection with 10⁵ PFU of IBV measured at 1, 3 or 6 d p.i.. Values are normalized to organ weight. All n represent the number of offspring from respective groups. All data are presented as mean and SD. Cytokine levels that were below detection limit were set to the kit's lower detection limit of 1 pg/g. The statistical significance was calculated by unpaired t test (two-tailed) with Welch's correction (*p<0.05, **p<0.01, ***p<0.001).

The cytokine measurements indicate that juvenile offspring born to IAV-infected or poly(I:C)-treated mice show stronger IL-2 activation upon viral infection during early life. This is in line with the observed increased morbidity and might be an implication for an overshooting cytotoxic immune activation in these animals.

In summary, these data provide clear evidence that offspring born to IAV-infected dams is more vulnerable towards infection with IBV and that maternal poly(I:C)-treatment does not affect offspring's vulnerability in the same way. Interestingly, these effects might be sex- and age-dependent. The IL-2 response seems to play a key role, as it is upregulated in juvenile offspring that shows increased vulnerability but downregulated in adult offspring born to IAV-infected dams. Although IL-2 expression might be linked to CD4⁺ cell hyperactivation in juvenile offspring, the exact mode of action and its consequence remains elusive.

5.3.2. Offspring infection with *Staphylococcus aureus*

To confirm this finding and to strengthen the model, the second hit was additionally performed with a bacterial pathogen that encounters different immune pathways upon infection.

Methicillin-resistant *Staphylococcus aureus* (MRSA), if applied intra-nasally, cause a local infection of the lung from where it can induce systemic infection and inflammation. Also, mouse models are well established for MRSA infection^{172,173}.

Infection with 10⁸ Colony Forming Units (CFU) of MRSA resulted in increased lethality in 2-week-old but not 6-week-old offspring born to IAV-infected dams (Figure 19). Because these animals died before sex determination was possible, we were not able to detect any sex-specific effects for MRSA-infected, juvenile offspring.

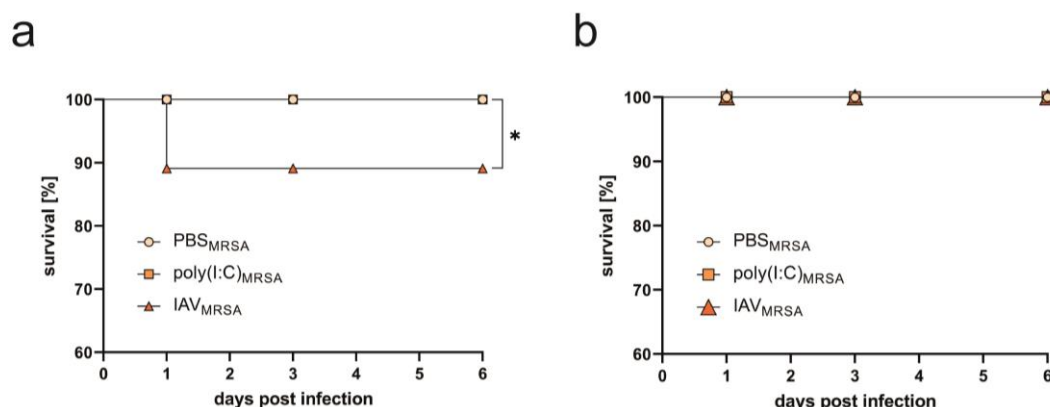


Figure 19. 2nd hit: Offspring born to IAV-infected dams show increased vulnerability towards early life MRSA infection. (a) 2-week-old offspring (both sexes) born to poly(I:C)-treated (n = 21 [day 1], 14 [day 3], 7 [day 6]) or IAV-infected (n = 55 [day 1], 34 [day 3], 16 [day 6]) dams were infected with 10^8 CFU of MRSA. Offspring born to PBS-treated dams (n = 38 [day 1], 25 [day 3], 12 [day 6]) were used as controls. (b) 6-week-old offspring (both sexes) born to poly(I:C)-treated (n = 21 [day 1], 14 [day 3], 7 [day 6]) or IAV-infected (n = 36 [day 1], 25 [day 3], 13 [day 6]) dams infected with 10^8 CFU of MRSA. Offspring born to PBS-treated dams (n = 34 [day 1], 22 [day 3], 11 [day 6]) were used as controls. Survival was determined at day 1, 3 or 6 p.i. The statistical significance was calculated by Log Rank test for trend (*p<0.05).

Again, lung cytokines were measured at 1, 3 and 6 days post infection. Importantly, no cytokine measurement was possible from mice that succumbed to infection prior to organ explant; thus, a survivorship bias needs to be considered. Measurement of cytokines in offspring's lungs showed no clear difference between offspring born to infected or uninfected mice upon infection with MRSA except for a slight upregulation of TNF- α in mice born to poly(I:C)-treated mice three days after infection with MRSA (Figure 20). No changes were observed for IL-1 β , IL-10 or IL-17A (Supplementary figure 8). Nevertheless, it needs to be considered that increased cytokine levels might be missed due to infection-related lethality as indicated above.

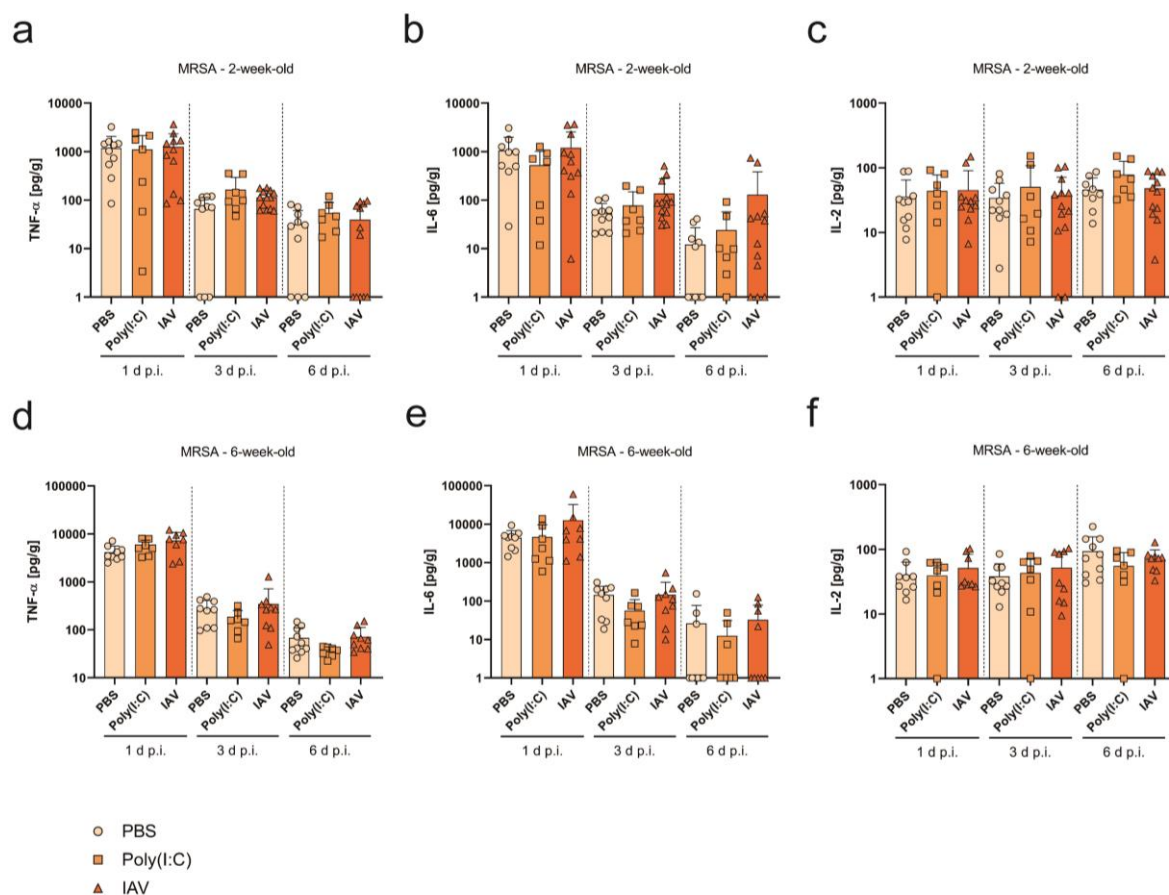


Figure 20. 2nd hit: Offspring born to IAV-infected dams show increased vulnerability towards early life MRSA infection. (a-c) Cytokines (TNF- α [a], IL-6 [b], and IL-2 [c]) determined by Luminex assay in lungs of 2-week-old offspring (both sexes) born to PBS- (n = 10) or poly(I:C)-treated (n = 7) or IAV-infected offspring (n = 11) after infection with 10^8 CFU of MRSA measured at 1, 3 or 6 d p.i. (d-f) Cytokines (TNF- α [d], IL-6 [e], and IL-2 [f]) determined by Luminex assay in lungs of 6-week-old offspring (both sexes) born to PBS-, poly(I:C) or IAV-infected offspring (n = 7-10) infected with 10^8 CFU of MRSA measured at 1, 3 or 6 d p.i. Values are normalized to organ weight. All n represent number of offspring from respective groups. All data are presented as mean and SD. Cytokine levels that were below detection limit were set to the kit's lower detection limit of 1 pg/g. The statistical significance was calculated by unpaired t-test (two-tailed) with Welch's correction (no effects achieved statistical significance).

Another important aspect of functional immunity that was addressed in this study is pathogen clearance. Healthy mice should be able to clear an MRSA infection rapidly¹⁷². To evaluate bacterial clearance, lung homogenates for juvenile and adult offspring isolated at 1, 3 and 6 days post infection were titrated. Whereas offspring born to PBS or poly(I:C)-treated mice was able to clear the infection within three to six days post infection, offspring born to IAV-infected mothers were only partially able to clear the infection and some mice continued to show high bacterial load six days post infection (Figure 21). Noteworthy, bacterial clearance was not only

affected in juvenile but also adult offspring (Figure 21b, data on sex not plotted). Differentiation of sex-specific effects was not possible due to limited group sizes.

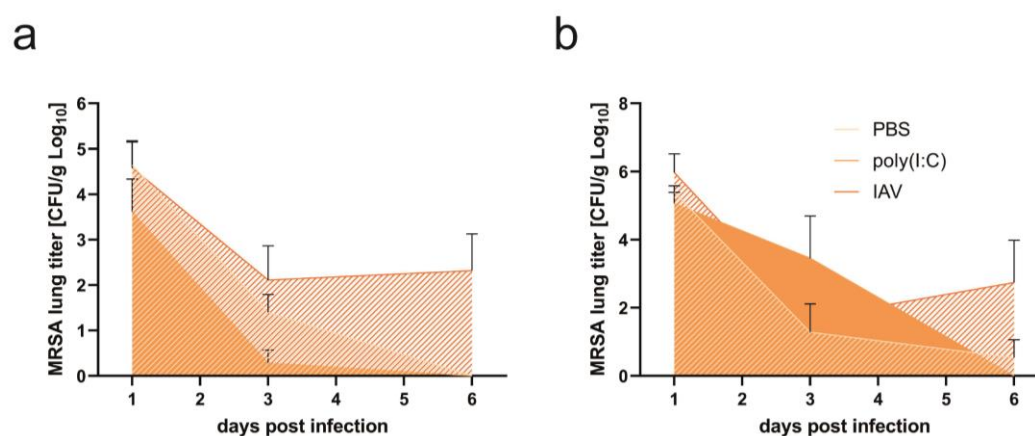


Figure 21. 2nd hit: Offspring born to IAV-infected mothers present delayed bacterial clearance. (a) MRSA lung titer in 2-week-old offspring (both sexes) born to PBS- (n = 7 – 10), poly(I:C)-treated (n = 4 – 7) or IAV-infected (n = 9 – 13) dams, measured on day 1, 3 and 6 p.i. (b) MRSA lung titer in 6-week-old offspring (both sexes) born to PBS- (n = 6–7), poly(I:C)-treated (n = 3–4) or IAV-infected (n = 5–6) dams, measured on day 1, 3 and 6 p.i. Values are normalized to organ weight. All n represent number of offspring from respective groups. All data are presented as mean and SD. The statistical significance was calculated by unpaired t-test (two-tailed) with Welch’s correction (no effects achieved statistical significance).

In summary these data show that juvenile offspring born to IAV-infected mice is not only more likely to develop severe disease upon bacterial infection but also show delayed clearance of the pathogen. Taken together, offspring born to IAV-infected but not poly(I:C)-treated mothers show increased vulnerability towards respiratory infection with MRSA. This is reflected by increased, mortality, delayed clearance of bacteria and at least in part an overshooting immune response early after infection. Importantly, not only juvenile offspring but also adult offspring is affected, indicating long-lasting impairments of the immune system. This phenotype goes in line with observed alterations of major immune cell populations after MIA during early pregnancy. Combined with the findings from the viral second hit, these experiments provide strong evidence, that maternal IAV infection conveys a life-long legacy to the offspring with increased vulnerability towards subsequent infections. Importantly, this phenotype cannot be reflected using an artificial model for MIA such as poly(I:C).

To understand the underlying mechanisms behind this increased vulnerability, further studies need to be done. As a first step to further pinpoint the observed effects like an overshooting

immune activation that is accompanied by a delayed clearance, we decided to focus on the role of alveolar macrophages, as they are within the first line of defense against respiratory challenge.

5.3.3. Adoptive transfer of alveolar macrophages

Alveolar macrophages (AMs) are known to play a crucial role during respiratory infections. They act as a first line of defense and are an important player in innate immunity. Additionally, alveolar macrophages act as antigen presenting cells and are important for the activation of the adaptive immune system. To find the underlying mechanisms behind MIA-associated immune dysregulation, alveolar macrophages are a good target to pinpoint explicit effects. Thus, two-week-old mice born to MIA affected mothers were used for an adoptive transfer of these macrophages before subsequent challenge with IBV. Because the effects described so far were more pronounced in 2-week-old offspring, AM transfer experiments were performed in juvenile offspring exclusively.

Offspring that were born to healthy mothers received either AMs from offspring born to poly(I:C)-treated or from offspring born to IAV-infected mothers (*poly(I:C) macrophages* or *IAV-macrophages* respectively). Offspring born to poly(I:C)-treated, or IAV-infected mothers received AMs from offspring born to PBS-treated dams (*PBS-macrophages*). AMs were isolated from litter mates of the respective groups and purified by fluorescence-activated cell sorting. Transfer of AMs to the respective, sex-matched recipient animals occurred intranasally immediately after purification. Twelve hours post transfer, these mice were infected with a sublethal dose of IBV (10^5 PFU) and monitored for signs of disease and weight development until organ explants on 3 days post infection (Figure 22a).

Adoptive transfer of AMs derived from offspring born to poly(I:C)-treated or IAV-infected mice into pups from healthy mothers did not affect relative weight development upon subsequent infection with IBV compared to offspring that did not receive any AMs in both males and females (Figure 22b,e). Also, transfer of *PBS-macrophages* into offspring born to poly(I:C)-treated mice did not affect immediate morbidity (Figure 22c,f). In contrast, offspring born to IAV-infected mothers that received *PBS-macrophages* were able to show significantly

increased weight gain compared to offspring that was born to IAV-infected mothers but did not receive *PBS-macrophages* (Figure 22d,g). These data suggest that early gestational influenza virus infection affects functionality of the offspring's AMs and this effect can be rescued by transfer of unaffected AMs prior to infection.

To further strengthen this hypothesis, we performed a growth kinetic of the IBV in vitro and investigated the effect of murine AMs isolated from 2-week-old offspring that was born to PBS-treated or IAV-infected dams on viral replication. Indeed, we were able to show that AMs isolated from offspring born to IAV-infected dams lead to increased viral replication compared to AMs isolated from control offspring. Interestingly, this effect was only observed in AMs isolated from male offspring born to IAV-infected mothers (Figure 22h).

These data show that alveolar macrophages might be one important contributor on increased vulnerability in offspring born to IAV-infected mothers. Aberrant frequency of alveolar macrophages or dysfunction, e.g. hyperactivation, as it was observed in offspring born to IAV-infected dams, might be a direct consequence of an impaired hematopoiesis that was affected by early gestational MIA. MIA associated dysfunction of these important immune cells might directly contribute to severe disease outcome as it was shown in this study.

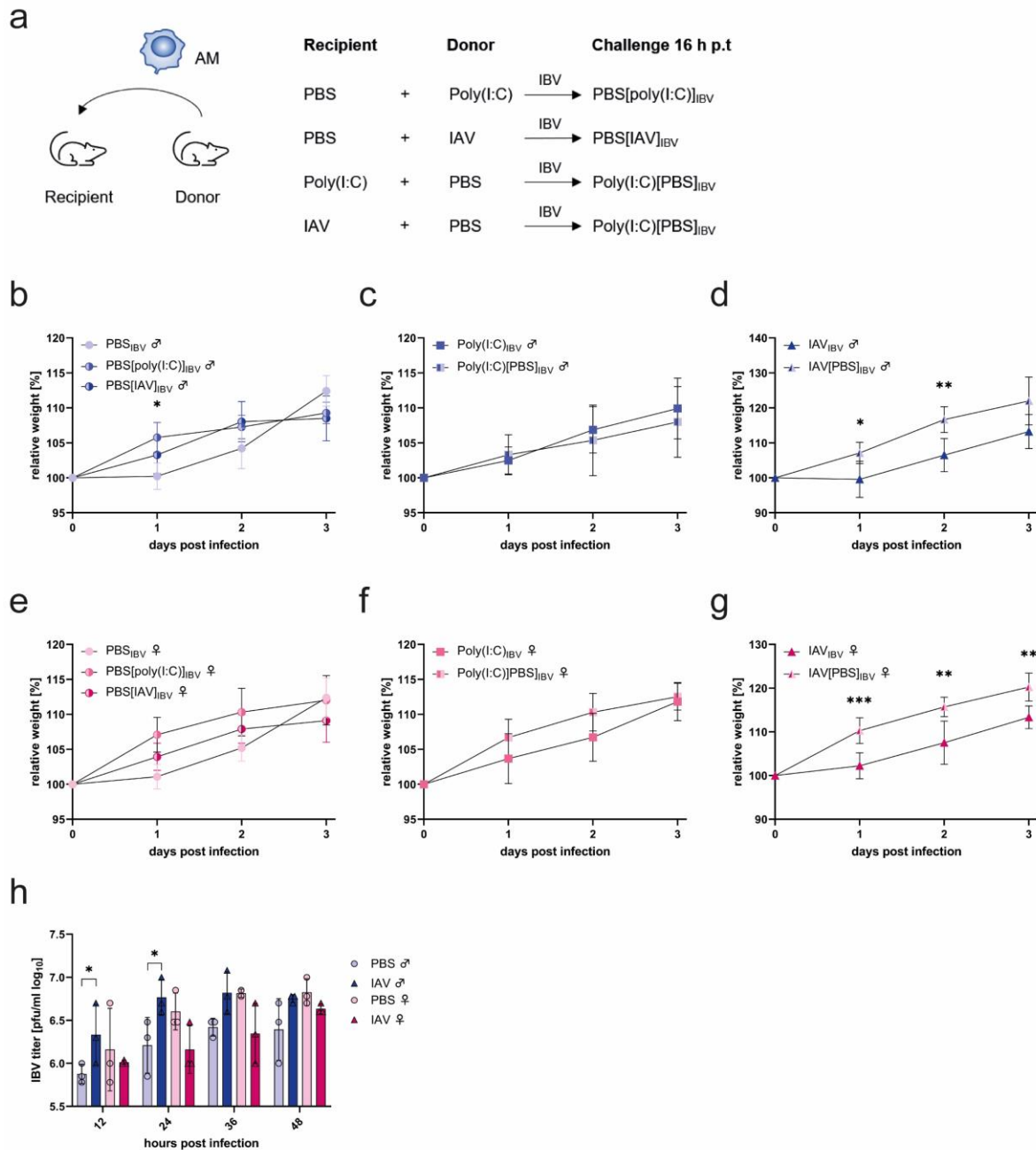


Figure 22. Alveolar macrophages of offspring born to IAV-infected mothers are functionally impaired. (a) Adoptive transfer experiments were performed in two-week-old offspring followed by IBV infection 16 hours post transfer (h p.t.). (b,e) Alveolar macrophages of 2-week-old male (b) and female (e) offspring born to poly(I:C)-treated ($n = 10$ males, 10 females) or IAV-infected mothers ($n = 11$ males, 14 females) were pooled and 10^5 AMs were transferred into offspring of the same sex ($n = 5-8$) born to PBS-treated mothers with infection of the sentinel-offspring 16 h p.t. with 10^5 PFU of IBV. (c,d,f,g) Alveolar macrophages of 2-week-old male (c,d) and female (f,g) offspring born to PBS-treated mothers ($n = 22$ males, 29 females) were pooled and 10^5 AMs were transferred into offspring of the same sex ($n = 6-8$) born to poly(I:C)- (c,f) or IAV-infected (d,g) mothers with infection of the sentinel-offspring 16 h p.t. with 10^5 PFU of IBV. Weight development was observed until 3 d p.i. (h) Growth kinetic of IBV on MDCK II-cells after the addition of 5×10^4 pooled AMs isolated from offspring ($n = 3$) born to PBS-treated or IAV-infected dams 4 hours after cell infection. Virus titers were determined in 12-hour intervals until 48 h p.i. All data are presented as mean and SD. The statistical significance for weight data was calculated by multiple, unpaired t-test (two-tailed) using Bonferroni-Dunn correction (b-g). Grouped data were analyzed unpaired t-test (two-tailed) with Welch's correction (h) (* $p < 0.05$, ** $p < 0.01$, *** $p < 0.001$).

5.4. Discussion

MIA is commonly defined as an increase of pro-inflammatory cytokines like IL-6, TNF α and MCP-1 during pregnancy¹¹⁴. Also increased levels of corticosterone and progesterone during pregnancy have been previously correlated to MIA^{152,153}. In the present study, we used an allogeneic mouse pregnancy model to show that a single-dose application of poly(I:C) on gestational day 5.5 results in a short immune activation early after application. In contrast, infection with IAV results in a stronger and prolonged increase of MIA markers and thus a more severe disease outcome during pregnancy. As we have previously shown, using an allogeneic mouse pregnancy model is key to understand viral pathogenicity during pregnancy-related immune adaptation and subsequently also potential effects on the offspring¹⁰⁰. We chose dosages that lead to mild but pronounced immune activation in the dams as they best resemble the clinical situation. Higher doses of virus or poly(I:C) applied at E 5.5 resulted in maternal death or high rates of pregnancy abortion, the latter especially upon poly(I:C)-treatment with 20 mg/kg. Although MIA seems to be stronger in dams infected with IAV compared to poly(I:C), both models present comparable SGA phenotypes in the fetuses. Since low birth weight is a major risk factor for later life disease in the offspring, a comparison of both models in this regard is reasonable and important to evaluate findings from other studies restricted to the use of poly(I:C) or other artificial immunogens^{159,161}. Notably, repetitive instead of single-dose stimulation with poly(I:C) might be a suitable tool to mimic infection more precisely. Nevertheless, most previously published models use single-dose application of artificial immunogens, hence we followed this scheme to accurately reflect potential mechanistical differences¹⁷⁴.

We further decided to study the effects of MIA in early pregnancy, since studies in humans have shown that early gestational hits are more likely to cause long-term health deficits in the offspring, while strong stress during late gestation is more likely to cause abortion or maternal death^{149,151}. It needs to be highlighted, that most studies on MIA in mice are carried out in mid or late gestational settings¹³³. One possible reason might be, that early gestational hits are experimentally more difficult to achieve, since the early pregnancy-status cannot be easily confirmed in mice. Common assessment of a copulation plug goes in line with high false-positive pregnancy rates and palpation cannot be reliably used before gestational day 10¹⁷⁵.

Additionally, measurement of pregnancy hormones needs invasive methods that might influence subsequent experiments. While some work has been done on the effects of timing of MIA on the offspring's neurocognitive development, a detailed understanding on the effects of MIA timing on the offspring's immune system remains elusive^{117,140}. In this study we show that early gestation indeed represents a critical phase of fetal development and that gestational stress has a long-lasting effect on the offspring's immune development.

We also showed that long-term consequences of MIA do not necessarily go in line with immediate effects in pregnancy outcome. Mild maternal influenza as well as poly(I:C)-application during early gestation did not affect gestational length, litter size and sex-distribution of the offspring. Only increased placental weight and a dysregulation of genes related to trans-placental nutrition and metabolism indicate disruption of pregnancy homeostasis and present a link to SGA offspring^{156,176}. This further highlights the importance of birth weight as a marker for MIA-related effects on the offspring. Importantly, offspring born to poly(I:C)-treated mice recovered the phenotype of relatively reduced bodyweight within the first two weeks of life, whereas offspring born to IAV-infected dams continued to show low body weight until early adulthood. Although developmental delay seems to be an important indicator for increased vulnerability to respiratory infectious disease, no differences were observed in lung physiology and function in adult offspring born to either control or MIA dams.

Infection of juvenile, 2-week-old offspring revealed increased vulnerability towards respiratory infection with both viral and bacterial hits. Notably, upon challenge with IBV, increased vulnerability was restricted to male offspring. This is interesting, since 2-week-old mice are considered as infantile and do not yet display mature sex-specific hormonal features¹⁷⁷. Due to experimental restrictions, we were not able to detect sex-specificity in the offspring's vulnerability against MRSA. Nevertheless, like the infection with IBV, offspring born to IAV-infected dams showed increased lethality upon MRSA infection, compared to offspring born to PBS- or poly(I:C)-treated dams. These data clearly show that early gestational influenza, but not poly(I:C)-induced MIA affects functional immunity towards respiratory infection in juvenile offspring. Influenza-related morbidity is often a consequence of the immune activation rather than direct effects of the viral infection¹⁷⁸. Thus, over-shooting immune activation, or cytokine-storms are a hallmark for severe disease. In our study, we

found that offspring born to IAV-infected mothers generally tend to present higher levels of inflammatory cytokines in the lung. Importantly, the functional capacity of the offspring's immune system was impaired as shown by decreased clearance of MRSA in the lung. Overall, these findings suggest that upon early life infection the offspring's immune system is highly activated but lacks efficient functionality in these mice. Experiments on 6-week-old adult offspring did not show detectable differences in morbidity and cytokine expression upon infection with IBV or MRSA. Though, bacterial clearance was still strikingly delayed in adult offspring born to IAV-infected dams. This might indicate on one hand aberrations in immune activation and control might be restricted to early stages of life, but on the other hand functional immune competence remains altered until adulthood.

These results provide first evidence that early gestational influenza in mice directly affects the offspring's hematopoiesis. Flow cytometric analysis revealed that frequencies of myeloid progenitor cells were increased in the bone marrow of offspring born to IAV-infected mice. Noteworthy, these mice were fully naïve when sacrificed for analysis, reinforcing that all effects are linked to in-utero effects. Stem cell aberrations also translated into abnormal frequencies of various functional immune cells in the offspring's lung and spleen. Reduced NK and B cell frequencies in the lungs from offspring born to IAV-infected dams might be associated with increased vulnerability to a respiratory second hit. These findings may provide a first link towards impaired immune competence in these offspring but certainly reveal many aspects that need to be taken in consideration for future research about the role of MIA and long-term health deficiencies in the offspring.

Alveolar macrophages and monocytes mainly coordinate the inflammatory immune activation towards viral and bacterial infection¹⁶⁸. Alveolar macrophages are of special interest, because seeding into the lung already upon fetal development, they remain long-lived in the lung mainly by self-renewal and thus might be a good correlate to in utero priming^{169,179}. Although only subtle differences in AM frequencies were observed in the offspring of all groups, functional experiments in vivo and in vitro revealed that the functionality of alveolar macrophages is affected by maternal influenza. Improving the offspring's recovery after infection with IBV was possible by transferring AMs from control animals to offspring born to IAV-infected dams, prior to infection. These data suggest that alveolar macrophage function can be rescued by adding unaffected cells into the system. On the other side, transfer of AMs

from offspring born to MIA dams, did not affect disease outcome in control animals. In any case, it is important to highlight, that we decided not to deplete host macrophages to avoid further disturbance of the AM niche and subsequent recruitment of new cells from the bone marrow into the lungs, prior to the experiment. Thus, any adverse effects of AMs derived from offspring born to IAV infected mothers, might be rescued by healthy host macrophages. Also, protective effects of healthy macrophages in offspring born to infected mothers, might be due to an overall increase of alveolar macrophages in the lung.

Nevertheless, these results provide strong evidence towards functional impairments of MIA offspring macrophages by also showing decreased viral clearance capacity *in vitro*.

In summary, this study shows, that early gestational influenza affects offspring's immune system in a functional way that renders the offspring more vulnerable towards early life respiratory infection. Comparing two important models for maternal immune activation by using either poly(I:C) or IAV clearly revealed that only influenza-related MIA but not poly(I:C)-stimulation results in impaired immunity in the offspring. We further hypothesize that early gestational influenza virus infection affects offspring's hematopoiesis *in utero* with long-lasting effects on immune cell frequency and functionality. Highlighting the multi-dimensional consequences of early gestational influenza on offspring's health, this study provides additional evidence favoring maternal vaccination against influenza as well as new opportunities to further study offspring's immunity in the context of MIA.

6. Outlook

This study provides a first model to directly compare artificial MIA and IAV-derived MIA in mice. Importantly, this model also utilizes allogeneic breeding and early gestational infection and by this overcomes important limitations that are given by previously established models. This model can now be used to study the explicit effects of maternal influenza on offspring's health.

Whereas this study shows that maternal IAV infection has a deregulatory effect on the offspring's hematopoiesis, the underlying mechanisms are still not known. Epigenetic profiling of hematopoietic stem cells and progenitors will provide a better understanding of these mechanisms and might provide a direct link between maternal infection and aberrant immune cell frequencies in the offspring. In order to understand how maternal infection can interfere with in-utero development of the fetus, cytokine-levels in the fetus should be assessed, as it is known, that cytokines might cross the placenta and can affect fetal development^{103,124}. On the other side also pathogen-derived antigens might cross the placenta and could cause a direct – and pathogen specific – imprinting of the fetal immune system. Thus, the fetus should be screened for antigen-burden and antigen-specific antibodies, pre-natally. These experiments might provide a better understanding about how a maternal IAV infection could interfere with fetal immunity towards later-life infection.

Another important question is, which alteration in fetal development also translate into a functional outcome like impaired immunity. In this study many immune cell populations were found to be dysregulated in otherwise healthy offspring that was born to MIA mothers. A first experiment in this study showed, that alveolar macrophages seem to play an important role in increased vulnerability towards respiratory infection in these animals. But it is rather likely, that many other mechanisms contribute to this phenotype. The “two hit” model presented in this study is a suitable tool to study the effect of immune cells that are involved in adaptive immunity, for example B-cells or CD4⁺ and CD8⁺ T-cells. Especially regulatory CD4⁺ and NK cells were found to be dysregulated in offspring born to IAV-infected mothers. In-vitro stimulation assays as well as in vivo transfer experiments could provide a detailed understanding of potential mal-function of these cells. On the other hand, the bacterial second hit model provides a strong tool to study effects of the innate immune system, since healthy mice can

clear this infection before the adaptive immune system is fully activated. Further experiments on alveolar macrophages, for example in vitro stimulation assays, or on NK-cells could provide a direct link to the elevated cytokine levels that were observed upon challenge.

Furthermore, this study implicates that maternal infection has a long-lasting effect on the offspring's immune system that is not restricted to the immediate response but also towards adaptive immunity. Subsequently, maternal infection could also influence vaccine efficacy and safety in the offspring that should be assessed thoroughly. On the other hand, also maternal vaccination could have effects on the offspring that go beyond the transfer of antibodies and micro-chimeric memory cells. Vaccination experiments in this model could provide first evidence, especially combined with epigenetic analysis and subsequent transcriptomics of the fetal hematopoietic niche.

Finally, some of the findings from this study could be translated into humans by studying placental aberrations (after delivery) and by investigating the immune response towards respiratory infection in children that were born to IAV infected mothers. These studies could provide additional implications for maternal vaccinations, especially in regards of the timing during gestation. Additionally, potential risk groups for severe respiratory disease could be assessed early on.

7. Materials and Methods

7.1. Materials

7.1.1. Chemicals

Chemical	Manufacturer
Agarose	Serva
Ampicillin sodium-salt	Serva
Avicel	FMC BioPolymer
Bovine serum albumin (BSA)	Sigma-Aldrich/Merck
Crystal violet	Merck
Diethylpyrocarbonate (DEPC)	Sigma-Aldrich/Merck
Dimethylsulfoxide (DMSO)	Sigma-Aldrich/Merck
Ethanol	Sigma-Aldrich/Merck
Ethanol (denatured, for disinfection)	Sigma-Aldrich/Merck
Formaldehyde solution (37%)	Merck
Glacial acetic acid	Merck
Hematoxylin	Shandon
Hydrochloric acid (HCl) (37%)	Merck
Methanol	ChemSolute
Paraffin	DCS
Paraformaldehyde	AppliChem
Polyinosinic-polycytidylic acid sodium salt, TLR tested (50 mg)	Sigma-Aldrich/Merck P9582-50MGM
Potassium chloride (KCl)	Merck
Potassium dihydrogen phosphate	Merck
Pursept-A Xpress (for disinfection)	Schülke & Mayr AG
Sodium chloride (NaCl)	ChemSolute
Sodium hydrogen phosphate	Merck
Sodium hydroxide (NaOH)	Merck
Tris (hydroxymethyl) amino methane	Merck

7.1.2. Buffers and solutions

Buffer / solution	Content / manufacturer
Avicel solution (2.5 %)	2.5 % Avicel in H ₂ O (autoclaved)
Citrate buffer (0.1 M)	12.0 g citrate 11.3 g citric acid In 800 ml H ₂ O final pH = 6.0 (adjusted with NaOH)
Chicken whole blood, with citrate	Lohmann Tierzucht (#570001)
Crystal violet solution	270 ml formaldehyde (37%) 1 g crystal violet In 1 l H ₂ O
DEPC-H ₂ O	0.1 % DEPC in H ₂ O (autoclaved)
DNase/RNase-free H ₂ O	Gibco/Life Technologies
dNTP mix (10 mM)	Life Technologies
EDTA solution (0.5 M, 100x)	Thermo Scientific
Ethidium bromide solution (10 mg/ml)	Roth
FACS buffer	2% FBS in PBS
FACS lysis buffer	12.5 mg Collagenase D 91.7 µl DNase I In 5 ml RPMI
FD Green buffer (10x)	Thermo Scientific
Halt™ Protease & Phosphatase Inhibitor Cocktail (100x)	Thermo Scientific
HF buffer (5x)	Thermo Scientific
MassRuler DNA ladder mix	Thermo Scientific
MassRuler DNA loading dye	Thermo Scientific
Paraformaldehyde solution (4%)	20g PFA 200 µl 5N NaOH (for solubility) 80 µl 37% HCl In PBS, final pH ~ 7.5, storage at 4 °C

Buffer / solution	Content / manufacturer
Phosphate buffered saline (PBS)	1.37 M NaCl 26.8 mM KCl 51.3 mM Na ₂ HPO ₄ ·2H ₂ O 17.6 mM KH ₂ PO ₄ pH 7.2 – 7.4, autoclaved
RBC lysis buffer (10x)	BioLegend
Ribolock RNase Inhibitor (40U/μl)	Thermo Scientific
RNAlater RNA Stabilization Reagent	Qiagen
RNase free DNase Set	Qiagen
SuperBlock T20	Thermo Scientific
TAE buffer (50x)	2 M Tris base 1 M glacial acetic acid 0.05 M EDTA pH 8.0

7.1.3. Kits

Kit	Manufacturer
FastStart Essential DNA Green Master	Roche
Superscript™ III Reverse Transcriptase Kit	Invitrogen/Life Technologies
Innuprep RNA Mini Kit 2.0	Analytik Jena
Multiplex mouse immunoassay, custom: (IL-1β, IL-2, IL-6, IL-10, IL-17A, TNFα, MCP-1)	Life Technologies
Zombie NIR Fixable Viability Kit	BioLegend
Progesterone ELISA	Cayman Chemical
Corticosterone ELISA	ARBOR Assays
Zytochem-Plus HPR kit	ZytoChem

7.1.4. Antibodies

Antibody	Species / dilution / manufacturer
Anti-IAV nucleoprotein (primary)	Mouse, 1:1000; Abcam #ab128193
Anti-mouse-HRP (secondary)	Goat, 1:1000; Sigma-Aldrich #A4416
Anti-rabbit IgG (H+L)	Donkey Jackson ImmunoResearch AB2310593
Anti-Mouse CD11b (Integrin alpha M, Mac-1 alpha) Monoclonal Antibody, Alexa Fluor 647 Conjugated, [M1/70]	Thermo Fisher Scientific
Anti-Mouse CD11c (Integrin aX, p150 / 90) Monoclonal Antibody, Phycoerythrin-Cy5.5 (PE-Cy5.5) Conjugated, [N418]	Thermo Fisher Scientific
F4/80 Monoclonal Antibody [BM8], PE, eBioscience™	Thermo Fisher Scientific
Brilliant Violet 421™ anti-mouse CD45 antibody [30-F11]	BioLegend
CD170 (Siglec F) Monoclonal Antibody [1RNM44N], eBioscience™	Thermo Fisher Scientific
CD45R (B220) Monoclonal Antibody [RA3-6B2], PE, eBioscience™	Thermo Fisher Scientific
CD11b Monoclonal Antibody [M1/70], PE-Cyanine7, eBioscience™	Thermo Fisher Scientific
CD11c Monoclonal Antibody [N418], PerCP-Cyanine5.5, eBioscience™	Thermo Fisher Scientific
PE anti-mouse CD16/32 antibody [93]	BioLegend
CD25 Monoclonal Antibody [PC61.5], PE-Cyanine7, eBioscience™	Thermo Fisher Scientific
APC/Cyanine7 anti-mouse CD3 antibody [145c11]	BioLegend

Antibody	Species / dilution / manufacturer
CD3e Monoclonal Antibody [145-2C11], PE-Cyanine7, eBioscience™	Thermo Fisher Scientific
CD34 Monoclonal Antibody [RAM34], FITC, eBioscience™	Thermo Fisher Scientific
CD4 Monoclonal Antibody [RM4-5], FITC, eBioscience™	Thermo Fisher Scientific
CD4 Monoclonal Antibody [RM4-59], PerCP-Cyanine5.5, eBioscience™	Thermo Fisher Scientific
CD49b (Integrin alpha 2) Monoclonal Antibody [DX5], PE, eBioscience™	Thermo Fisher Scientific
APC/Cyanine7 anti-mouse CD117 (c-kit) antibody [2B8]	BioLegend
FOXP3 Monoclonal Antibody [150D/E4], PE, eBioscience™	Thermo Fisher Scientific
PE/Cy7 anti-mouse Ly-6A/E (Sca-1) antibody [E13-161.7]	BioLegend
V450 Mouse Lineage Antibody Cocktail, BD Horizon	BD Bioscience
APC Rat Anti-Mouse CD8a [53-6.7]	BD Bioscience
CD86 (B7-2) Monoclonal Antibody [GL1], APC, eBioscience™	Thermo Fisher Scientific
PE Rat Anti-Mouse Ly-6G [1A8]	BD Bioscience
Ly-6C Rat anti-Mouse, PerCP-Cyanine5.5, [HK1.4], eBioscience™	Thermo Fisher Scientific
MHC Class II (I-A/I-E) Monoclonal Antibody (M5/114.15.2), FITC, eBioscience™	Thermo Fisher Scientific
PerCP/Cyanine5.5 anti-mouse CD206 (MMR) antibody [C068C2]	BioLegend

7.1.5. Enzymes

Enzyme	Manufacturer
Taq DNA polymerase	Qiagen
Proteinase K	Qiagen
Collagenase D (<i>Chlostridium histolyticum</i>)	Sigma-Aldrich

7.1.6. DNA oligonucleotides

Oligonucleotide ID	Sequence / manufacturer
SX_F	5'-GATGATTTGAGTGGAAATGTGAGGTA-3'
SX_R	5'-CTTATGTTTATAGGCATGCACCATGTA-3'
Ywhaz_forward	5'-CACGCTCCCTAACCTTGCTT-3'
Ywhaz_reverse	5'-ATCGTAGAAGCCTGACGTGG-3'
Grb10_forward	5'-AAGCGAAGACCGAGATGAAG-3'
Grb10_reverse	5'-CATAGGTGCGTTGAAAGGAG-3'
Igf2_forward	5'-CTTGATCCCAGAACCCAAGAA-3'
Igf2_reverse	5'-CCCCTTGGTGACATGGGGAC-3'
Slc38a1_forward	5'-CGGGAGAGTAGGAGGAGTCT-3'
Slc38a1_reverse	5'-GTCTGCTCCCACACATCGTT-3'
Slc38a2_forward	5'-AATGCGATTGTGGGCAGTGG-3'
Slc38a2_reverse	5'-AGCTTCCAGCCAGACCATAC-3'

7.1.7. Narcotics and supplements

Substance	Manufacturer
Isoflurane (100%)	Abbott
Ketamine (100 mg/ml)	WDT
Sodium chloride 0.9%	B. Braun Melsungen AG
Xylazine (20 mg/ml)	WDT

7.1.8. Bacterial strains

Organism	Strain
Methicillin-resistant <i>Staphylococcus aureus</i>	USA300

7.1.9. Media for bacterial culture

Medium	Manufacturer
Mannitol Salt Phenol Red Agar	Sigma-Aldrich/Merck
Tryptic Soy Broth (TSB) medium	Sigma-Aldrich/Merck
Tryptic Soy Broth (TSB) agar	Sigma-Aldrich/Merck

7.1.10. Eukaryotic cell lines

Cell line	Origin / manufacturer
Mardin-Darby Canine Kidney (MDCK II)	Immortalized canine cell line (♀) ATCC (CCL-34)

7.1.11. Media and supplements for eukaryotic cell culture

Medium / supplement	Content / manufacturer
Bovine serum albumin solution (BSA, 35% in D-PBS)	Sigma-Aldrich/Merck
Cryoconservation medium	FBS 10% DMSO
Dulbecco's Phosphate Buffered Saline (D-PBS)	Sigma-Aldrich/Merck
Fetal bovine serum (FBS) superior	Biochrom GmbH

Medium / supplement	Content / manufacturer
Infection medium	MEM 1% L-Glutamine 1% Penicillin & Streptomycin (P/S) 0.2% BSA TPCK trypsin, 1:1000
L-Glutamine (200 mM)	Sigma-Aldrich/Merck
Growth medium	MEM 10% D-PBS 1% L-Glutamine 1% Penicillin & Streptomycin (P/S)
Minimum Essential Medium (MEM)	Sigma-Aldrich/Merck
Modified Eagle Medium 2x (2x MEM) without Phenol Red	Sigma-Aldrich/Merck
Overlay medium for plaque test	1:1 mixture of 2xMEM and 2.5% Avicel in H ₂ O + 0.4% BSA
Penicillin & Streptomycin (P/S)	Sigma-Aldrich/Merck
TPCK-treated trypsin	Sigma-Aldrich/Merck
Trypsin-EDTA	Sigma-Aldrich/Merck
RPMI 1640 medium	Life Technologies

7.1.12. Virus strains

Virus strain	Origin
A/Hamburg/NY1580/09 (H1N1)	Sigrid Baumgarte, Institut für Hygiene und Umwelt, Hamburg, Germany ([248])
B/Lee/40	Kindly provided by Thorsten Wolff, Robert Koch Institute, Berlin, Germany
A/Aichi/63 (H3N2) (6+2 gene reassortant in WSN background)	Eva Fiebertshäuser-Böttcher, Institute for Virology, Philipps University Marburg

7.1.13. Consumables

Article	Manufacturer
12-well tissue culture plate	Greiner bio-one Cellstar
24-well tissue culture plate	Falcon / BD Biosciences
6-well tissue culture plate	Falcon / BD Biosciences
96-well v-bottom microwell plate	Nunc
96-well tissue culture plate	Sarstedt
Disposable needles Sterican™ (26G)	Roth
Capillaries (EDTA tubes for blood collection)	Kabe Labortechnik GmbH
Cryo vials (1.5 ml)	Sarstedt
Metal beads (Ø 2.0 mm)	RETSCH (#22.455.0010)
PCR tubes	Sarstedt
Petri dishes (100 mm)	Falcon / BD Biosciences
Pipette tips, with filter (10, 100, 1000 µl)	Sarstedt
Precision wipe tissue	Kimtech Science
Reaction tubes (1.5 ml, 2.0 ml)	Sarstedt
SafeSeal reaction tubes + screw cap	Sarstedt
Syringe TERUMO®, without needle, U-100 Insulin (1 ml, 6 % Luer)	TERUMO Cooperation
T25 cell culture flask	Falcon / BD Biosciences
T75 cell culture flask	Sarstedt
Transfer pipettes (5, 10, 25 ml)	Sarstedt
Eggs (specified pathogen free, SPF)	VALO Biomedica
Corning cell strainer 70 µm	Sigma-Aldrich

7.1.14. Safety gear

Article	Manufacturer
Filter mask, type 9332 FFP3	3M
Gloves Latex	Kimberly-Clark
Gloves Purple Nitrile	Kimberly-Clark
Lab coat	Leiber
Lab shoes	Suecos
OP mask	Mölnlycke Health Care
OP Nurse Cap	Mölnlycke Health Care
Overall	ProFit

7.1.15. Laboratory equipment

Article	Manufacturer
Animal scale	Kern
Biological safety cabinet HeraSafe KS12	Thermo Scientific
Biological safety cabinet HeraSafe KS18	Thermo Scientific
Centrifuge Avanti J-E	Beckham Coulter
Centrifuge 5417R	Eppendorf
Centrifuge Varifuge 3.0R	Thermo Scientific
Cryo conservation container Mr. Frosty	Nalgene
Documentation System Imagequant LAS 4000 GE	Amersham Biosciences
FACS Aria-Fusion (5-laser, 18-fluorescence system)	BD Biosciences
Gel documentation system Gel Doc XR	Bio-Rad
Gel electrophoresis system Sub-Cell GT (15 x 15 cm)	Bio-Rad
Heraeus temperature-controlled CO ₂ incubator B6120	Kendro

Article	Manufacturer
Heraeus temperature-controlled CO ₂ incubator BBD 6220	Thermo Scientific
Heraeus temperature-controlled CO ₂ incubator Heracell 150	Thermo Scientific
Isoflurane vaporizer	UNO
LightCycler® 96	Roche
Magnetic stirrer MR3001 (with heating element)	Heidolph
Microliter pipettes Eppendorf Reference (1-10, 10-100, 100-1000 µl)	Eppendorf
Microplate reader Tecan Safire2	Tecan
Microwave Supratomic M754	Miele
Mixer mill MM 400	RETSCH
Multichannel pipettes (8 channel; 5-50 µl; 20-200 µl)	Brand
Neubauer counting chamber, bright light	Marienfeld
Nikon Eclipse 80i upright light microscope, coupled with Color Camera Nikon DS-Ri2	Nikon (Japan)
PCR cycler GeneAmp PCR System 9700	Applied Biosystems
pH calculation device pHenomenal®	VWR
Pipetus	Hirschmann Laborgeräte
Precision scale Extend ED224S	Sartorius
Precision scale ExtendED3202S-CW	Sartorius
Roche LightCycler® 96	Roche
Shaker MaxQ 6000	Thermo Scientific
Shaker WT 17	Biometra
Shaking waterbathSW22	Julabo
Small centrifuge (1.5 reactions tubes)	Biozym
Small centrifuge (PCR 8-strips)	Biozym
Spectrophotometer NanoDrop 1000	Peqlab

Article	Manufacturer
Spectrophotometer SpectronicGenesys 10	Thermo Scientific
Surgical forceps (for organ harvesting)	F.S.T.
Surgical scissors (for organ harvesting)	F.S.T.
Thermomixer TMix 220V	Analytik Jena
ThermoMixer® C, including Thermoblock	Eppendorf
Thermostat Precitherm PFV	Labora Mannheim
Transmitted-light microscope	Zeiss
Ultrapure water system Milli Q Aca	Millipore
Vortex-Mixer 7-2020	neoLab
Motorbrüter Type 168D	BRUJA
ADVIA Centaur Testosterone II assay	Siemens Healthcare Diagnostics

7.1.16. Software

Software	Provider
Adobe Photoshop CS4	Adobe Systems Inc.
BD FACS Diva™ Software v.8.0.1	BD Biosciences
ELISA online analysis tool	https://www.myassays.com/
GraphPad Prism v.8.3.1	GraphPad Software Inc.
ImageJ	National Center for Biotechnology Information
LightCycler® 96 software, V 1.1.0.1320	Roche
LinRegPCR	Ruijter et al., 2014
Microsoft Office	Microsoft
Nikon NIS-Elements Advanced Research 4.51	Nikon (Japan)
ADVIA Centaur XP	Siemens Healthcare Diagnostics
Primer BLAST	NCBI (http://www.ncbi.nlm.nih.gov/tools/primer-blast/index.cgi)

7.2. Methods

7.2.1. Ethics statement

Animal experiments were performed in strict accordance with the guidelines of German animal protection law. All animal protocols were approved by the relevant German authority (Behörde für Gesundheit und Verbraucherschutz); license numbers 124/12, 075/17 and 097/19.

7.2.2. Cells and virus

Cell lines of canine cocker spaniel kidney (MDCK II) were grown in modified Eagle's medium (MEM) supplemented with 10 % fetal bovine serum (FBS), 1 % penicillin/streptomycin (P/S) and 1 % L-Glutamine and were cultivated at 5 % CO₂, 96 % rH and 37 °C. The pH1N1 influenza A virus A/Hamburg/NY1580/09 (pH1N1 2009) was grown on MDCK II cells using a multiplicity of infection (MOI) of 0.2. Virus was harvested after 36 hours. Virus titration was performed 72 h post infection on MDCK II cells by plaque assay. The influenza B virus B/Lee/40 was grown in embryonated specified pathogen free (SPF) eggs at 33 °C for three days. 100 µl of virus containing 200 plaque forming units (PFU) were injected into the allantoic fluid of eggs. The virus was harvested by aspirating the allantoic fluid after euthanizing the embryo at 4 °C for four hours. All subsequent steps were performed on ice or at 4 °C. The allantoic fluid of individual eggs was tested for the presence of virus by hemagglutination assay and positive aliquots were pooled. The virus was purified by centrifugation of the allantoic fluid at 5.000 g and 4 °C for 10 min and isolation of the supernatant. Aliquots were stored at -80 °C.

7.2.3. Hemagglutination assay

To confirm productive infection of IBV inoculated eggs after harvest, hemagglutination assays were performed. The hemagglutination assay is a method for virus titration, based on the viral ability to attach to sialic acids on the surface of red blood cells, thus preventing coagulation of these cells in suspension¹⁸⁰. Two-fold dilutions of the samples were prepared in 96-well microtiter plates in PBS and a final volume of 50 µl. 50 µl of a 0.5% chicken red blood cell

solution (in PBS) was added to all wells. After incubation at 4 °C for 30 min, positive wells were identified by negative sedimentation.

7.2.4. Determination of viral titers

Viral titers were determined by plaque assay. 6-well cell culture plates were seeded with 3 ml of MEM containing 2.0×10^5 MDCK II cells and incubated at 37 °C overnight. The virus was 10-fold serially diluted in phosphate buffered saline (PBS). After removing the media from the cells and washing them once with PBS, the cells were infected with 333 μ l virus dilution or diluted organ homogenate per well and incubated at 33 °C (B/Lee/40) or 37 °C (pH1N1 2009) for 1 h. The plates were agitated every 10 minutes to ensure even distribution of the virus. After incubation, the virus supernatant was removed and overlay medium containing 1.25 % Avicel and 0.001 % TPCK-Trypsin in MEM was added to the plates. The cells were incubated 3 days at 37 °C or 4 days at 33 °C for pH1N1 2009 or B/Lee/40 respectively. After incubation, the cells were fixed in 4 % paraformaldehyde solution at 4 °C for 30 min to 24 h. Plaques were visualized by either counterstaining with crystal violet solution (B/Lee/40) or by using IAV nucleoprotein-specific antibody staining and development via a horseradish conjugated secondary antibody and peroxidase substrate.

7.2.5. Methicillin resistant *Staphylococcus aureus* (MRSA)

Methicillin resistant *Staphylococcus aureus* (MRSA) were grown from a CryoBank stem conservation system JB1 for *S. aureus* strain USA300. A stem plate was prepared by plating one unit from the stem conservation system onto a TS-agar plate and overnight incubation at 37 °C. Stem plates were kept for further use at 4 °C for up to three months. Pre-cultures were prepared by transferring one colony from a stem plate into 2 ml of trypticase soy broth (TSB) medium and incubation overnight at 37 °C while shaking at 180 rpm. Main culture for infection were started by preparing a 1:100 dilution of the pre culture in TSB medium. The main culture was incubated at 37 °C and 180 rpm until the bacteria concentration reached 1.42×10^8 colony forming units (CFU)/ml. The bacteria concentration was determined by measuring the optical density (OD_{600}) that was found to correlate to the desired concentration by previous

experiments. For infection, the bacteria were concentrated and subsequently diluted in PBS to a final dose of 1×10^8 CFU per animal. The final concentration was confirmed by re-titration.

7.2.6. Determination of bacterial titers

The bacterial load in murine lung tissue was determined by plating tissue homogenates onto mannitol salt phenol red (MS) agar plates. This is a selective agar and the primary screening medium for detection and identification of MRSA¹⁸¹. Organ homogenates were prepared fresh by homogenizing the lung tissue in 1 ml of PBS in a bead mill at 30 Hz and 4 °C for 10 min. Fresh preparation of the homogenate without any centrifugation steps are necessary to avoid sedimentation of bacteria. 10-fold serial dilutions of the homogenates were prepared in ice cold PBS. 1 ml of homogenate dilution was added to 14 ml of melted MS agar at 65 °C (kept in a water bath after autoclaving) and plated onto 10 cm Petri dishes. MS agar was kept hot for no longer than 6 hours to avoid degradation of components. All measurements were performed in technical duplicates. MS agar plates were incubated at 37 °C for two days before MRSA colonies were identified by shape and color change of the agar.

7.2.7. Animal experiments

Animal experiments were performed in strict accordance with the guidelines of German animal protection law. All animal protocols were approved by the relevant German authority (Behörde für Gesundheit und Verbraucherschutz; protocols 124/12, 075/17 and 097/19).

Eight to ten weeks old female C75BL/6J mice were mated allogenuically to male BALB/c mice (institutional breeding colonies) following standard protocols. Mice were kept under standard housing conditions (21 ± 2 °C, 40–50 % humidity, food and water ad libitum) with a 12:12 light–dark cycle. Animals with an unclear pregnancy status were excluded from subsequent experiments. Pregnant mice at embryonic days (E) E5.5 were anaesthetized with 100 mg/kg ketamine and 10 mg/kg Xylazine and intra-nasally inoculated according to Table 2.

Table 2: Inoculation scheme for pregnant mice at E5.5.

Inoculum	Dose	Volume	Route
PBS	n. a.	50 μ l	Intra-nasally
pH1N1 2009	10^3 PFU	50 μ l	Intra-nasally
Poly(I:C)	4 mg/kg	150 – 250 μ l	Intra-peritoneally

All infection experiments were performed under BSL-2 conditions. Mice were monitored for weight loss and signs of disease until 14 days post infection (d p.i.) or until organ explants and euthanized when reaching the human endpoint, according to the guidelines of animal protection law and the approved protocols by the relevant German authority (Behörde für Gesundheit und Verbraucherschutz Hamburg, approval number 124/12 and 075/17). Some mice were sacrificed on 1, 3 and 6 d p.i. and organs removed for subsequent analysis. Additional groups of mice were euthanized at E17.5 and full-term vital fetuses were counted and morphologically assessed. E17.5 corresponds to 1 – 2 days before birth, to avoid mothers killing potentially sick offspring directly after birth, which would limit the assessment of the reproductive outcome. Additionally, organs were isolated for subsequent analysis. Blood of the fetuses were taken after immediate decapitation. Blood was centrifugated for 15 min at 3,000 g and 4 °C, and the respective plasma was stored at -80 °C. Organs were stored in 4 % formalin solution at 4 °C or dry at -80 °C for subsequent homogenization. For experiments with foster mothers, whole litters of neonates were exchanged between mothers with similar litter size (\pm 2 neonates) within 12 hours after birth. Neonates were marked via tail tip painting and individually weighed every day until 14 days post-partum. Sex of mice were determined by PCR (fetuses and neonates only) or by visual identification. For second hit experiments two- or six-week-old offspring were infected according to Table 3 and Table 4.

Table 3: Inoculation scheme for two-week-old mice

Inoculum	Dose	Volume	Route
PBS	n. a.	10 μ l	Intra-nasally
pH1N1 2009	10^3 PFU	10 μ l	Intra-nasally
B/Lee/40	10^6 PFU	10 μ l	Intra-nasally
MRSA	10^8 CFU	10 μ l	Intra-nasally

Table 4: Inoculation scheme for six-week-old mice

Inoculum	Dose	Volume	Route
PBS	n. a.	50 μ l	Intra-nasally
pH1N1 2009	10^3 PFU	50 μ l	Intra-nasally
B/Lee/40	10^6 PFU	50 μ l	Intra-nasally
MRSA	10^8 CFU	50 μ l	Intra-nasally

All infection experiments were performed under BSL-2 conditions. Mice were monitored for weight loss and signs of disease until 14 days post infection (d p.i.) or until organ explants and euthanized when reaching the human endpoint, according to the guidelines of animal protection law and the approved protocols by the relevant German authority (Behörde für Gesundheit und Verbraucherschutz Hamburg, approval numbers 124/12, 075/17 and 097/19). Some mice were sacrificed on 1, 3 and 6 d p.i. and organs removed for subsequent analysis. Mice were euthanized by cervical dislocation after Isoflurane sedation (3 Vol%) or by decapitation (mice below 2 weeks of age only).

For the analysis of the immune cell profile by flow cytometry as well as the sorting of immune cells by fluorescence activated cell sorting (FACS), two- and six-week-old mice born to treated mothers were euthanized for organ explants without further treatment.

For the adoptive transfer of alveolar macrophages (AMs), donor mice were euthanized with an age of 14 days for isolation of AMs as described below. Sentinel mice with the same age were administered isolated AMs the same day via intra-nasal application. For the adoptive transfer, 1×10^6 AMs were transferred in 20 μ l of sterile PBS. One day after the transfer, the sentinel offspring was subsequently challenged with B/Lee/40 or PBS as described above. After infection offspring was sacrificed on day 3 post infection for organ harvest.

7.2.8. Lung function

All experiments on the assessment of lung function were performed at the Comprehensive Pneumology Center (CPC), Institute of Lung Biology and Disease, Helmholtz Center Munich, German Research Center for Environmental Health, 85764 Neuherberg, Germany (see collaborations).

Mice were anesthetized with ketamine-xylazine, tracheostomized and the lung function analyzed¹⁸². In brief, respiratory function was measured using a flexiVent system (Scireq). Mice were ventilated with a tidal volume of 10 ml/kg at a frequency of 150 breaths/min to reach a mean lung volume similar to that of spontaneous breathing. Testing of lung mechanical properties including dynamic lung compliance was carried out by a software-generated script that took four readings per animal.

7.2.9. Immunohistology and histopathology

Lungs of infected animals were processed for pathological examination and immunohistochemistry according to established protocols. Deparaffinized slides were treated with 0.1 M citrate buffer (pH 6.0) and a rabbit anti-H7N1 serum. The primary antibody (anti-IAV NP) was detected by a biotin-conjugated anti-rabbit antibody (Jackson ImmunoResearch) followed by the application of the Zytochem-Plus HPR kit (Zytomed). Tissues were counterstained with hematoxylin for pathological analysis.

7.2.10. Immune cell analysis and sorting

Two- or six-week-old offspring born to treated mothers (see 7.2.7) was euthanized and organs were explanted for cell isolation. Immune cell analysis was done in collaboration with Prof. Dr. Sonja Loges and Dr. Isabel Ben-Batalla (UKE Hamburg) and Prof. Dr. Bianca Schneider as well as Dr. Jochen Behrens (Research Center Borstel). Cells from lung, spleen, blood, and bone marrow were analyzed.

Table 5: Cell types and corresponding surface markers for FACS analysis of offspring immune cells.

Cell type	Surface marker
B cells	CD3 ⁻ , B220 ⁺
T cells	CD3 ⁺ , B220 ⁻
CD4 ⁺ T cells	CD3 ⁺ , CD4 ⁺ , CD8 ⁻ , B220 ⁻
CD8 ⁺ T cells	CD3 ⁺ , CD4 ⁻ , CD8 ⁺ , B220 ⁻
Treg cells	CD3 ⁺ , CD4 ⁺ , CD25 ⁺ , FoxP3 ⁺
Natural killer cells (NK)	CD3 ⁻ , CD49b ⁺
Macrophages (except lung)	F4/80 ⁺
M1 macrophages (except lung)	F4/80 ⁺ , MHC II ⁺
M2 macrophages (except lung)	F4/80 ⁺ , MRC I ⁺
Hematopoietic progenitor cells	Lin ⁻ , Sca1 ⁻ , cKit ⁺
Hematopoietic stem cells (HSC)	Lin ⁻ , Sca1 ⁺ , cKit ⁺
Granulocyte-monocyte progenitor cells (GMP)	Lin ⁻ , Sca1 ⁻ , cKit ⁺ , CD16/32 ⁺ , CD34 ⁺
Common myeloid progenitor cells (CMP)	Lin ⁻ , Sca1 ⁻ , cKit ⁺ , CD16/32 ^{low} , CD34 ⁺
Megakaryocyte-erythroid progenitor cells (MEP)	Lin ⁻ , Sca1 ⁻ , cKit ⁺ , CD16/32 ⁻ , CD34 ⁻

All cells except for lung macrophages were analyzed by Dr. Isabel Ben-Batalla and Dr. Jochen Behrends. Due to specific characteristics of lung macrophages, they were analyzed separately (Table 6).

Table 6: Cell types and corresponding surface markers for FACS analysis of lung macrophages.

Cell type	Surface marker
Alveolar macrophages (AM, lung only)	SiglecF ⁺ , CD64 ⁺ , cd11c ⁺ , cd11b ⁻
Interstitial macrophages (IM, lung only)	SiglecF ⁺ , CD64 ⁺ , cd11c ⁻ , cd11b ⁺

Organs were harvested immediately after euthanizing the mice by cervical dislocation (six-week-old mice) or decapitation (two-week-old offspring) and full exsanguination. Lung and spleen were minced on ice and transferred into FACS lysis buffer. Organ homogenates were lysed for 30 min at 37 °C with constant agitation. Bone marrow was isolated by cutting the tips of tibia and femur, transferring them into a 0.2 ml reaction tube with a small hole on the bottom, placed into a 1.5 ml reaction tube and subsequent centrifugation at 1.000 g and room

temperature (RT) for 5 min. Single cells were obtained by pushing the lysed organ homogenates through a 70 µm cell strainer. After centrifugation of the single cell solution at 1.500 rpm and 4 °C for 5 min, the supernatant was discarded, and 1 ml red blood cell (RBC) lysis buffer was added. After 5 min of incubation on ice, the cells were centrifuged at 1.500 rpm and 4 °C for 5 min and the supernatant was discarded. After one washing step with FACS buffer, the cell pellet was resuspended in 100 µl of Zombie NIR solution (1:500 in PBS) and incubated for 20 min in the dark and at RT. After one washing step with FACS buffer, the cells were resuspended in the corresponding antibodies using 2 µl antibody for 300 µl FACS buffer containing the cells. Staining was performed for 30 min at RT in the dark. After one washing step using FACS buffer, the supernatant was discarded, and the cells were resuspended in FACS buffer (cell analysis) or RPMI + 2 % BSA for transfer experiments. A representative example gating strategy that was used for sorting alveolar macrophages is shown in Supplementary figure 9.

7.2.11. Cytokine and hormone measurement

Cytokines were determined in supernatants of homogenized lungs, collected from mice at 1, 3 or 6 d p.i. Therefore, lung tissue (approx. 0.05 – 0.10 g) was weighed into 2 ml-O-Ring tubes filled with four to eight metal beads on the day of explant and stored at -80 °C until further use. On the day of measurement, 1 ml of PBS was added to the tissue and the tissue was homogenized as described above. After centrifugation at 6.000 g and 4 °C for 10 min, the supernatants were transferred to a new tube and centrifuged again at 10.000 g and 4 °C for 10 min directly before addition to the Luminex plate. Cytokines (IFN- α , IL-1 β , IL-2, IL-6, IL-10, IL-17A and TNF- α) were then determined using a custom-made Bio-Plex Pro Mouse Cytokine I 7-plex assay (Bio-Rad) following the manufacturer's instructions in a Bio-Plex 200 System with high-throughput fluidics (HTF; Bio-Rad). All measurements were run in duplicate. Progesterone (Cayman Chemical) and corticosterone (ARBOR ASSAYS) levels in maternal serum were evaluated by ELISA following the manufacturer's instructions. For progesterone analysis, serum was diluted 1:100 or 1:200 and measured after 70 min of substrate incubation. All ELISAs were measured on a Sapphire2 ELISA microplate reader (Tecan) and evaluated using a four-parameter logistic regression (MyAssays). To determine serum testosterone levels, a chemiluminescence immunoassay (ADVIA Centaur Testosterone II assay; Siemens Healthcare

Diagnostics) was employed. Measurement was performed with the ADVIA Centaur XP (Siemens Healthcare Diagnostics).

7.2.12. Nutrient gene RT-qPCR of placental tissue

Nutrient gene expression was measured from RNA of homogenized placental tissue taken at E17.5. RNA was isolated using the Analytik Jena kit Innuprep 2.0 following the manufacturer's instructions with additional on-column DNase I-treatment. cDNA was generated using the Superscript™ III Reverse Transcriptase kit (Invitrogen) using random nonamere primers d(N)9 (Gene Link). RT-qPCR was performed to analyze placental gene expression levels of two labyrinthine-specific, growth stimulatory genes, the growth inhibitory Grb10 (growth factor receptor bound protein 10) and the growth stimulatory gene Igf2 (insulin-like growth factor II) and two isoforms of the system A family of amino acid transporters, Slc38a1 (solute carrier family 38, member 1) and Slc38a2 (solute carrier family 38, member 2), which are responsible for transplacental transport of neutral amino acids¹⁵⁶. DNA oligonucleotides for amplification of the target genes as well as the housekeeping gene *Ywhaz* (Tyrosine 3-Monooxygenase/tryptophan 5-monoxygenase activation protein, zeta polypeptide)¹⁸³ were designed using primer-BLAST (<http://www.ncbi.nlm.nih.gov/tools/primer-blast/index.cgi>) and are shown in Table 7.

Table 7: oligonucleotides for placental nutrient gene RT-qPCR

gene	forward 5'-3'	reverse 5'-3'
<i>Ywhaz</i>	CACGCTCCCTAACCTTGCTT	ATCGTAGAAGCCTGACGTGG
<i>Grb10</i>	AAGCGAAGACCGAGATGAAG	CATAGGTGCGTTGAAAGGAG
<i>Igf2</i>	CTTGGATCCCAGAACCCAAGAA	CCCCTTGGTGACATGGGGAC
<i>Slc38a1</i>	CGGGAGAGTAGGAGGAGTCT	GTCTGCTCCCACACATCGTT
<i>Slc38a2</i>	AATGCGATTGTGGGCAGTGG	AGCTTTCCAGCCAGACCATAC

Data were analyzed using LinReg PCR¹⁸⁴.

7.2.13. Sex determination by PCR

The sex of murine fetuses were determined by PCR using SX primers as described in the original publication¹⁸⁵. Fetal tail tips were used for sex determination.

7.2.14. Data analysis

All data were analyzed using Graph Pad Prism v.8.4.2. Statistical details of all experiments are indicated in the respective figure legends. Level of statistical significance was defined as $p < 0.05$ (*equals $p < 0.05$; ** equals $p < 0.01$; *** equals $p < 0.001$). All effects were analyzed for statistical significance as indicated in the respective figure legends, but only significant effects are depicted in the figures.

In general, data sets were not analyzed for normal distribution since small sample size ($n \leq 6$) as well as unequal sample size within data sets that were compared do not allow for proper analysis of normal distribution. Instead, normal distribution of all data sets were assumed due to biological considerations unless indicated otherwise. Technical outliers were defined following good laboratory practice and are clearly indicated in all figure legends. Mathematical outliers were defined within data sets that were considered normally distributed only. Grubb's test was used to identify mathematical outliers for data sets with $n \geq 7$ and mathematical outliers are clearly indicated in all figure legends.

Data sets for weight loss were analyzed using multiple t-testing with one unpaired t-test per row. Tests were performed assuming unequal variances for each group. Statistical significance was corrected for multiple comparisons using the Bonferroni-Dunn method with an α -error of 0.05. Data sets for weight loss were not analyzed by ANOVA because respective treatment groups were compared to control groups independently and results were analyzed in a time-point dependent manner. Thus, single time-point related t-tests were considered ideal.

Survival data were analyzed using a log rank test for trend.

Grouped or column-presented data sets like titers and cytokines were analyzed using two-tailed, unpaired t-test with Welch's correction assuming unequal variances. As described above a normal distribution of these data sets was presupposed by biological consideration. When multiple time-points were applicable, data sets were only analyzed per respective time-point. Thus, no ANOVA or correction for multiple comparisons were performed.

In general, it should be considered, that statistical analysis of these data should be evaluated with care. No case number planning was possible, since all experiments were performed in a novel setup without known effect size for the parameters to be measured. Hence, statistical claims of this study should be considered as descriptive.

7.2.15. Collaborations

Listed below are all methods performed by internal and external collaboration partners. This does not include experimental design, data evaluation and interpretation.

7.2.15.1. Lung function

Assessment of lung function and pathology in adult offspring (Supplementary figure 4) was performed by Aicha Jeridi and Ali Önder Yildirim. These analysis were performed in the context of a pipeline screening that is offered by the German Mouse Clinic in Munich (<https://www.mouseclinic.de/screens/lung-function-optional/lung-function-optional/index.html>).

Contact: Dr. Ali Önder Yildirim
Comprehensive Pneumology Center (CPC), Institute of Lung Biology and Disease, Helmholtz Center Munich, German Research Center for Environmental Health, 85764 Neuherberg, Germany

7.2.15.2. Nutrition gene RT-qPCR of placental tissue

The analysis of nutrition genes (Table 7) by qPCR was performed by Nancy Kouassi. This includes performance of the assay and primer design.

Contact: Nancy Kouassi
Heinrich Pette Institute
Department 61

7.2.15.3. Analysis of cell populations by flow cytometry

Flow cytometric analysis of immune cells as listed in Table 5 were performed by Dr. Isabel Ben-Batalla. This includes cell preparation, staining and the analysis of immune cells from two- and six-week-old offspring born to PBS or poly(I:C)-treated as well as IAV-infected dams. Per each group four male and four female mice were analyzed.

Contact:	Dr. Isabel Ben-Batalla	Medical Center Hamburg-Eppendorf
	Prof. Dr. Sonja Loges	Medical Center Hamburg-Eppendorf

All data acquired by Dr. Isabel Ben-Batalla were additionally analyzed by Dr. Jochen Behrens who revised the gating. Additionally, Dr. Jochen Behrens performed the analysis of all immune cells listed in Table 6. This includes gating and data analysis.

Contact:	Dr. Jochen Behrens	Research Center Borstel
	Prof. Dr. Bianca Schneider	Research Center Borstel

7.2.15.4. Measurement of testosterone from plasma

Measurements of murine plasma testosterone were performed at the Medical Centre Hamburg-Eppendorf, Central Centre for Diagnostics.

Contact:	Prof. Dr. Dr. Thomas René	Medical Center Hamburg-Eppendorf
----------	---------------------------	----------------------------------

7.2.15.5. Immunohistology and histopathology

Histological preparations and staining were performed by Gundula Pilnitz-Stolze. This includes treatment of formalin fixed samples, preparation of slides, staining and fixation.

Contact:	Gundula Pilnitz-Stolze	Heinrich Pette Institute
		Core facility: Imaging

8. Literature

1. Iuliano, A. D. *et al.* Estimates of global seasonal influenza-associated respiratory mortality: a modelling study. *The Lancet* **391**, 1285–1300 (2018).
2. Lofgren, E., Fefferman, N. H., Naumov, Y. N., Gorski, J. & Naumova, E. N. Influenza Seasonality: Underlying Causes and Modeling Theories. *Journal of Virology* **81**, 5429–5436 (2007).
3. Matsuzaki, Y. *et al.* Clinical Features of Influenza C Virus Infection in Children. *J Infect Dis* **193**, 1229–1235 (2006).
4. Hay, A. J., Gregory, V., Douglas, A. R. & Lin, Y. P. The evolution of human influenza viruses. *Philos Trans R Soc Lond B Biol Sci* **356**, 1861–1870 (2001).
5. Kawaoka Y, Palese P. Family Orthomyxoviridae. *Elsevier Academic Press* 681–693 (2005).
6. Kaul, K. L. *et al.* Influenza A Subtyping. *J Mol Diagn* **12**, 664–669 (2010).
7. Tong, S. *et al.* A distinct lineage of influenza A virus from bats. *Proc. Natl. Acad. Sci. U.S.A.* **109**, 4269–4274 (2012).
8. Mehle, A. Unusual Influenza A Viruses in Bats. *Viruses* **6**, 3438–3449 (2014).
9. Bouvier, N. M. & Palese, P. The biology of influenza viruses. *Vaccine* **26 Suppl 4**, D49-53 (2008).
10. Noda, T. Native Morphology of Influenza Virions. *Front Microbiol* **2**, (2012).
11. Palese P, Shaw ML. Orthomyxoviridae: The Viruses and their Replication. *Fields Virology* (2007).
12. Zebedee, S. L. & Lamb, R. A. Influenza A virus M2 protein: monoclonal antibody restriction of virus growth and detection of M2 in virions. *J Virol* **62**, 2762–2772 (1988).
13. Noda, T. & Kawaoka, Y. Structure of influenza virus ribonucleoprotein complexes and their packaging into virions. *Rev. Med. Virol.* **20**, 380–391 (2010).
14. Horimoto, T. & Kawaoka, Y. Influenza: lessons from past pandemics, warnings from current incidents. *Nat. Rev. Microbiol.* **3**, 591–600 (2005).
15. Webster, R. G., Bean, W. J., Gorman, O. T., Chambers, T. M. & Kawaoka, Y. Evolution and ecology of influenza A viruses. *Microbiol Rev* **56**, 152–179 (1992).
16. Mostafa, A., Abdelwhab, E. M., Mettenleiter, T. C. & Pleschka, S. Zoonotic Potential of Influenza A Viruses: A Comprehensive Overview. *Viruses* **10**, (2018).
17. Daszak, P., Cunningham, A. A. & Hyatt, A. D. Emerging infectious diseases of wildlife--threats to biodiversity and human health. *Science* **287**, 443–449 (2000).
18. Verhagen, J. H., Herfst, S. & Fouchier, R. A. M. How a virus travels the world. *Science* **347**, 616–617 (2015).
19. van Dijk, J. G., Verhagen, J. H., Wille, M. & Waldenström, J. Host and virus ecology as determinants of influenza A virus transmission in wild birds. *Current Opinion in Virology* **28**, 26–36 (2018).
20. Parrish, C. R., Murcia, P. R. & Holmes, E. C. Influenza Virus Reservoirs and Intermediate Hosts: Dogs, Horses, and New Possibilities for Influenza Virus Exposure of Humans. *Journal of Virology* **89**, 2990–2994 (2015).
21. Hinshaw, V. S., Webster, R. G., Easterday, B. C. & Bean, W. J. Replication of avian influenza A viruses in mammals. *Infect. Immun.* **34**, 354–361 (1981).
22. Long, J. S., Mistry, B., Haslam, S. M. & Barclay, W. S. Host and viral determinants of influenza A virus species specificity. *Nat. Rev. Microbiol.* **17**, 67–81 (2019).
23. Neumann, G., Noda, T. & Kawaoka, Y. Emergence and pandemic potential of swine-origin H1N1 influenza virus. *Nature* **459**, 931–939 (2009).

24. Yassine, H. M., Lee, C.-W. & Saif, Y. M. Interspecies Transmission of Influenza A Viruses Between Swine and Poultry. in *Swine Influenza* (eds. Richt, J. A. & Webby, R. J.) 227–240 (Springer, 2013). doi:10.1007/82_2011_180.
25. Couceiro, J. N., Paulson, J. C. & Baum, L. G. Influenza virus strains selectively recognize sialyloligosaccharides on human respiratory epithelium; the role of the host cell in selection of hemagglutinin receptor specificity. *Virus Res.* **29**, 155–165 (1993).
26. Matrosovich, M. N., Matrosovich, T. Y., Gray, T., Roberts, N. A. & Klenk, H.-D. Human and avian influenza viruses target different cell types in cultures of human airway epithelium. *Proc. Natl. Acad. Sci. U.S.A.* **101**, 4620–4624 (2004).
27. van Riel, D. *et al.* Human and Avian Influenza Viruses Target Different Cells in the Lower Respiratory Tract of Humans and Other Mammals. *Am J Pathol* **171**, 1215–1223 (2007).
28. Beare, A. S. & Webster, R. G. Replication of avian influenza viruses in humans. *Archives of Virology* **119**, 37–42 (1991).
29. Long, J. S., Mistry, B., Haslam, S. M. & Barclay, W. S. Host and viral determinants of influenza A virus species specificity. *Nat. Rev. Microbiol.* **17**, 67–81 (2019).
30. Steinhauer, D. A. & Holland, J. J. Rapid evolution of RNA viruses. *Annu. Rev. Microbiol.* **41**, 409–433 (1987).
31. Holland, J. *et al.* Rapid evolution of RNA genomes. *Science* **215**, 1577–1585 (1982).
32. Steel, J. & Lowen, A. C. Influenza A Virus Reassortment. in *Influenza Pathogenesis and Control - Volume I* (eds. Compans, R. W. & Oldstone, M. B. A.) 377–401 (Springer International Publishing, 2014). doi:10.1007/82_2014_395.
33. Ito, T. *et al.* Molecular basis for the generation in pigs of influenza A viruses with pandemic potential. *J. Virol.* **72**, 7367–7373 (1998).
34. Scholtissek, C. Molecular evolution of influenza viruses. *Virus Genes* **11**, 209–215 (1995).
35. Webster, R. G., Sharp, G. B. & Claas, E. C. Interspecies transmission of influenza viruses. *Am. J. Respir. Crit. Care Med.* **152**, S25–30 (1995).
36. Kilbourne, E. D. Influenza Pandemics of the 20th Century. *Emerg Infect Dis* **12**, 9–14 (2006).
37. Murray, C. J. L., Lopez, A. D., Chin, B., Feehan, D. & Hill, K. H. Estimation of potential global pandemic influenza mortality on the basis of vital registry data from the 1918–20 pandemic: a quantitative analysis. *Lancet* **368**, 2211–2218 (2006).
38. Johnson, N. P. A. S. & Mueller, J. Updating the accounts: global mortality of the 1918–1920 ‘Spanish’ influenza pandemic. *Bull Hist Med* **76**, 105–115 (2002).
39. Emergence of a Novel Swine-Origin Influenza A (H1N1) Virus in Humans | NEJM. https://www.nejm.org/doi/10.1056/NEJMoa0903810?url_ver=Z39.88-2003&rfr_id=ori%3Arid%3Acrossref.org&rfr_dat=cr_pub%3Dwww.ncbi.nlm.nih.gov.
40. Dawood, F. S. *et al.* Estimated global mortality associated with the first 12 months of 2009 pandemic influenza A H1N1 virus circulation: a modelling study. *Lancet Infect Dis* **12**, 687–695 (2012).
41. Allen, J. D. & Ross, T. M. H3N2 influenza viruses in humans: Viral mechanisms, evolution, and evaluation. *Hum Vaccin Immunother* **14**, 1840–1847 (2018).
42. CDC. How to Prevent Flu. https://www.cdc.gov/flu/prevent/prevention.htm?CDC_AA_refVal=https%3A%2F%2Fwww.cdc.gov%2Fflu%2Fconsumer%2Fprevention.htm (2019).
43. WHO. Influenza (Seasonal). [https://www.who.int/news-room/fact-sheets/detail/influenza-\(seasonal\)](https://www.who.int/news-room/fact-sheets/detail/influenza-(seasonal)) (2018).

44. ECDC. Factsheet about seasonal influenza. <https://www.ecdc.europa.eu/en/seasonal-influenza/facts/factsheet> (2020).
45. Houser, K. & Subbarao, K. Influenza Vaccines: Challenges and Solutions. *Cell Host Microbe* **17**, 295–300 (2015).
46. Wong, S.-S. & Webby, R. J. Traditional and new influenza vaccines. *Clin. Microbiol. Rev.* **26**, 476–492 (2013).
47. Estrada, L. D. & Schultz-Cherry, S. Development of a Universal Influenza Vaccine. *J Immunol* **202**, 392–398 (2019).
48. Cox, M. M. J., Patriarca, P. A. & Treanor, J. FluBlok, a recombinant hemagglutinin influenza vaccine. *Influenza Other Respir Viruses* **2**, 211–219 (2008).
49. Hoffmann, E. *et al.* Multiple gene segments control the temperature sensitivity and attenuation phenotypes of ca B/Ann Arbor/1/66. *J. Virol.* **79**, 11014–11021 (2005).
50. Jin, H. *et al.* Multiple amino acid residues confer temperature sensitivity to human influenza virus vaccine strains (FluMist) derived from cold-adapted A/Ann Arbor/6/60. *Virology* **306**, 18–24 (2003).
51. Hoft, D. F. *et al.* Live and inactivated influenza vaccines induce similar humoral responses, but only live vaccines induce diverse T-cell responses in young children. *J. Infect. Dis.* **204**, 845–853 (2011).
52. Mohn, K. G.-I. *et al.* Longevity of B-cell and T-cell responses after live attenuated influenza vaccination in children. *J. Infect. Dis.* **211**, 1541–1549 (2015).
53. European Centre for Disease Prevention and Control. Seasonal influenza vaccination and antiviral use in EU/EEA Member States – Overview of vaccine recommendations for 2017–2018 and vaccination coverage rates for 2015–2016 and 2016–2017 influenza seasons. *ECDC Technical Report* (2018).
54. Nachbagauer, R. *et al.* A universal influenza virus vaccine candidate confers protection against pandemic H1N1 infection in preclinical ferret studies. *npj Vaccines* **2**, 1–13 (2017).
55. Nachbagauer, R. & Krammer, F. Universal influenza virus vaccines and therapeutic antibodies. *Clin. Microbiol. Infect.* **23**, 222–228 (2017).
56. CDC. 2016–2017 Flu Vaccine Nearly 50 Percent Effective. <https://www.aafp.org/news/health-of-the-public/20170221fluvacceffect.html> (2017).
57. CDC. What You Should Know for the 2017–2018 Influenza Season. *Centers for Disease Control and Prevention* <https://www.cdc.gov/flu/about/season/flu-season-2017-2018.htm> (2019).
58. Flannery, B. Interim Estimates of 2017–18 Seasonal Influenza Vaccine Effectiveness — United States, February 2018. *MMWR Morb Mortal Wkly Rep* **67**, (2018).
59. Uyeki, T. M. *et al.* Clinical Practice Guidelines by the Infectious Diseases Society of America: 2018 Update on Diagnosis, Treatment, Chemoprophylaxis, and Institutional Outbreak Management of Seasonal Influenza a. *Clin. Infect. Dis.* **68**, e1–e47 (2019).
60. European Medicines Agency. Antiviral medicines for pandemic influenza. <https://www.ema.europa.eu/en/human-regulatory/overview/public-health-threats/pandemic-influenza/antiviral-medicines-pandemic-influenza> (2018).
61. Hwang, S. G. *et al.* Rapid and simple detection of Tamiflu-resistant influenza virus: Development of oseltamivir derivative-based lateral flow biosensor for point-of-care (POC) diagnostics. *Scientific Reports* **8**, 1–11 (2018).
62. Hayden, F. G. & Shindo, N. Influenza virus polymerase inhibitors in clinical development. *Curr Opin Infect Dis* **32**, 176–186 (2019).

63. Chow, E. J., Doyle, J. D. & Uyeki, T. M. Influenza virus-related critical illness: prevention, diagnosis, treatment. *Crit Care* **23**, (2019).
64. CDC. Burden of Influenza. *Centers for Disease Control and Prevention* <https://www.cdc.gov/flu/about/burden/index.html> (2020).
65. Thompson, W. W. *et al.* Estimates of US influenza-associated deaths made using four different methods. *Influenza Other Respir Viruses* **3**, 37–49 (2009).
66. Ompad, D. C., Galea, S. & Vlahov, D. Distribution of Influenza Vaccine to High-Risk Groups. *Epidemiol Rev* **28**, 54–70 (2006).
67. Incidence of Influenza in Healthy Adults and Healthcare Workers: A Systematic Review and Meta-Analysis. <https://journals.plos.org/plosone/article?id=10.1371/journal.pone.0026239>.
68. CDC. People at High Risk of Flu. *Centers for Disease Control and Prevention* <https://www.cdc.gov/flu/highrisk/index.htm> (2018).
69. Risk groups for severe influenza. *European Centre for Disease Prevention and Control* <https://www.ecdc.europa.eu/en/seasonal-influenza/prevention-and-control/vaccines/risk-groups>.
70. Thompson, W. W., Comanor, L. & Shay, D. K. Epidemiology of seasonal influenza: use of surveillance data and statistical models to estimate the burden of disease. *J. Infect. Dis.* **194 Suppl 2**, S82-91 (2006).
71. Rothberg, M. B., Haessler, S. D. & Brown, R. B. Complications of Viral Influenza. *The American Journal of Medicine* **121**, 258–264 (2008).
72. Smetana, J., Chlibek, R., Shaw, J., Splino, M. & Prymula, R. Influenza vaccination in the elderly. *Hum Vaccin Immunother* **14**, 540–549 (2017).
73. Goodwin, K., Viboud, C. & Simonsen, L. Antibody response to influenza vaccination in the elderly: a quantitative review. *Vaccine* **24**, 1159–1169 (2006).
74. Moro-García, M. A., Alonso-Arias, R. & López-Larrea, C. Molecular mechanisms involved in the aging of the T-cell immune response. *Curr. Genomics* **13**, 589–602 (2012).
75. Miller, R. A. The aging immune system: primer and prospectus. *Science* **273**, 70–74 (1996).
76. Han, S. N. & Meydani, S. N. Antioxidants, Cytokines, and Influenza Infection in Aged Mice and Elderly Humans. *J Infect Dis* **182**, S74–S80 (2000).
77. Angstwurm, M. W. A., Gaertner, R. & Schopohl, J. Outcome in elderly patients with severe infection is influenced by sex hormones but not gender. *Crit. Care Med.* **33**, 2786–2793 (2005).
78. Jiang, Y. *et al.* Adiponectin exacerbates influenza infection in elderly individuals via IL-18. *Signal Transduction and Targeted Therapy* **5**, 1–3 (2020).
79. Fowlkes, A. L. *et al.* Epidemiology of 2009 pandemic influenza A (H1N1) deaths in the United States, April-July 2009. *Clin. Infect. Dis.* **52 Suppl 1**, S60-68 (2011).
80. Veerapandian, R., Snyder, J. D. & Samarasinghe, A. E. Influenza in Asthmatics: For Better or for Worse? *Front Immunol* **9**, (2018).
81. Jain, S. *et al.* Hospitalized patients with 2009 H1N1 influenza in the United States, April-June 2009. *N. Engl. J. Med.* **361**, 1935–1944 (2009).
82. Van Kerkhove, M. D. *et al.* Risk factors for severe outcomes following 2009 influenza A (H1N1) infection: a global pooled analysis. *PLoS Med.* **8**, e1001053 (2011).
83. Rothberg, M. B. & Haessler, S. D. Complications of seasonal and pandemic influenza. *Crit. Care Med.* **38**, e91-97 (2010).
84. Bramley, A. M. *et al.* Intensive care unit patients with 2009 pandemic influenza A (H1N1pdm09) virus infection - United States, 2009. *Influenza Other Respir Viruses* **6**, e134-142 (2012).

85. Díaz, E. *et al.* Impact of obesity in patients infected with 2009 influenza A(H1N1). *Chest* **139**, 382–386 (2011).
86. Thompson, W. W. *et al.* Influenza-associated hospitalizations in the United States. *JAMA* **292**, 1333–1340 (2004).
87. Neuzil, K. M. *et al.* Burden of Interpandemic Influenza in Children Younger than 5 Years: A 25-Year Prospective Study. *J Infect Dis* **185**, 147–152 (2002).
88. O’Brien, M. A. *et al.* Incidence of outpatient visits and hospitalizations related to influenza in infants and young children. *Pediatrics* **113**, 585–593 (2004).
89. Izurieta, H. S. *et al.* Influenza and the rates of hospitalization for respiratory disease among infants and young children. *N. Engl. J. Med.* **342**, 232–239 (2000).
90. Halasa, N. B. Update on the 2009 pandemic influenza A H1N1 in children. *Curr. Opin. Pediatr.* **22**, 83–87 (2010).
91. Nair, H. *et al.* Global burden of respiratory infections due to seasonal influenza in young children: a systematic review and meta-analysis. *Lancet* **378**, 1917–1930 (2011).
92. Viboud, C. *et al.* Risk factors of influenza transmission in households. *Br J Gen Pract* **54**, 684–689 (2004).
93. Rasmussen, S. A., Jamieson, D. J. & Uyeki, T. M. Effects of influenza on pregnant women and infants. *American Journal of Obstetrics & Gynecology* **207**, S3–S8 (2012).
94. Louie, J. K. *et al.* Children hospitalized with 2009 novel influenza A(H1N1) in California. *Arch Pediatr Adolesc Med* **164**, 1023–1031 (2010).
95. Libster, R. *et al.* Pediatric hospitalizations associated with 2009 pandemic influenza A (H1N1) in Argentina. *N. Engl. J. Med.* **362**, 45–55 (2010).
96. Fiore, A. E. *et al.* Antiviral agents for the treatment and chemoprophylaxis of influenza --- recommendations of the Advisory Committee on Immunization Practices (ACIP). *MMWR Recomm Rep* **60**, 1–24 (2011).
97. Jamieson, D. J. H1N1 2009 influenza virus infection during pregnancy in the USA. **374**, 8 (2009).
98. van Riel, D. *et al.* Influenza pathogenicity during pregnancy in women and animal models. *Semin Immunopathol* **38**, 719–726 (2016).
99. Raj, R. S., Bonney, E. A. & Phillippe, M. Influenza, Immune System, and Pregnancy. *Reprod Sci* **21**, 1434–1451 (2014).
100. Engels, G. *et al.* Pregnancy-Related Immune Adaptation Promotes the Emergence of Highly Virulent H1N1 Influenza Virus Strains in Allogeneically Pregnant Mice. *Cell Host & Microbe* **21**, 321–333 (2017).
101. ács, Ná., Bánhidly, F., Puhó, E. & Czeizel, A. E. Maternal influenza during pregnancy and risk of congenital abnormalities in offspring. *Birth Defect Res A* **73**, 989–996 (2005).
102. Fell, D. *et al.* Maternal influenza and birth outcomes: systematic review of comparative studies. *BJOG: Int J Obstet Gy* **124**, 48–59 (2017).
103. Smith, S. E. P., Li, J., Garbett, K., Mirnics, K. & Patterson, P. H. Maternal Immune Activation Alters Fetal Brain Development through Interleukin-6. *Journal of Neuroscience* **27**, 10695–10702 (2007).
104. Mosby, L. G., Rasmussen, S. A. & Jamieson, D. J. 2009 pandemic influenza A (H1N1) in pregnancy: a systematic review of the literature. *American Journal of Obstetrics and Gynecology* **205**, 10–18 (2011).
105. Arck, P. C. & Hecher, K. Fetomaternal immune cross-talk and its consequences for maternal and offspring’s health. *Nature Medicine* **19**, 548–556 (2013).

106. Nancy, P. *et al.* Chemokine gene silencing in decidual stromal cells limits T cell access to the maternal-fetal interface. *Science* **336**, 1317–1321 (2012).
107. Blois, S. M. *et al.* A pivotal role for galectin-1 in fetomaternal tolerance. *Nature Medicine* **13**, 1450–1457 (2007).
108. Segerer, S. E. *et al.* The glycoprotein-hormones activin A and inhibin A interfere with dendritic cell maturation. *Reprod Biol Endocrinol* **6**, 17 (2008).
109. Solano, M. E. *et al.* Progesterone and HMOX-1 promote fetal growth by CD8⁺ T cell modulation. *J Clin Invest* **125**, 1726–1738 (2015).
110. Moffett, A. & Colucci, F. Uterine NK cells: active regulators at the maternal-fetal interface. *J Clin Invest* **124**, 1872–1879 (2014).
111. Muzzio, D. O. *et al.* B Cell Development Undergoes Profound Modifications and Adaptations During Pregnancy in Mice. *Biol Reprod* **91**, (2014).
112. Gabriel, G. & Arck, P. C. Sex, Immunity and Influenza. *J Infect Dis* **209**, S93–S99 (2014).
113. Grimaldi, C. M., Cleary, J., Dagtas, A. S., Moussai, D. & Diamond, B. Estrogen alters thresholds for B cell apoptosis and activation. *J. Clin. Invest.* **109**, 1625–1633 (2002).
114. Boulanger-Bertolus, J., Pancaro, C. & Mashour, G. A. Increasing Role of Maternal Immune Activation in Neurodevelopmental Disorders. *Front. Behav. Neurosci.* **12**, (2018).
115. Graham, A. M. *et al.* Maternal Systemic Interleukin-6 During Pregnancy is Associated with Newborn Amygdala Phenotypes and Subsequent Behavior at 2-years-of-age. *Biol Psychiatry* **83**, 109–119 (2018).
116. Meyer, U., Feldon, J., Schedlowski, M. & Yee, B. K. Immunological stress at the maternal–foetal interface: A link between neurodevelopment and adult psychopathology. *Brain, Behavior, and Immunity* **20**, 378–388 (2006).
117. Meyer, U., Yee, B. K. & Feldon, J. The Neurodevelopmental Impact of Prenatal Infections at Different Times of Pregnancy: The Earlier the Worse? *Neuroscientist* **13**, 241–256 (2007).
118. Brown, A. S. & Susser, E. S. In utero infection and adult schizophrenia. *Mental Retardation and Developmental Disabilities Research Reviews* **8**, 51–57 (2002).
119. Cannon, M. & Clarke, M. C. Risk for schizophrenia — broadening the concepts, pushing back the boundaries. *Schizophrenia Research* **79**, 5–13 (2005).
120. Francis, D. *et al.* The Role of Early Environmental Events in Regulating Neuroendocrine Development: Moms, Pups, Stress, and Glucocorticoid Receptors. *Annals of the New York Academy of Sciences* **794**, 136–152 (1996).
121. Gunnar, M. R. Quality of Early Care and Buffering of Neuroendocrine Stress Reactions: Potential Effects on the Developing Human Brain. *Preventive Medicine* **27**, 208–211 (1998).
122. van der Lubbe, J. E. M. *et al.* Maternal antibodies protect offspring from severe influenza infection and do not lead to detectable interference with subsequent offspring immunization. *Virology Journal* **14**, 123 (2017).
123. Wilcox, C. R. & Jones, C. E. Beyond Passive Immunity: Is There Priming of the Fetal Immune System Following Vaccination in Pregnancy and What Are the Potential Clinical Implications? *Front. Immunol.* **9**, (2018).
124. Hodyl, N. A., Krivanek, K. M., Lawrence, E., Clifton, V. L. & Hodgson, D. M. Prenatal exposure to a pro-inflammatory stimulus causes delays in the development of the innate immune response to LPS in the offspring. *Journal of Neuroimmunology* **190**, 61–71 (2007).
125. Kay, G., Tarcic, N., Poltyrev, T. & Weinstock, M. Prenatal Stress Depresses Immune Function in Rats. *Physiology & Behavior* **63**, 397–402 (1998).

126. Mandal, M., Marzouk, A. C., Donnelly, R. & Ponzio, N. M. Preferential development of Th17 cells in offspring of immunostimulated pregnant mice. *Journal of Reproductive Immunology* **87**, 97–100 (2010).
127. Thornburg, K. L., Shannon, J., Thuillier, P. & Turker, M. S. In utero life and epigenetic predisposition for disease. *Adv. Genet.* **71**, 57–78 (2010).
128. Gluckman, P. D., Hanson, M. A., Cooper, C. & Thornburg, K. L. Effect of In Utero and Early-Life Conditions on Adult Health and Disease. *N Engl J Med* **359**, 61–73 (2008).
129. Hodyl, N. A., Stark, M. J., Osei-Kumah, A. & Clifton, V. L. Prenatal programming of the innate immune response following in utero exposure to inflammation: a sexually dimorphic process? *Expert Review of Clinical Immunology* **7**, 579–592 (2011).
130. Brown, A. S. & Meyer, U. Maternal Immune Activation and Neuropsychiatric Illness: A Translational Research Perspective. *AJP* **175**, 1073–1083 (2018).
131. Meyer, U. & Feldon, J. Epidemiology-driven neurodevelopmental animal models of schizophrenia. *Progress in Neurobiology* **90**, 285–326 (2010).
132. Estes, M. L. & McAllister, A. K. Maternal immune activation: Implications for neuropsychiatric disorders. *Science* **353**, 772–777 (2016).
133. Weber-Stadlbauer, U. & Meyer, U. Challenges and opportunities of a-priori and a-posteriori variability in maternal immune activation models. *Current Opinion in Behavioral Sciences* **28**, 119–128 (2019).
134. Frost, E. L., Lammert, C. R., Johanson, D. M., Zunder, E. R. & Lukens, J. R. Sex bias in maternal immune activation-induced neurodevelopmental disease begins at the maternal-fetal interface. *The Journal of Immunology* **204**, 79.13–79.13 (2020).
135. Gogos, A., Sbisa, A., Witkamp, D. & Buuse, M. van den. Sex differences in the effect of maternal immune activation on cognitive and psychosis-like behaviour in Long Evans rats. *European Journal of Neuroscience*.
136. Matsumoto, M. & Seya, T. TLR3: interferon induction by double-stranded RNA including poly(I:C). *Advanced drug delivery reviews* **60**, 805–812 (2008).
137. Van Amersfoort, E. S., Van Berkel, T. J. C. & Kuiper, J. Receptors, Mediators, and Mechanisms Involved in Bacterial Sepsis and Septic Shock. *Clin Microbiol Rev* **16**, 379–414 (2003).
138. Reisinger, S. *et al.* The Poly(I:C)-induced maternal immune activation model in preclinical neuropsychiatric drug discovery. *Pharmacology & Therapeutics* **149**, 213–226 (2015).
139. Cunningham, C., Campion, S., Teeling, J., Felton, L. & Perry, V. H. The sickness behaviour and CNS inflammatory mediator profile induced by systemic challenge of mice with synthetic double-stranded RNA (poly I:C). *Brain, Behavior, and Immunity* **21**, 490–502 (2007).
140. Meyer, U. *et al.* The Time of Prenatal Immune Challenge Determines the Specificity of Inflammation-Mediated Brain and Behavioral Pathology. *J. Neurosci.* **26**, 4752–4762 (2006).
141. Wolff, Amy. R. & Bilkey, David. K. The maternal immune activation (MIA) model of schizophrenia produces pre-pulse inhibition (PPI) deficits in both juvenile and adult rats but these effects are not associated with maternal weight loss. *Behavioural Brain Research* **213**, 323–327 (2010).
142. Fortier, M.-E., Luheshi, G. N. & Boksa, P. Effects of prenatal infection on prepulse inhibition in the rat depend on the nature of the infectious agent and the stage of pregnancy. *Behavioural Brain Research* **181**, 270–277 (2007).
143. Mednick, S. A., Machon, R. A., Huttunen, M. O. & Bonett, D. Adult schizophrenia following prenatal exposure to an influenza epidemic. *Arch. Gen. Psychiatry* **45**, 189–192 (1988).
144. Barr, C. E., Mednick, S. A. & Munk-Jorgensen, P. Exposure to influenza epidemics during gestation and adult schizophrenia. A 40-year study. *Arch. Gen. Psychiatry* **47**, 869–874 (1990).

145. O'Callaghan, E., Sham, P., Takei, N., Glover, G. & Murray, R. M. Schizophrenia after prenatal exposure to 1957 A2 influenza epidemic. *Lancet* **337**, 1248–1250 (1991).
146. Chan, K.-H. *et al.* Wild Type and Mutant 2009 Pandemic Influenza A (H1N1) Viruses Cause More Severe Disease and Higher Mortality in Pregnant BALB/c Mice. *PLOS ONE* **5**, e13757 (2010).
147. Marcelin, G. *et al.* Fatal outcome of pandemic H1N1 2009 influenza virus infection is associated with immunopathology and impaired lung repair, not enhanced viral burden, in pregnant mice. *J. Virol.* **85**, 11208–11219 (2011).
148. Kim, H. M., Kang, Y. M., Song, B. M., Kim, H. S. & Seo, S. H. The 2009 pandemic H1N1 influenza virus is more pathogenic in pregnant mice than seasonal H1N1 influenza virus. *Viral Immunol.* **25**, 402–410 (2012).
149. Meyer, U., Yee, B. K. & Feldon, J. The Neurodevelopmental Impact of Prenatal Infections at Different Times of Pregnancy: The Earlier the Worse? *Neuroscientist* **13**, 241–256 (2007).
150. Kim, J. C. *et al.* Severe pathogenesis of influenza B virus in pregnant mice. *Virology* **448**, 74–81 (2014).
151. O'Hare, T. & Creed, F. Life Events and Miscarriage. *The British Journal of Psychiatry* **167**, 799–805 (1995).
152. Arck, P. C. Stress and Pregnancy Loss: Role of Immune Mediators, Hormones and Neurotransmitters. *American Journal of Reproductive Immunology* **46**, 117–123 (2001).
153. MacNiven, E. & de Catanzaro, D. Reversal of stress-induced pregnancy blocks in mice by progesterone and metyrapone. *Physiology & Behavior* **47**, 443–448 (1990).
154. Cuffe, J. S. M., O'Sullivan, L., Simmons, D. G., Anderson, S. T. & Moritz, K. M. Maternal corticosterone exposure in the mouse has sex-specific effects on placental growth and mRNA expression. *Endocrinology* **153**, 5500–5511 (2012).
155. Vaughan, O. R., Sferruzzi-Perri, A. N. & Fowden, A. L. Maternal corticosterone regulates nutrient allocation to fetal growth in mice. *The Journal of Physiology* **590**, 5529–5540 (2012).
156. Coan, P. M. *et al.* Adaptations in placental nutrient transfer capacity to meet fetal growth demands depend on placental size in mice. *J. Physiol. (Lond.)* **586**, 4567–4576 (2008).
157. He, S., Allen, J. C., Malhotra, R., Østbye, T. & Tan, T. C. Association of maternal serum progesterone in early pregnancy with low birth weight and other adverse pregnancy outcomes. *J. Matern. Fetal. Neonatal. Med.* **29**, 1999–2004 (2016).
158. Hutcheon, J. A., McNamara, H., Platt, R. W., Benjamin, A. & Kramer, M. S. Placental weight for gestational age and adverse perinatal outcomes. *Obstet Gynecol* **119**, 1251–1258 (2012).
159. Nomura, Y. *et al.* Low birth weight and risk of affective disorders and selected medical illness in offspring at high and low risk for depression. *Comprehensive Psychiatry* **48**, 470–478 (2007).
160. Kehl, S. *et al.* Induction of Labour in Growth Restricted and Small for Gestational Age Foetuses – A Historical Cohort Study. *Geburtshilfe Frauenheilkd* **79**, 402–408 (2019).
161. Schlaudecker, E. P. *et al.* Small for gestational age: Case definition & guidelines for data collection, analysis, and presentation of maternal immunisation safety data. *Vaccine* **35**, 6518 (2017).
162. Zager, A., Pinheiro, M. L., Ferraz-de-Paula, V., Ribeiro, A. & Palermo-Neto, J. Increased cell-mediated immunity in male mice offspring exposed to maternal immune activation during late gestation. *Int. Immunopharmacol.* **17**, 633–637 (2013).
163. Onore, C. E., Schwartzer, J. J., Careaga, M., Bennan, R. F. & Ashwood, P. Maternal immune activation leads to activated inflammatory macrophages in offspring. *Brain Behav Immun* **38**, 220–226 (2014).
164. Cheng, H., Zheng, Z. & Cheng, T. New paradigms on hematopoietic stem cell differentiation. *Protein Cell* **11**, 34–44 (2020).

165. Choi, K.-D., Vodyanik, M. & Slukvin, I. I. The Hematopoietic Differentiation and Production of Mature Myeloid Cells from Human Pluripotent Stem Cells. *Nat Protoc* **6**, 296–313 (2011).
166. Basilico, S. & Göttgens, B. Dysregulation of haematopoietic stem cell regulatory programs in acute myeloid leukaemia. *J Mol Med (Berl)* **95**, 719–727 (2017).
167. Iwasaki, H. & Akashi, K. Myeloid Lineage Commitment from the Hematopoietic Stem Cell. *Immunity* **26**, 726–740 (2007).
168. Coates, B. M. *et al.* Inflammatory Monocytes Drive Influenza A Virus–Mediated Lung Injury in Juvenile Mice. *The Journal of Immunology* **200**, 2391–2404 (2018).
169. Hussell, T. & Bell, T. J. Alveolar macrophages: plasticity in a tissue-specific context. *Nat. Rev. Immunol.* **14**, 81–93 (2014).
170. Joshi, N., Walter, J. M. & Misharin, A. V. Alveolar Macrophages. *Cell. Immunol.* **330**, 86–90 (2018).
171. Ramage, W. *et al.* Cross-Reactive and Lineage-Specific Single Domain Antibodies against Influenza B Hemagglutinin. *Antibodies* **8**, 14 (2019).
172. Martínez-Olondris, P., Rigol, M. & Torres, A. What lessons have been learnt from animal models of MRSA in the lung? *European Respiratory Journal* **35**, 198–201 (2010).
173. Kim, H. K., Missiakas, D. & Schneewind, O. Mouse models for infectious diseases caused by *Staphylococcus aureus*. *J Immunol Methods* **410**, 88–99 (2014).
174. Meyer, U. Prenatal Poly(I:C) Exposure and Other Developmental Immune Activation Models in Rodent Systems. *Biological Psychiatry* **75**, 307–315 (2014).
175. Heyne, G. W. *et al.* A Simple and Reliable Method for Early Pregnancy Detection in Inbred Mice. *J Am Assoc Lab Anim Sci* **54**, 368–371 (2015).
176. Eskild, A., Haavaldsen, C. & Vatten, L. J. Placental weight and placental weight to birthweight ratio in relation to Apgar score at birth: a population study of 522 360 singleton pregnancies. *Acta Obstetricia et Gynecologica Scandinavica* **93**, 1302–1308 (2014).
177. McGee, S. R. & Narayan, P. Precocious Puberty and Leydig Cell Hyperplasia in Male Mice With a Gain of Function Mutation in the LH Receptor Gene. *Endocrinology* **154**, 3900–3913 (2013).
178. Liu, Q., Zhou, Y. & Yang, Z. The cytokine storm of severe influenza and development of immunomodulatory therapy. *Cell Mol Immunol* **13**, 3–10 (2016).
179. Evren, E., Ringqvist, E. & Willinger, T. Origin and ontogeny of lung macrophages: from mice to humans. *Immunology* **160**, 126–138 (2020).
180. Killian, M. L. Hemagglutination assay for influenza virus. *Methods Mol. Biol.* **1161**, 3–9 (2014).
181. Lally, R. T., Ederer, M. N. & Woolfrey, B. F. Evaluation of mannitol salt agar with oxacillin as a screening medium for methicillin-resistant *Staphylococcus aureus*. *J. Clin. Microbiol.* **22**, 501–504 (1985).
182. John-Schuster, G. *et al.* Cigarette smoke-induced iBALT mediates macrophage activation in a B cell-dependent manner in COPD. *Am. J. Physiol. Lung Cell Mol. Physiol.* **307**, L692-706 (2014).
183. Solano, M. E., Thiele, K., Kowal, M. K. & Arck, P. C. Identification of suitable reference genes in the mouse placenta. *Placenta* **39**, 7–15 (2016).
184. Ruijter, J. M., Lorenz, P., Tuomi, J. M., Hecker, M. & van den Hoff, M. J. B. Fluorescent-increase kinetics of different fluorescent reporters used for qPCR depend on monitoring chemistry, targeted sequence, type of DNA input and PCR efficiency. *Microchim Acta* **181**, 1689–1696 (2014).
185. McFarlane, L., Truong, V., Palmer, J. S. & Wilhelm, D. Novel PCR assay for determining the genetic sex of mice. *Sex Dev* **7**, 207–211 (2013).

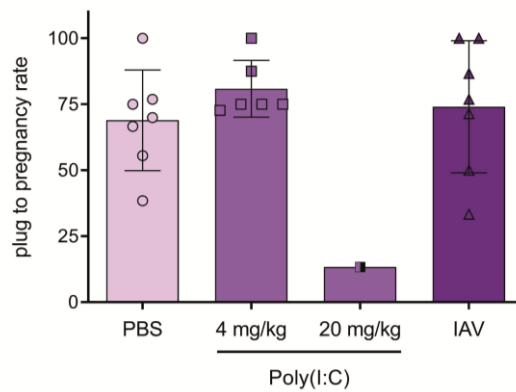
I. Supplements – Hazardous materials

Material	GHS pictograms	Hazard statements	Precautionary statements
Collagenase D		H315, H319, H334, H335	P261, P264, P271, P280, P285, P302+P351, P304+P340, P305+P351+P338, P332+P313, P337+P313, P342+P311, P362, P403+P233, P405, P501
Crystal violet		H302, H318, H351, H361, H373	P260, P264, P270, P280, P501 P305+P351+P338,
Diethylpyrocarbonate		H302, H315, H319, H335	P280, P302+P352, P304+P340, P312 P305+P351+P338,
Ethanol		H225, H319	P210, P233, P305+P351+P338
Ethidium bromide solution		H302, H330, H341	P201, P260, P280, P304+P340, P308+P311
Formaldehyde solution (37%)		H301+H311+H331, H314, H317, H335, H341, H350, H370	P260, P280, P303+P361+P353, P304+P340, P305+P351+P338, P308+P311
Glacial Acetic acid		H226, H314	P210, P233, P240, P241, P2242, P243, P254, P280, P301+P330+P331, P303+P361+P353, P304+P340+P310, P305+P351+P310, P363, P370+P378, P403+P235, P405, P501

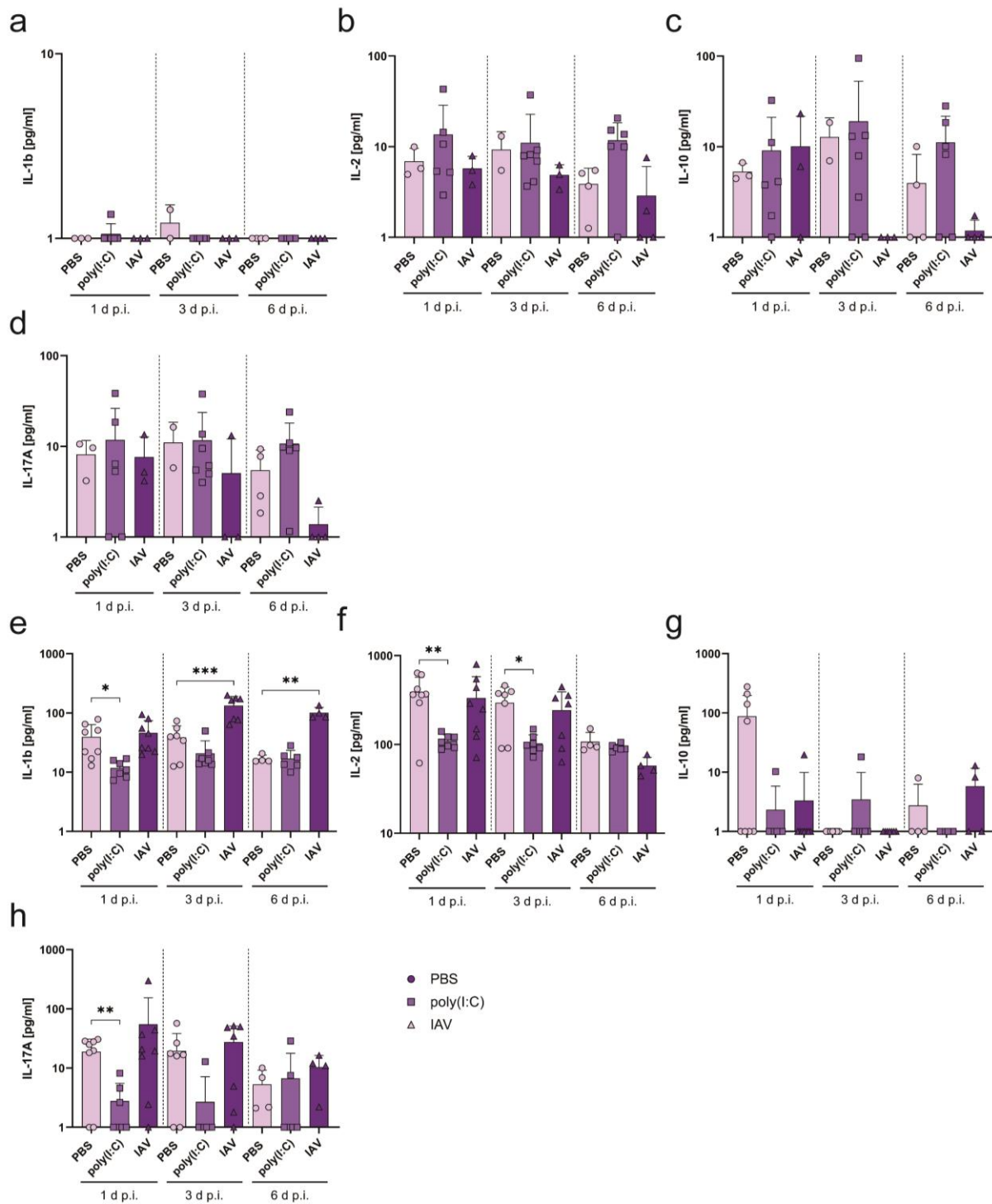
Material	GHS pictograms	Hazard statements	Precautionary statements
Halt™ Protease & Phosphatase Inhibitor		H302	P280, P264, P301+P312, P330, P501
Hematoxylin		H302, H315, H319, H335	P261, P305+P351+P338
Hydrochloric acid (37%)		H290, H314, H335	P280, P303+P361+P353, P304+P340, P305+P31+P338, P310
Isoflurane		H319, H315, H335, H336	P302+P352, P321, P332+P313, P362, P264, P280, P305+P351+P338, P337+P313, P261, P271, P304+P340, P312, P403+P233, P405, P501
Ketamine		H302, H332, H335	P261, P264, P301+P312, P304+P340, P330
Methanol		H225, H301+H311+H331, H370	P210, P270, P280, P303+P361+P353, P304+P340, P308+P311
Paraformaldehyde		H228, H302+H332, H315, H317, H318, H335, H341, H350	P202, P210, P270, P280, P305+P351+P338, P308+P313
Penicillin & Streptomycin		H302, H317	P280
Proteinase K		H315, H319, H334, H335	P261, P305+P351+P338, P324+P311
Pursept-A Xpress		H225, H319	P210, P271, P305+P351+P338, P337+P313, P403+P233

Material	GHS pictograms	Hazard statements	Precautionary statements
RBC lysis buffer		H319, H316, H412	P273, P280, P264, P332+P313, P305+P351+P338, P501
Sodium hydroxide		H290	P234, P390
TPCK-treated trypsin		H15, H319, H334, H335	P280, P284, P271, P261, P264, P304+P340, P342+P311, P302+P352, P361+P364, P305+P351+P38, P337+P313, P501
Trypsin-EDTA	 	H315, H319, H334	P280, P302+P352, P304+P341, P305+P351+P338, P342+P311
Xylazine		H301	P264, P301+P10, P330

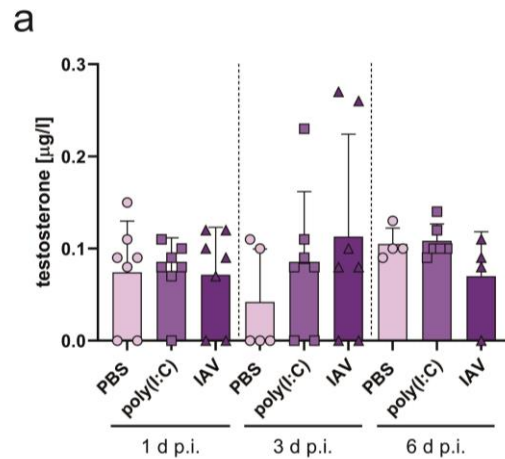
II. Supplements – Figures



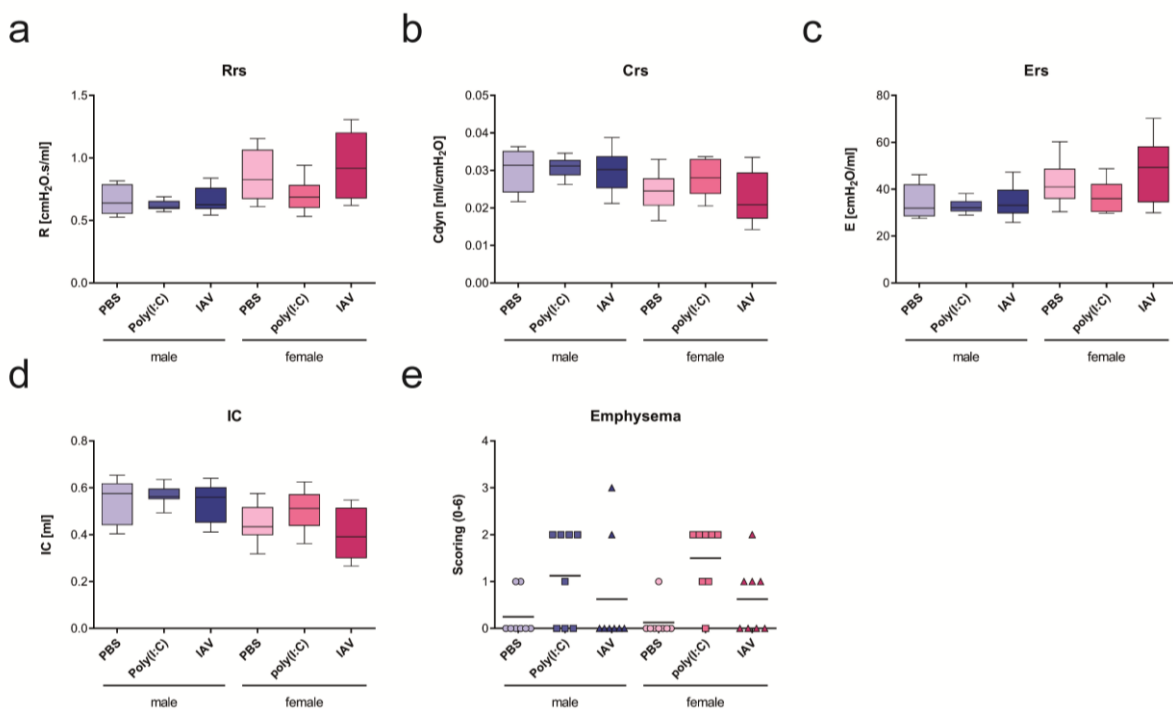
Supplementary figure 1: Plug to pregnancy rate in different treatment groups. Plug to pregnancy rate was determined within independent experiments for groups of plug positive mice treated with PBS (n = 7), poly(I:C) at a dosage of 4 mg/mg (n = 6), a dosage of 20 mg/kg (n = 1) or infected with IAV (n = 7). Treatment with 20 mg/kg was only performed once on 15 plug positive mice. Values are shown as mean and error bars as SD. Significance was calculated using unpaired t test with Welch's correction (no effects achieved statistical significance).



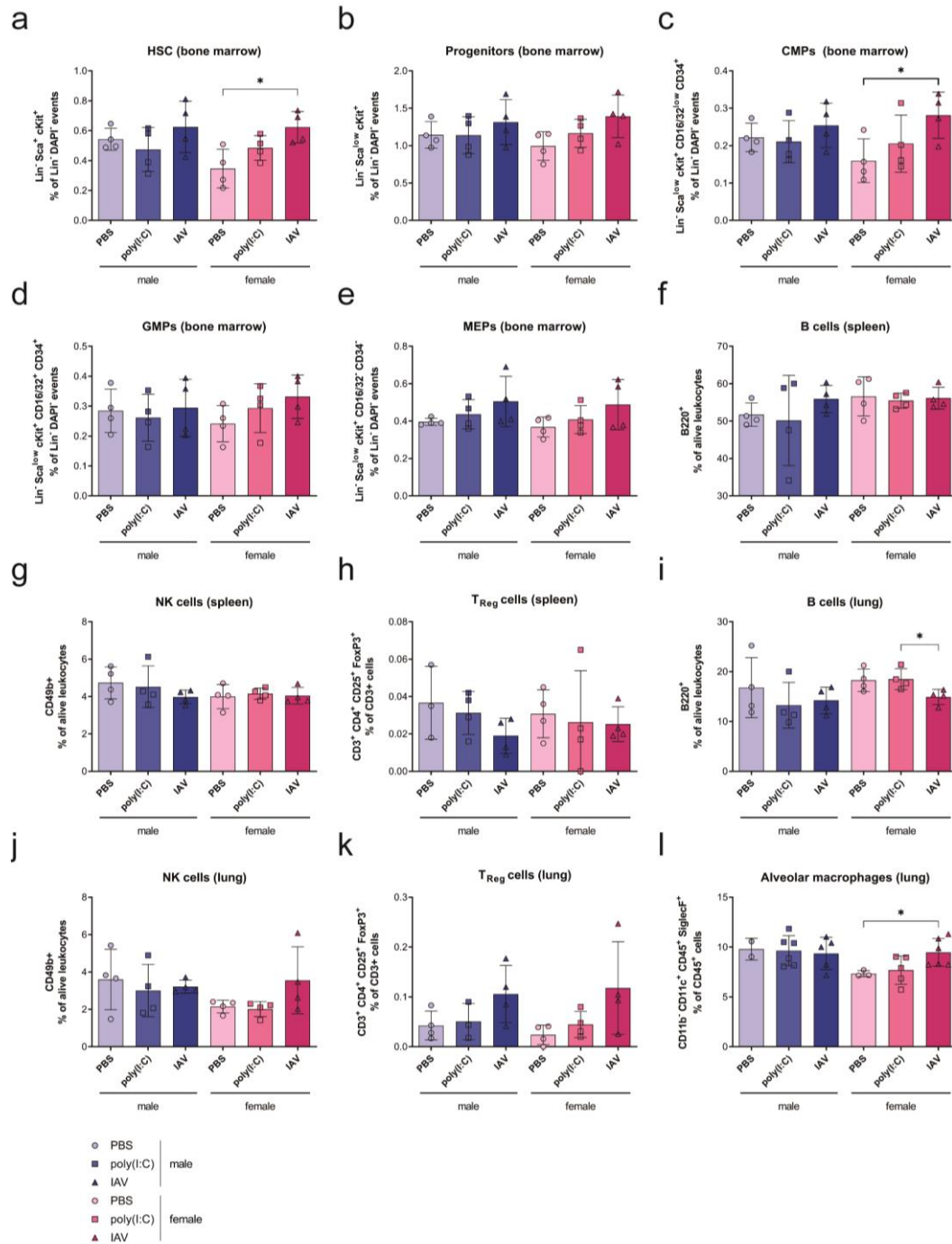
Supplementary figure 2. 1st hit: IAV-infection and poly(I:C)-treatment lead to MIA displayed by increased levels of pro-inflammatory cytokines. (a-d) Cytokines (IL-1 β [a], IL-2 [b], IL-10 [c] and IL-17A [d]) determined by Luminex assay in lungs of pregnant mice treated with PBS (n = 3), poly(I:C) (n = 6-7) or infected with IAV (n = 3-4) at E5.5, measured at 1, 3 and 6 d p.i. (e-h) Cytokines (IL-1 β [e], IL-2 [f], IL-10 [g] and IL-17A [h]) determined by Luminex assay in plasma of pregnant mice treated with PBS (n = 8, one outlier), poly(I:C) (n = 6-7) or infected with IAV (n = 4-8) at E5.5, measured at 1, 3 and 6 d p.i. Values are normalized to organ weight. All data are presented as mean and SD. Cytokine levels that were below detection limit were set to the kit's lower detection limit of 1 pg/g. The statistical significance was calculated by unpaired test (two-tailed) with Welch's correction (*p<0.05, **p<0.01, ***p<0.001). Mathematical outliers were determined using Grubb's test.



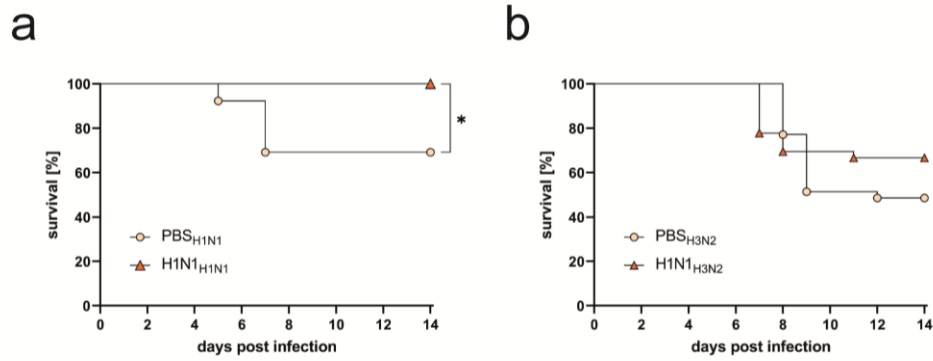
Supplementary figure 3. 1st hit: MIA does not affect maternal testosterone levels. Testosterone determined by ELISA in plasma of pregnant mice treated with PBS, poly(I:C) or infected with IAV ($n = 4 - 7$) at E5.5, measured at 1, 3 and 6 d p.i. All data are presented as mean and SD. The statistical significance was calculated by unpaired t-test (two-tailed) with Welch's correction (no effects achieved statistical significance).



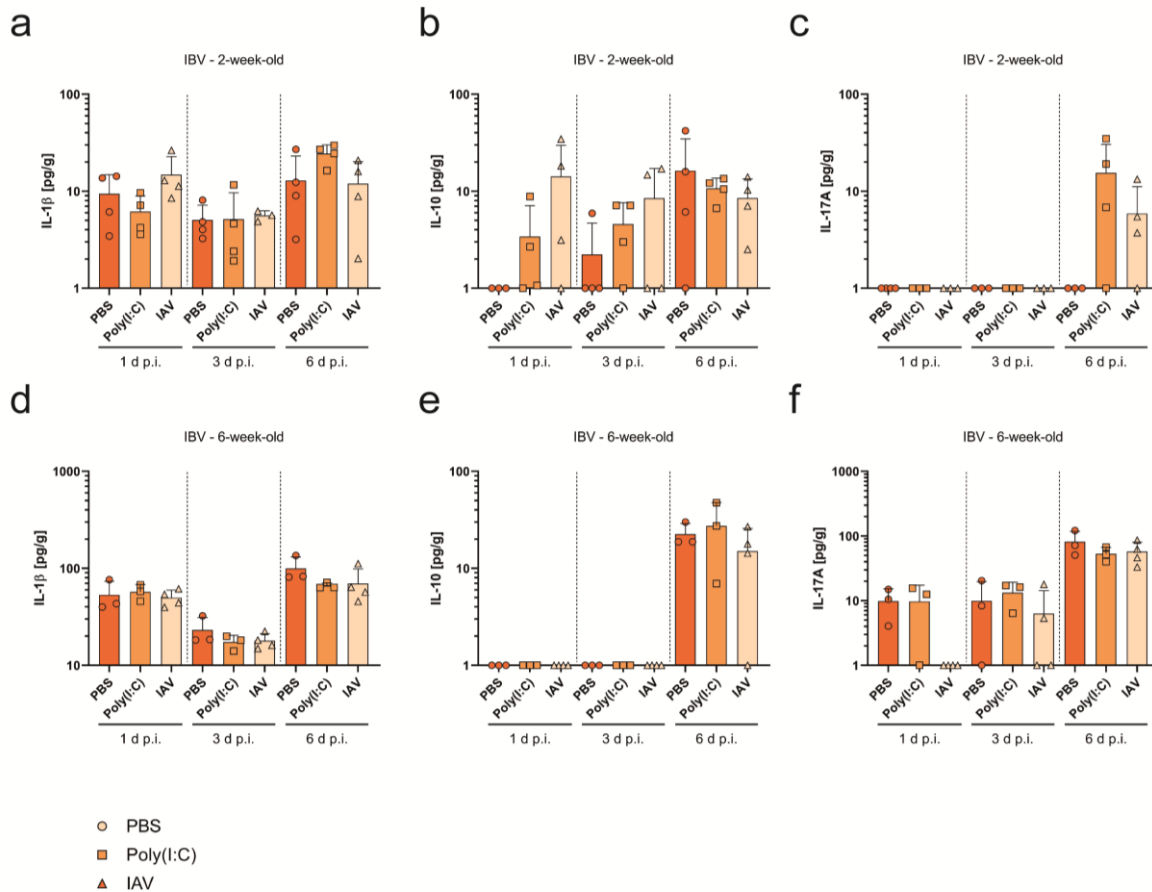
Supplementary figure 4: Offspring's lung physiology and function. (a) Resistance, (b) Compliance, (c) Elastance, (d) inspiratory capacity and (e) emphysema grading assessed in 20-week-old mice ($n = 8$) born to PBS-treated, poly(I:C)-treated or IAV-infected dams using a FlexiVent Research System (a-d) or by histological assessment. Values are shown as mean with bars as SD and error bars from min to max. Significance was calculated using unpaired t test with Welch's correction (no effects achieved statistical significance).



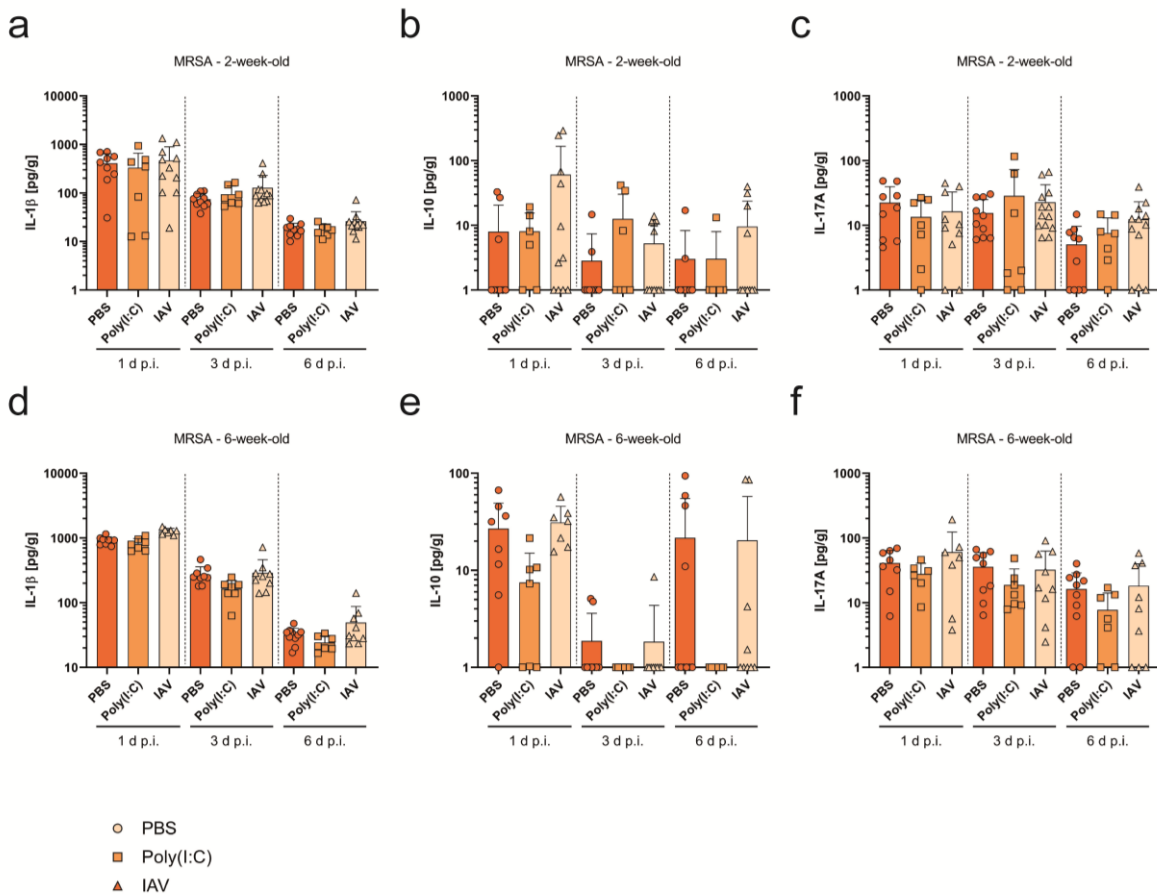
Supplementary figure 5. Stem- and immune cell frequencies in adult offspring. (a-e) Frequency of Lin⁻ Sca⁺ cKit⁺ cells (a), Lin⁻ Sca^{low} cKit⁺ cells (b), Lin⁻ Sca^{low} cKit⁺ CD16/32^{low} CD34⁺ cells (c), Lin⁻ Sca^{low} cKit⁺ CD16/32⁺ CD34⁺ cells (e) and Lin⁻ Sca^{low} cKit⁺ CD16/32⁻ CD34⁺ cells (e) as % of Lin⁻ DAPI events in the bone marrow of 6-week-old offspring (n = 4) born to early gestational PBS-treated, poly(I:C)-treated or IAV-infected dams, as assessed by flow cytometry. (g-k) Frequency of B220⁺ cells (f and i), CD49b⁺ cells (g and j), CD3⁺ CD4⁺ CD25⁺ FoxP3⁺ cells (h and k) as % of alive leukocytes in spleens (g-h) or lungs (i-k) of 6-week-old offspring (n = 4) born to early gestational PBS-treated, poly(I:C)-treated or IAV-infected dams, as assessed by flow cytometry. (l) Frequency of CD11b⁻ CD11⁺ CD45⁺ SiglecF⁺ cells as % of CD45⁺ cells in lung of 6-week-old offspring born to early gestational PBS-treated (n = 2-3), poly(I:C)-treated (n = 5-6) or IAV-infected dams (n = 5-6), as assessed by flow cytometry. If fewer measurement points than the indicated n are visible in the graphs, the ones not shown were excluded as technical outliers. All data are presented as mean and SD. The statistical significance was calculated by unpaired t-test (two-tailed) with Welch's correction (*p < 0.05).



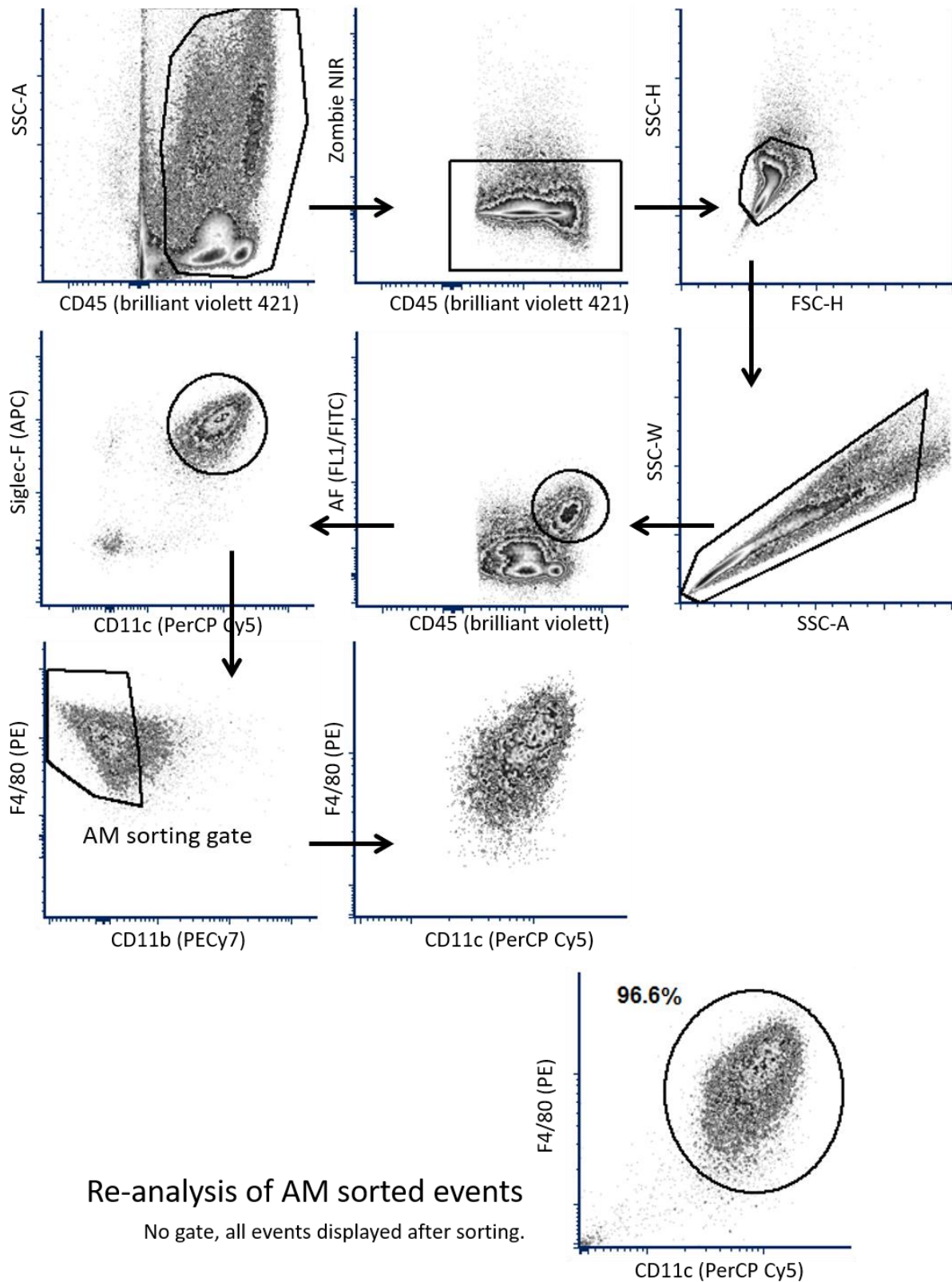
Supplementary figure 6. Homologous second hit experiments in juvenile offspring. (a) 2-week-old male offspring born to PBS- (n = 13) or IAV-infected (n = 14) dams infected with 10^3 PFU of IAV (H1N1). Survival was determined within 14 d p.i. (b) 2-week-old female offspring born to PBS- (n = 35) or IAV-infected (n = 37) dams infected with 10^2 PFU of IAV (H3N2 6+2 reassortant in WSN). Survival was determined within 14 d p.i. All n represent number of offspring from respective groups. The statistical significance was calculated Log Rank test for trend (* $p < 0.05$).



Supplementary figure 7. 2nd hit: Male offspring born to IAV-infected dams show increased vulnerability towards early life IBV infection. (a-c) Cytokines (IL-1 β [a], IL-10 [b], and IL-17A [c]) determined by Luminex assay in lungs of 2-week-old offspring (both sexes) born to PBS- or poly(I:C)-treated or IAV-infected offspring (n = 4) after infection with 10⁵ PFU of IBV measured at 1, 3 or 6 d p.i. (d-f) Cytokines (IL-1 β [d], IL-10 [e], and IL-17A [f]) determined by Luminex assay in lungs of 6-week-old offspring (both sexes) born to PBS- or poly(I:C)-treated or IAV-infected offspring (n = 3 - 4) after infection with 10⁵ PFU of IBV measured at 1, 3 or 6 d p.i.. Values are normalized to organ weight. All n represent number of offspring from respective groups. All data are presented as mean and SD. Cytokine levels that were below detection limit were set to the kit's lower detection limit of 1 pg/g. The statistical significance was calculated by unpaired t-test (two-tailed) with Welch's correction (no effects achieved statistical significance).



Supplementary figure 8. 2nd hit: Offspring born to IAV-infected dams show increased vulnerability towards early life MRSA infection. (a-c) Cytokines (IL-1 β [a], IL-10 [b], and IL-17A [c]) determined by Luminex assay in lungs of 2-week-old offspring (both sexes) born to PBS- (n = 10) or poly(I:C)-treated (n = 7) or IAV-infected offspring (n = 11) after infection with 10⁸ CFU of MRSA measured at 1, 3 or 6 d p.i. (d-f) (IL-1 β [a], IL-10 [b], and IL-17A [c]) determined by Luminex assay in lungs of 6-week-old offspring (both sexes) born to PBS-, poly(I:C) or IAV-infected offspring (n = 7-10) infected with 10⁸ CFU of MRSA measured at 1, 3 or 6 d p.i. Values are normalized to organ weight. All n represent number of offspring from respective groups. All data are presented as mean and SD. Cytokine levels that were below detection limit were set to the kit's lower detection limit of 1 pg/g. The statistical significance was calculated by unpaired t-test (two-tailed) with Welch's correction (no effects achieved statistical significance).



Supplementary figure 9: Example gating strategy for AM sort. After pre-gating CD45⁺ leucocytes, dead cells were excluded by positive Zombie NIR staining. After debris and doublet exclusion, alveolar macrophages were defined as auto fluorescent (AF) positive, Siglec-F⁺ CD11c⁺ CD11b⁻ cells. Purity was confirmed by re-analysis F4/80⁺, CD11c⁺.

III. Supplements – List of tables and figures

Tables

Table 1: EMA approved antiviral medications.....	10
Table 2: Inoculation scheme for pregnant mice at E5.5.....	66
Table 3: Inoculation scheme for two-week-old mice.....	66
Table 4: Inoculation scheme for six-week-old mice.....	67
Table 5: Cell types and corresponding surface markers for FACS analysis of offspring immune cells.....	69
Table 6: Cell types and corresponding surface markers for FACS analysis of lung macrophages.....	69
Table 7: oligonucleotides for placental nutrient gene RT-qPCR.....	71

Figures

Figure 1: Influenza A virion morphology and structure.....	4
Figure 2: Interspecies transmission and hosts of IAV.....	6
Figure 3: Influenza A virus pandemics.....	8
Figure 4: Contradictory demands for the immune system to adapt to pregnancy and to mount an immune response towards maternal infection with the influenza virus.....	14
Figure 5: Number of studies using a poly(I:C) based model of MIA from 2003 to 2018.....	17
Figure 6. 1 st hit: IAV-infection but not poly(I:C)-treatment during early gestation leads to mild and non-lethal disease.....	22
Figure 7. 1 st hit: IAV-infection during early gestation leads to viral replication and inflammation of the lung....	23
Figure 8. 1 st hit: IAV-infection and poly(I:C)-treatment lead to MIA displayed by increased levels of pro-inflammatory cytokines.....	24
Figure 9. 1 st hit: IAV-infection during early gestation causes increased levels of corticosterone and progesterone.....	25
Figure 10. 1 st hit: Poly(I:C)-treatment and IAV-infection during early gestation affect placental weight and nutrient gene expression.....	26
Figure 11. 1 st hit: IAV- and poly(I:C)-induced MIA does not affect primary pregnancy outcome.....	28
Figure 12: 1 st hit: IAV- and poly(I:C)-induced MIA leads to low-birth-weight offspring.....	29
Figure 13. Offspring's health: Offspring born to IAV-infected dams present prolonged low body weight that is not affected by brood care.....	30
Figure 14. Offspring's health: Early gestational influenza affects 2-week-old offspring's hematopoiesis.....	32
Figure 15. Offspring's health: Early gestational influenza affects 2-week-old offspring's peripheral immune cell frequencies.....	33
Figure 16. Offspring's health: Early gestational influenza might affect alveolar macrophages in 2-week-old offspring's lung.....	34
Figure 17. 2 nd hit: Male offspring born to IAV-infected dams show increased vulnerability towards early life IBV infection.....	36
Figure 18. 2 nd hit: Offspring born to IAV-infected dams show increased vulnerability towards early life IBV infection.....	37
Figure 19. 2 nd hit: Offspring born to IAV-infected dams show increased vulnerability towards early life MRSA infection.....	39
Figure 20. 2 nd hit: Offspring born to IAV-infected dams show increased vulnerability towards early life MRSA infection.....	40
Figure 21. 2 nd hit: Offspring born to IAV-infected mothers present delayed bacterial clearance.....	41
Figure 22. Alveolar macrophages of offspring born to IAV-infected mothers are functionally impaired.....	44

Supplementary figures

Supplementary figure 1: Plug to pregnancy rate in different treatment groups.....	87
Supplementary figure 2. 1 st hit: IAV-infection and poly(I:C)-treatment lead to MIA displayed by increased levels of pro-inflammatory cytokines.....	88
Supplementary figure 3. 1 st hit: MIA does not affect maternal testosterone levels.....	89
Supplementary figure 4: Offspring's lung physiology and function.	89
Supplementary figure 5. Stem- and immune cell frequencies in adult offspring.	90
Supplementary figure 6. Homologous second hit experiments in juvenile offspring.	91
Supplementary figure 7. 2 nd hit: Male offspring born to IAV-infected dams show increased vulnerability towards early life IBV infection.....	92
Supplementary figure 8. 2 nd hit: Offspring born to IAV-infected dams show increased vulnerability towards early life MRSA infection.	93
Supplementary figure 9: Example gating strategy for AM sort.	94

IV. License agreements, reprint of figures

Figure 1

Original publication: Structure of influenza virus nucleoprotein complexes and their packaging into virions
Author: Yoshihiro Kawaoka, Takeshi Noda
Publication: Reviews in Medical Virology
Publisher: John Wiley and Sons
License number (reuse in this thesis): 4867670437760

Original publication: Influenza: lessons from past pandemic, warnings from current incidents
Author: Taisuke Horimoto et al
Publication: Nature Reviews Microbiology
Publisher: Springer Nature
License number (reuse in this thesis): 4867670582455

Figure 2

Original publication: Host and viral determinants of influenza A virus species specificity
Author: Jason S. Long et al
Publication: Nature reviews Microbiology
Publisher: Springer Nature
License number (reuse in this thesis): 4867670866280

Figure 4

Original publication: Sex, Immunity and Influenza
Author: Gabriel, Gülsah; Arck Petra Clara
Publication: Journal of Infectious Diseases
Publisher: Oxford University Press
License number (reuse in this thesis): 4867670035536

Figure 5

Original publication: Challenges and opportunities of a-priori and a-posteriori variability in maternal immune activation models
Author: Ulrike Weber-Stadlbauer, Urs Meyer
Publication: Current Opinion in Behavioral Sciences
Publisher: Elsevier
License number (reuse in this thesis):
Creative Commons Attribution-NonCommercial-No Derivatives License
(CC BY NC ND)

Danksagung

Mein großer Dank gilt Prof. Dr. Gülsah Gabriel für die Bereitstellung dieses spannenden Forschungsprojektes sowie die hervorragende Unterstützung in all den Jahren. Ich habe außerordentlich viel lernen können und dabei sehr von deiner Expertise und vielfältigen Unterstützung profitiert. Ich werde viel aus dieser Zeit mitnehmen und immer gerne auf diese Zeit zurückblicken – vielen Dank!

In diesem Zuge danken möchte ich ebenfalls Prof. Dr. Zoya Ignatova in ihrer Funktion als Zweit-Gutachterin meiner Promotion und als Vorbild für eine stets unterstützende und auch fordernde Professorin. Unsere lange Zusammenarbeit, schon während meines Studiums, war für mich richtungsweisend und dafür möchte ich mich ausdrücklich bedanken.

Weiterhin möchte ich den Kollegen danken, mit denen ich im Rahmen meiner Promotion besonders eng zusammengearbeitet habe:

Dr. Kerstin Walendy-Gnirß hat mich vor allem in den ersten Zügen meiner Promotion maßgeblich unterstützt und ist mir bis heute in vielen Belangen ein Vorbild. Die Liebe zum Detail und vernünftige Dokumentation sind nur einige Aspekte, die du maßgeblich beeinflusst hast – vielen Dank!

Dr. Vinicius Pinho dos Reis möchte ich für die vielen faszinierenden Fachgespräche danken. Aber vor allem für seine unendliche Hilfsbereitschaft und gute Laune, die das wissenschaftliche Arbeiten noch wertvoller und schöner gemacht haben. Von den vielen Süßigkeiten ganz abgesehen!

My sincerest thanks also to Dr. Nilgün Tekin-Bubenheim, who joined our team in 2019 and brought so much enthusiasm and new expertise in our work. It was always a real pleasure to work with you!

Annette Gries, Ulla Müller und Hanna Jania möchte ich für die hervorragende technische Assistenz und die großartige Zusammenarbeit danken. Mit euch zu arbeiten war immer eine Freude und ohne euch wäre dieses große Projekt sicher nicht zu stemmen gewesen.

Ferner möchte ich meinen anderen Kollegen danken, allen voran Berfin Tuku, für die wirklich schöne Arbeitsatmosphäre, Hilfsbereitschaft und die Aktivitäten nach Feierabend. Mit euch zusammen waren die letzten Jahre eine wirklich großartige Zeit und ich hoffe sehr, dass wir in Kontakt bleiben.

Mein Dank gilt ebenfalls unseren Kooperationspartnern:

Prof. Dr. Bianca Schneider, Prof. Dr. Sonja Loges, Dr. Jochen Behrends, Dr. Isabel Ben-Batalla und Arne Düsedau für die fachliche und technische Unterstützung bei der *flow cytometry* und bei immunologischen Fragestellungen. Auch Prof. Ali Önder Yildirim, Prof. Thomas René, Gundula Pilnitz-Stolze und Nancy Kouassi möchte ich für die erfolgreiche Zusammenarbeit danken.

Special thanks also to Dr. Fiona Culley who allowed me to join her lab for two months and to learn about RSV and adoptive transfer experiments in mice at her side.

Ferner Dr. Raffael Nachbagauer, welcher mich während meiner Zeit in New York zur Anfertigung meiner Master-Thesis betreut hat. Raffael, die Arbeit mit dir war für mich unglaublich inspirierend und ganz sicher entscheidend für meine anhaltende Begeisterung für die Virologie und die Forschung.

Für die finanzielle Unterstützung meiner Promotion möchte ich der Claussen-Simon-Stiftung danken. Die Claussen-Simon-Stiftung aus Hamburg hat mich seit dem Master-Studium erst im Rahmen eines Stipendiums im Programm „Master Plus“ inklusive eines Auslandsstipendiums gefördert und anschließend auch während der Promotion im Programm „Dissertation Plus“. Die finanzielle Unterstützung hat es mir ermöglicht, mich vollständig auf mein Studium und die Promotion zu fokussieren und hat somit maßgeblich zu diesem Erfolg beigetragen. Auch die ideelle Unterstützung, sowie das breite und vielfältige Netzwerk, dass ich über die Stiftung aufbauen konnte sind ein großer Gewinn. In diesem Sinne möchte ich mich vor allem bei Frau Dr. Regina Back für diese Unterstützung und das anhaltende Vertrauen bedanken – vielen Dank!

Abschließend möchte ich mich bei jenen Menschen bedanken, die mir am wichtigsten sind und die mich in allen Lebenslagen unterstützen.

Bei meinen Eltern und Ihren Ehepartnern Annette & Christian Johannsen sowie Mario & Birgit Jacobsen für die unbegrenzte und liebevolle Unterstützung. Ihr wart mir immer ein sicherer Heimathafen und bei euch konnte ich den manchmal notwendigen Abstand zur Arbeit gewinnen und immer wieder Kraft tanken. Ohne euch wäre ich niemals an diesen Punkt gekommen und dafür möchte ich euch von Herzen danken!

An dieser Stelle möchte ich auch meiner Großmutter Helga Jacobsen stellvertretend für meine ganze Familie danken, da sie mich seit dem Studium ebenfalls in besonderem Maße unterstützt hat und deren Worte mir immer wieder neue Kraft mit auf den Weg gegeben haben. Sowie meiner Schwester Inga Jacobsen, die mir seit je her hilft auch über die Arbeit hinaus zu blicken und die Schönheit in allen Aspekten des Lebens zu finden.

Ebenfalls danken möchte ich meiner Lebensgefährtin Carina Jürgens, die ich während meiner Promotion kennengelernt habe und die mir seitdem ein neues Leben geschenkt hat. Danke für deine Geduld, deine Liebe und dass du immer für mich da bist.

Eidesstattliche Erklärung

Hiermit versichere ich an Eides statt, die vorliegende Dissertation selbst verfasst und keine anderen als die angegebenen Hilfsmittel benutzt zu haben. Die eingereichte schriftliche Fassung entspricht der auf dem elektronischen Speichermedium. Ich versichere, dass diese Dissertation nicht in einem früheren Promotionsverfahren eingereicht wurde.

Datum, Unterschrift